The Institute of Paper Chemistry

Appleton, Wisconsin

Doctor's Dissertation

The High Temperature Alkaline Degradation of Phenyl-β-D-Glucopyranoside

William E. Molinarolo

January, 1989

THE HIGH TEMPERATURE ALKALINE DEGRADATION OF PHENYL β-D-GLUCOPYRANOSIDE

A thesis submitted by

William E. Molinarolo

B.A. 1980, Illinois Wesleyan University
M.S. 1984, Lawrence University

in partial fulfillment of the requirements
of The Institute of Paper Chemistry
for the degree of Doctor of Philosophy
from Lawrence University,
Appleton, Wisconsin

January, 1989

TABLE OF CONTENTS

ABSTRACT

Random cleavage of glycosidic bonds of cellulose under alkaline pulping conditions is the degradation pathway responsible for the loss of pulp viscosity. Until recently, an intermolecular nucleophilic substitution with attack at the C(1) carbon by the conjugate base of OH-2, $S_N$icB(2), had been thought to be the only mechanism causing this type of bond cleavage. The carbohydrate model phenyl β-D-glucopyranoside, which forms 1,6-anhydro-β-D-glucopyranose (levoglucosan) and phenolate anion by the $S_N$icB(2) mechanism at 100°C, was examined under high temperature alkaline conditions to determine whether the reaction mechanism or product ratios changed with increased temperature.

Heating phenyl β-D-glucopyranoside at 100°C in alkali and monitoring reactant and product concentrations by gas chromatographic techniques yielded a degradation rate constant of 5.0×10^{-5} sec^{-1} and an 88% yield of levoglucosan that were consistent with literature values. Additional experiments were performed at the typical wood chemical pulping temperatures of 170°C using a modified fast flow reactor. Levoglucosan and phenol yields at 170°C were approximately 82% and 100%, respectively.

The extent of oxygen-aglycon cleavage determined by ^{18}O incorporation was negligible; indicating the lack of an S_N2Ar mechanism. Addition of a strong nucleophile (NaSH) did not greatly affect the reaction rate constants but affected the levoglucosan yield; thus the S_N2 pathway was eliminated. A 1300 times decrease in the reaction rate constant due to blocking the C(2)-OH reaction site indicated an S_Ni type mechanism. The apparent thermodynamic functions of activation ($\Delta H^{\ddagger}$ 28.3 kcal $mol^{-1}$and $\Delta S^{\ddagger}$ -1.3 kcal mol^{-1} $°K^{-1}$) were indicative of an $S_N$icB(2) pathway rather than the $S_N$icB(2)-ro or S_N1 mechanisms. The 2% decrease in reaction rate

constants with a fivefold increase of the reaction medium's ionic strength and a kinetically derived linear relationship of reaction rate constants with varying the hydroxide ion concentration at constant ionic strength were also consistent with the $S_N$icB(2) mechanism.

Thus, phenyl β-D-glucopyranoside degradation proceeds by an $S_N$icB(2) pathway at both 100 and 170°C. The fact that the expected $S_N$icB(2) product, levoglucosan, was formed in less than quantitative yields was probably due to competing reactions which occur after the $S_N$icB(2) rate-determining step. From the observed levoglucosan yields, it may be possible to determine the extent of $S_N$icB(2) reactions occurring with other, slower reacting carbohydrate models at 170°C.

INTRODUCTION

The Kraft pulping process accounts for the majority of pulp produced in North America.[1] Prior to fiber liberation, carbohydrate losses are 10% for cellulose and 50% for the hemicelluloses.[2] A drop in pulp viscosity also accompanies this yield loss.[3]

Possible oxygen-free, carbohydrate reactions that can occur during Kraft pulping include: swelling, dissolution, hydrolysis of acetyl groups, peeling, stopping, and random chain cleavage of β-glycosidic bonds.[4] The most widely studied degradation reactions are cellulosic peeling and random chain cleavage.

Peeling is a well characterized reaction that becomes significant below 100°C and accounts for a large portion of the carbohydrate yield losses.[5] For cellulose, this reaction is the stepwise depolymerization by removal of glucosyl units from the chain's reducing end. Peeling proceeds until the chain is totally peeled, chemically stopped,[4] or physically stopped.[6]

Random chain cleavage, in contrast to peeling, can occur at any cellulosic glycosidic linkage. This reaction produces two shorter cellulosic chains, which causes the pulp viscosity drop,[4] and produces a new reducing end group.[7] Random chain cleavage is generally believed to occur at temperatures greater than 130°C.[4] However, Gentile *et al.*[6] have found that cleavage may have already begun at temperatures below 100°C. To date, the reaction mechanism for random chain cleavage is still unresolved.

Recognition of the random chain cleavage reaction came in 1957 by Corbett and Richards.[7] Samuelson[3] reported in 1953 a rapid pulp viscosity drop for both

acidic and alkaline hydrolyses of cellulosic fibers. These results were unexpected to Corbett and Richards,[7] because the alkaline hydrolyses exhibited random chain cleavage behavior associated with acidic hydrolysis not the recognized alkaline reaction of peeling. Originally, the alkaline viscosity losses were thought to be due to an experimental artifact, but experimental evidence indicated otherwise. Corbett and Richards[7] proposed that the mechanism for this cellulose degradation was similar to that proposed for the simple glucoside models of Lindberg.[8] From the study of alkaline degradations of alkyl β-D-glucoside and cellodextrins at 170°C, Lindberg indicated that carbohydrate glycosidic cleavage may occur by the mechanism illustrated in Figure 1. The C(2)-OH has already ionized and the oxyanion bridges to C(1) to displace the remainder of the chain. This pathway has been used to explain cellulosic random chain cleavage.[4]

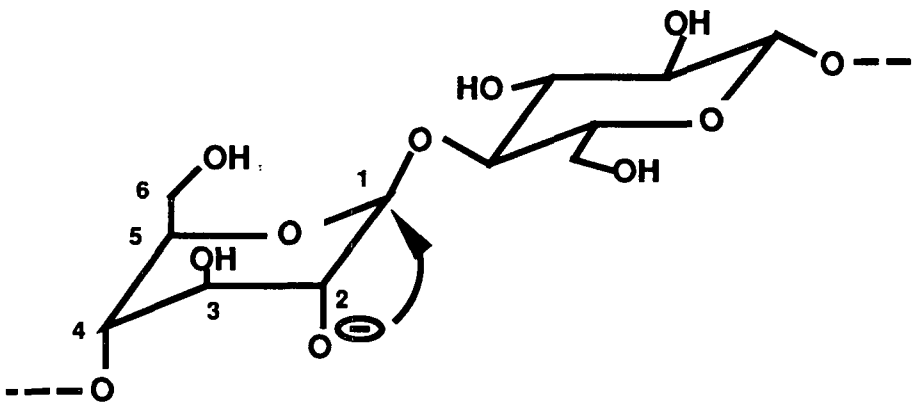

Figure 1. Proposed random chain cleavage reaction for cellulose.[4]

ALKALINE DEGRADATION OF MODEL COMPOUNDS

Model compound studies[9-19] have provided the majority of the current information on cellulosic random chain cleavage. These studies eliminated problems associated with the examination of the alkaline degradation of cellulose by eliminating competing peeling reactions, allowing for homogeneous kinetics, and limiting product analyses to known compounds. Ballou,[20] Capon,[21] and Brandon[11] have presented comprehensive reviews on the possible carbohydrate degradation reaction mechanisms in oxygen-free alkaline media. Only model compounds that can react by the pathway suggested by Lindberg[8] will be examined below.

Aryl Glycosides

The mechanism for carbohydrate random chain cleavage postulated by Lindberg[8] was based on the differences in reactivities of α-D- and β-D- linked glucosides and the appearance of trace amounts of levoglucosan from β-D-glucopyranoside models at 170°C in 2.5M NaOH. Levoglucosan only appeared in trace amounts, because it was much more reactive than the starting material. This work inferred that the alkaline degradation pathways of alkyl β-D-glucopyranosides and phenyl β-D-glucopyranoside were similar. McCloskey and Coleman[22] had observed that phenyl β-D-glucopyranoside formed an 88% levoglucosan yield in boiling 1.3M KOH and proposed a mechanism which will be called intermolecular nucleophilic substitution with attack at the C(1) carbon by the conjugate base of C(2)-OH ($S_N$icB(2)).

The $S_N$icB(2) mechanism for phenyl β-D-glucopyranoside (**1**) (Figure 2) begins with ionization of the C(2)-hydroxyl. The pyranose ring flips from the stable $^4C_1$ to the $^1C_4$ conformation. The C(2)-oxyanion and the phenyl ring are now in the anti

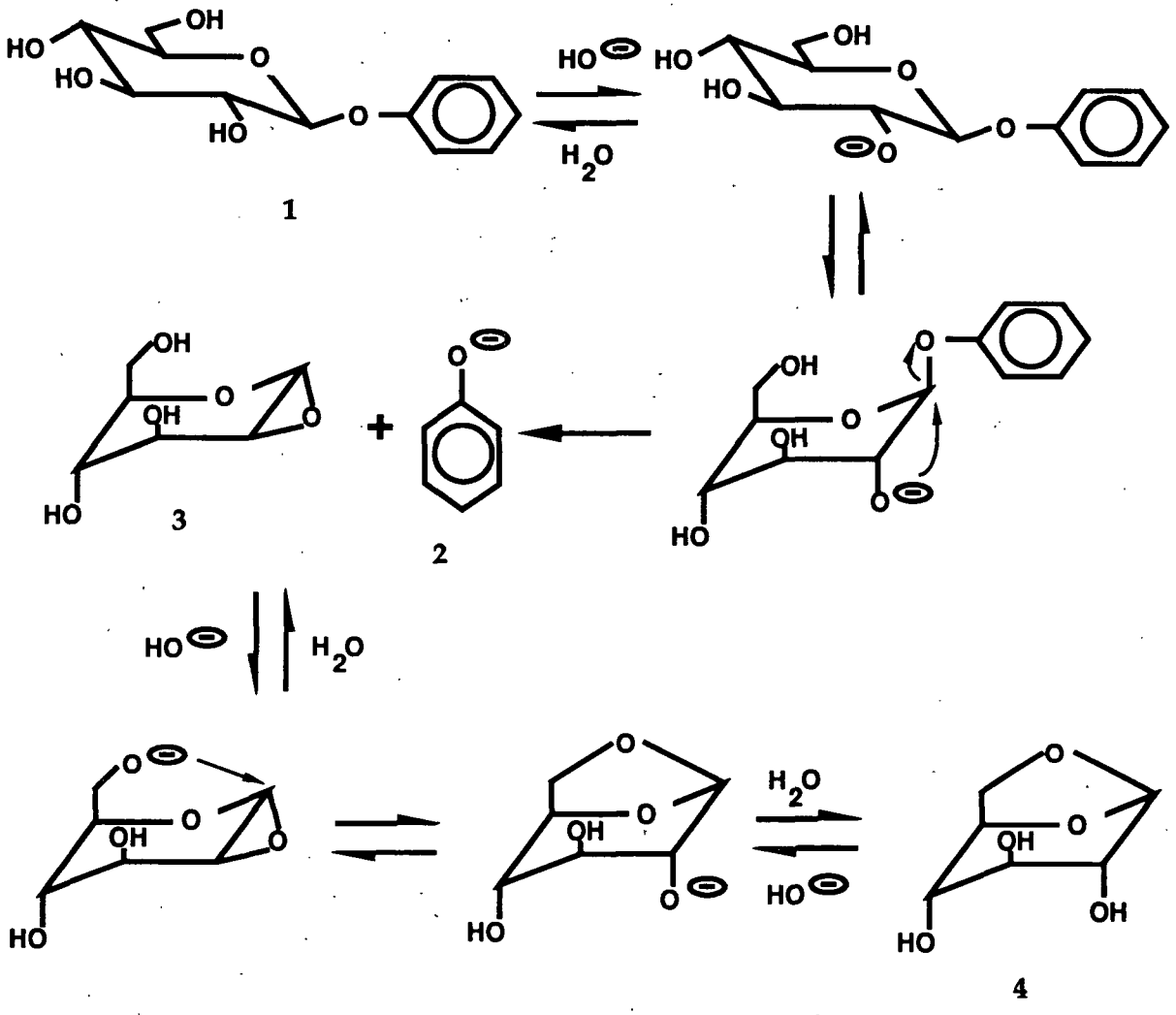

Figure 2. Degradation of phenyl β-D-glucopyranoside by the $S_N$icB(2) mechanism.[22]

periplanar position necessary for further reaction. In the presumed rate-determining step, the C(2)-oxyanion bridges to C(1) to displace a phenolate ion (**2**) and form 1,2-anhydro-α-D-glucopyranose (**3**). The C(6)-hydroxyl ionizes to form an oxyanion which opens the 1,2-epoxide ring at C(1) to form levoglucosan (**4**).

Another product-determining pathway exists for opening the 1,2-epoxide ring of 1,2-anhydro-α-D-glucopyranose. Hydroxide ions (Figure 3) can directly attack at C(1) to form glucose which degrades rapidly to acidic products under the alkaline conditions. This alternative pathway for compounds that react by the $S_N$icB(2) mechanism was observed by McCloskey and Coleman[22] when the C(6)-hydroxyl was either absent or in a position in which the 1,6-anhydride could not be formed.

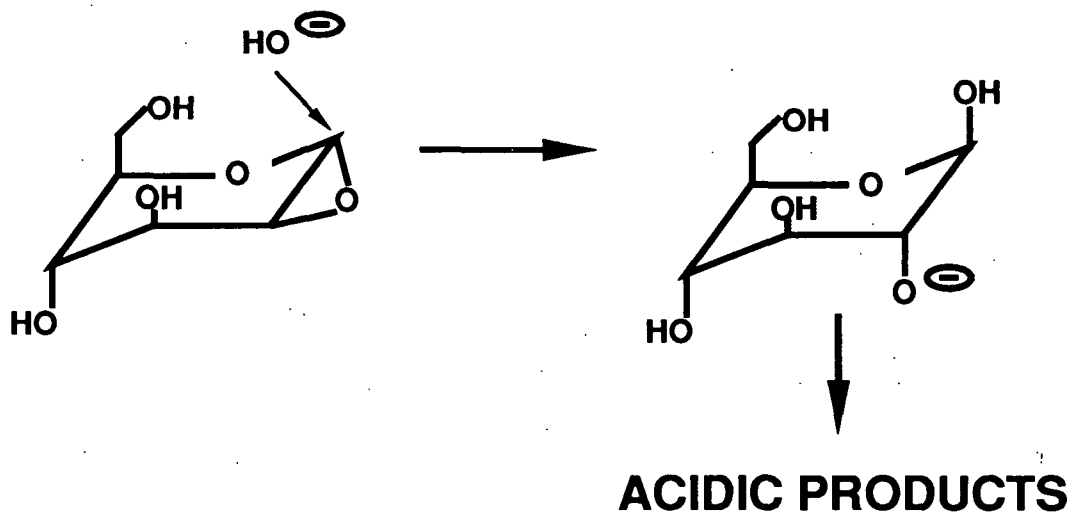

Figure 3. Hydroxide ion degradation of 1,2-anhydro-α-D-glucopyranose.[22]

Several pieces of indirect evidence supported the proposed $S_N$icB(2) pathway. Model compound degradation was absent when the C(2)-hydroxyl was replaced with a non-ionizable methoxide group.[22,23] The change from the β-D- to α-D-glucose anomer caused the reaction to stop.[22,24] At room temperature, Brigl's anhydride (5) (Figure 4), 1,2-anhydro-3,4,6-tri-O-acetyl-α-D-glucopyranose, rapidly formed levoglucosan in hydroxide solutions[25] or methyl β-D-glucopyranoside (6) in a sodium methoxide solution.[26] Brigl's anhydride studies indicated that 1,2-anhydro-α-D-glucopyranose was a viable intermediate in the $S_N$icB(2) mechanism and was extremely reactive from it's room temperature behavior.

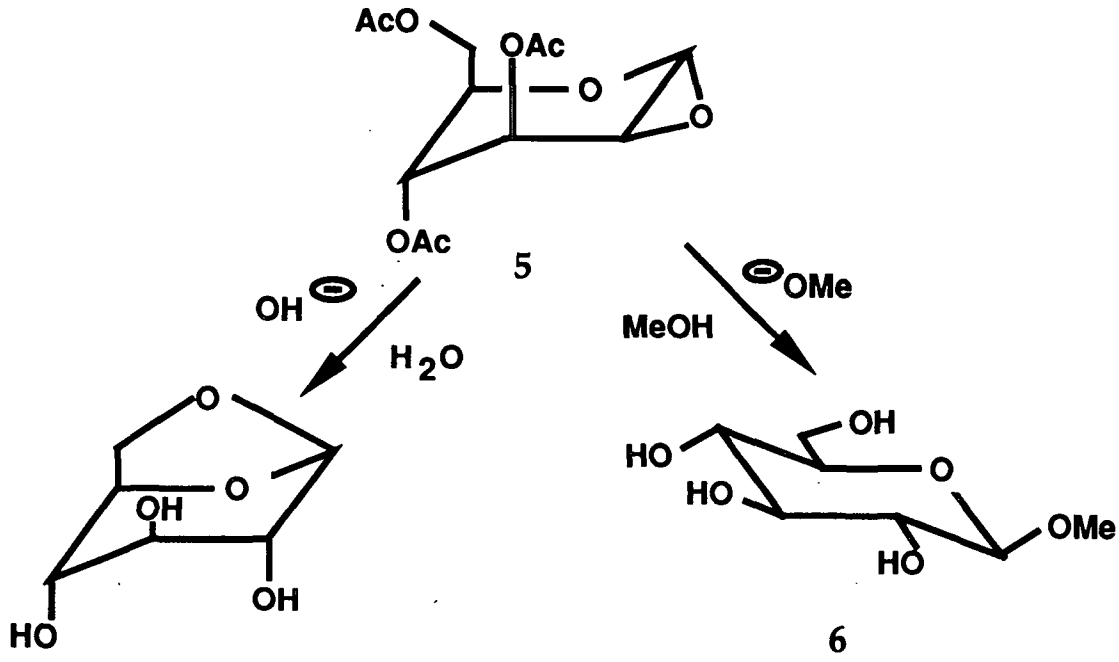

Figure 4. Brigl's anhydride (5) reactions with aqueous hydroxide[25] and methanolic sodium methoxide[26] solutions.

In aryl glycoside studies[22,27-29] in which the model could proceed by the $S_N$icB(2) pathway, researchers have proposed that other mechanisms also occur. McCloskey and Coleman[22] found that levoglucosan yield dropped from 88 to 60% when a nitro group was placed in the para position of the phenyl ring. They hypothesized that another mechanism was taking place along with the $S_N$icB(2) mechanism.

One possible mechanism is the unimolecular nucleophilic substitution (S_N1) pathway. As seen in Figure 5, the glucosyl-oxygen bond ruptures to form a glucosyl cation and an aryloxy anion. Hydroxide can then attack on the glucosyl cation to form glucose which degrades rapidly to acidic products under the reaction conditions.

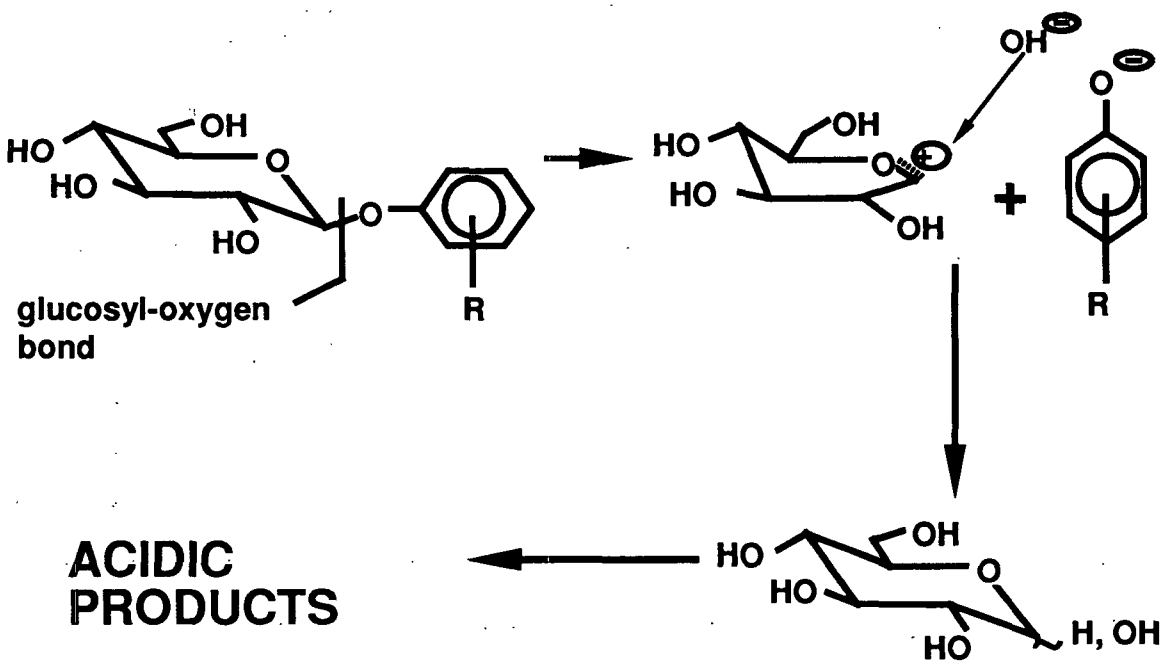

Figure 5. Proposed S_N1 mechanism for substituted phenyl β-D-glucopyranosides.

Another possible pathway, bimolecular nucleophilic substitution (S_N2), involves backside attack of hydroxide at C(1) with simultaneous release of an aryloxy anion (Figure 6). Again, glucose forms and rapidly degrades to acidic products in the alkaline conditions.

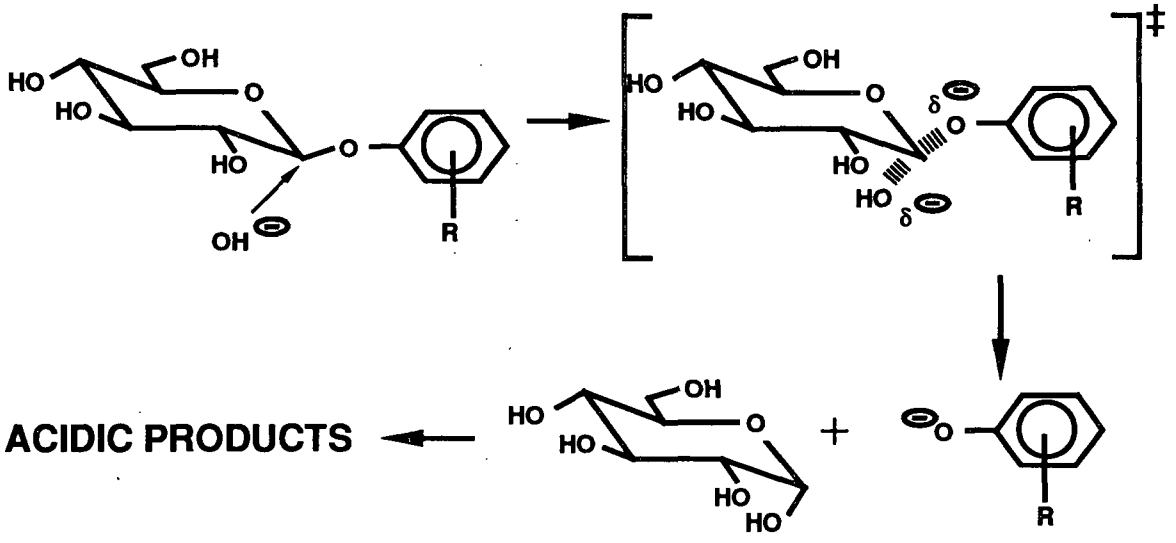

Figure 6. S_N2 mechanism for substituted phenyl β-D-glucopyranosides.

The previously presented mechanisms considered only glucosyl-oxygen cleavage (see Figure 5). In 1966, Gasman and Johnson[27] reported a large amount of the $S_N$icB(2) pathway and a minor amount of a bimolecular nucleophilic substitution on the aromatic ring (S_N2Ar) mechanism in the alkaline degradation of p-nitrophenyl β-D-galactopyranoside. The S_N2Ar pathway (Figure 7) in methanolic sodium methoxide begins with methoxide attack at C(1) of the phenyl ring.

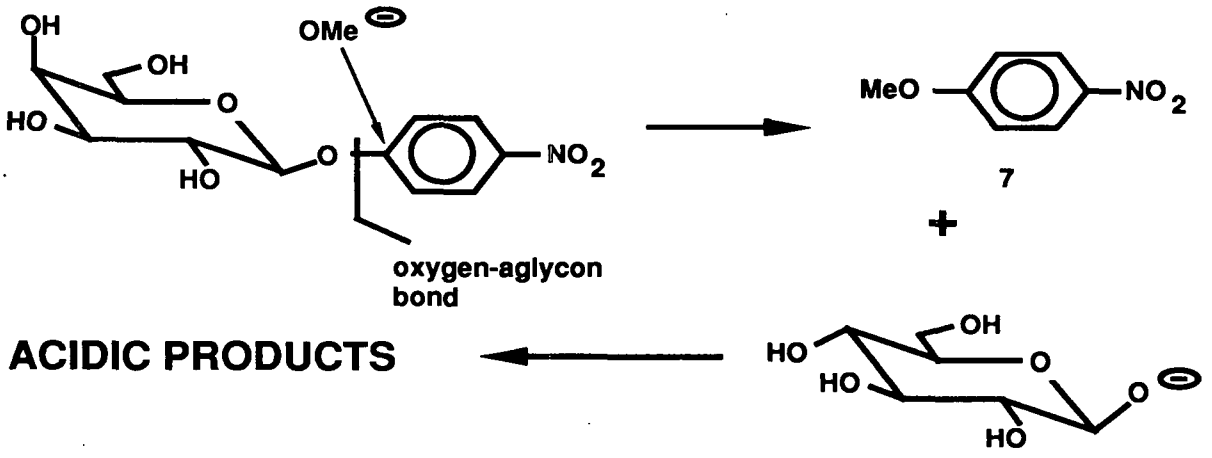

Figure 7. S_N2Ar mechanism for p-nitrophenyl β-D-glucopyranoside.[27]

Cleavage of the oxygen-aglycon bond produces a β-D-galactosyl anion and p-nitroanisole (7). The β-D-galactosyl anion would then degrade to acidic products. The use of a methanolic sodium methoxide was helpful in discovering this reaction pathway. In earlier aqueous studies this mechanism would have been undetected, because cleavage of either the glucosyl-oxygen or oxygen-aglycon bond would yield p-nitrophenol. In methanolic sodium methoxide, glucosyl-oxygen cleavage yielded p-nitrophenol, while oxygen-aglycon cleavage produced p-nitroanisole.

Lai, *et al.*[18] and Moody and Richards[30] reported on kinetic examinations of phenyl β-D-glucopyranoside degradation under alkaline reactions at 100°C. Their studies used ultraviolet (UV) spectroscopy to follow phenolate production to calculate the amount of phenyl β-D-glucopyranoside degraded. Lai, *et al.*[18] postulated a mixed $S_NicB(2)/S_N2$ mechanism for the phenyl β-D-glucopyranoside

degradation, while Moody and Richards[30] suggested that only the $S_N$icB(2) pathway occurred. These conclusions should only be considered preliminary results, because they used extrapolated 25°C and 70°C hydroxide activities to 100°C for their analyses and failed to provide any supporting evidence for their proposed mechanisms.

The aryl glycoside studies indicate that the $S_N$icB(2) pathway may be a major degradation mechanism. However, other reaction mechanisms, which include S_N1, S_N2, and S_N2Ar, may also be occurring.

Alkyl β-D-Glucoside and Cellodextrin Models

Alkyl glucoside and cellodextrin model compound studies[11-16] have provided the majority of the cellulosic random chain cleavage data. These studies have used mechanistic probes to attempt to quantify the amount of each mechanism present in the model system. Cleavage of both the glucosyl-oxygen and oxygen-aglycon bond were noted by the researchers. Only literature pertinent to glucosyl-oxygen bond cleavage, with emphasis on compounds that can proceed by the $S_N$icB(2) mechanism, will be examined here.

The $S_N$icB(2) mechanism has been postulated through levoglucosan production to be the most predominant reaction pathway present in selected model compound studies,[11-15] but alternative reaction pathways have also been reported in these systems. The S_N1 reaction mechanism has been indicated to be the major alternative reaction pathway.[11,14] The possible S_N2 mechanism was shown to be unlikely to occur, because upon addition of a strong nucleophile, which should increase the reaction rate constant, no effect was seen on the degradation rate constant of 1,5-anhydrocellobiitol.[15]

In 1986 Henderson[16] reported results associated with the degradation of 1,5-

anhydromannibiitol. For alkyl β-D glucoside and cellodextrin models, a new mechanism, intermolecular nucleophilic substitution with attack at the C(1) carbon by the conjugate base of the C(2)-OH with ring opening ($S_N$icB(2)-ro), was suggested for consideration. The proposed $S_N$icB(2)-ro mechanism for phenyl β-D-glucopyranoside (Figure 8) begins with formation of a C(2)-oxyanion. In contrast to the $S_N$icB(2) pathway, the ring flip is not necessary for C(2) oxyanion attack at C(1), because the C(2)-oxyanion and the pyranose ring oxygen are already in an anti periplanar configuration. The C(2)-oxyanion bridges to C(1) and displaces the pyranose ring oxygen as an oxyanion. The resultant oxyanion then degrades to products in the alkaline medium.

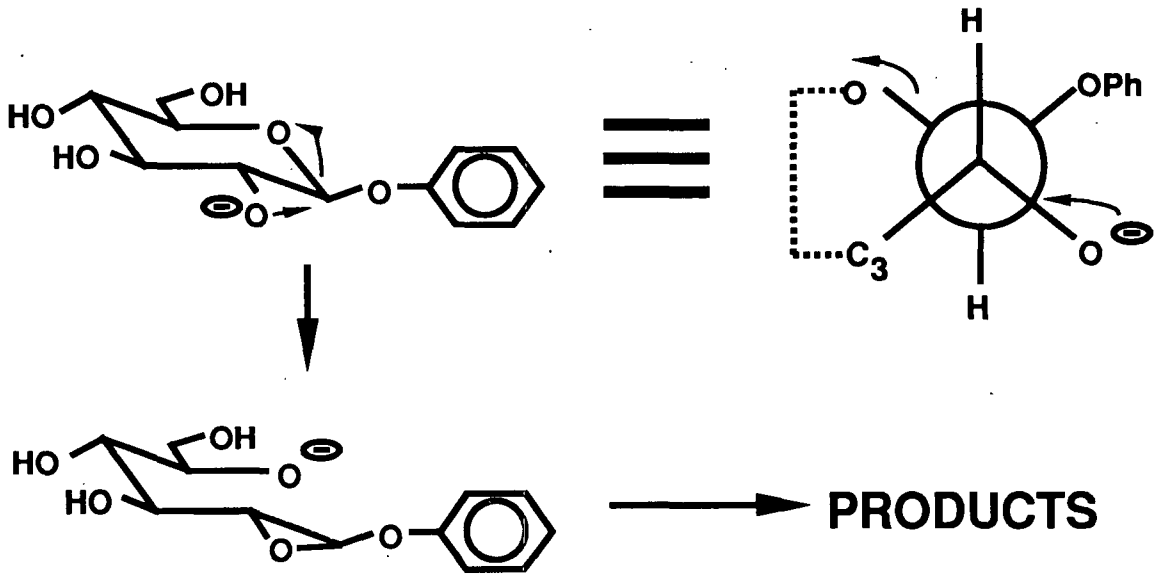

Figure 8. Proposed $S_N$icB(2)-ro mechanism for the C(2)-oxyanion of phenyl β-D-glucopyranoside and Newman projection of the C(2)-oxyanion.[16]

Throughout the alkyl β-D glucoside and cellodextrin studies,[12-15] researchers have used levoglucosan yield as an indicator of the extent of the $S_N$icB(2) mechanism. However, the levoglucosan yield varied considerably with changes in the model compound and the reaction conditions. The yield changed from 28% for methyl β-D-glucopyranoside[14] to 85% for 1,5-anhydro-2,3,6-tri-O-methyl-cellobiitol.[13] Also, the levoglucosan yield for the same model (Table 1) was observed to be dependent upon several factors; higher levoglucosan yields occurred at (1) lower temperatures, (2) lower sodium hydroxide concentrations, and (3) higher ionic strengths at the same sodium hydroxide level.[13]

Table 1. Levoglucosan yield from 1,5-anhydro-2,3,6-tri-O-methyl-cellobiitol under various conditions.[13]

NaOH, M	Salt, M	Temp., °C	% Levo[a]
2.5	-	151.4	76.1
2.5	-	171.4	59.0
2.5	-	182.7	51.6
0.5	-	170	67.1
0.5	2.0 NaOTs[b]	170	84.1

a. Levo is for levoglucosan.
b. NaOTs is sodium p-toluenesulfonate (sodium tosylate).

Blythe *et al.*[15] reported for 1,5-anhydrocellobiitol that the levoglucosan yield dropped from 41.9% for the sodium hydroxide case to 37.6% when sodium hydrosulfide (a strong nucleophile) was present, when compared at a constant

sodium hydroxide ion concentrations and ionic strengths. Since the reaction rate constants of these degradations appeared to be unaffected by addition of the strong nucleophile, Blythe *et al.*[15] proposed that hydrosulfide was acting after the rate-determining step, and like hydroxide (Figure 3), by favoring the formation of acidic products.

With these yield variations, it is difficult to determine the exact extent of the $S_N$icB(2) mechanism in those model systems and the implied behavior they may have on wood carbohydrates during chemical pulping. The behavior of phenyl β-D-glucopyranoside under pulping conditions might provide some useful information of the significance of levoglucosan formation and the $S_N$icB(2) mechanism.

In summary, cellulose random chain cleavage in an oxygen-free alkaline medium has been believed to occur by an $S_N$icB(2) mechanism. This conclusion has been reached by inference from model compounds, such as alkyl β-D-glucopyranosides, and not by direct experimental evidence. Originally, it was believed that alkyl β-D-glucopyranosides degraded by the $S_N$icB(2) reaction pathway as characterized by levoglucosan formation. This reaction was thought to be similar to that of phenyl β-D-glucopyranoside at 100°C. However, recent cellulose model compound studies, including work on methyl β-D-glucopyranoside, have shown that quantitative levoglucosan formation does not occur and have suggested the viability of alternative reaction pathways. These findings have indicated that the proposed $S_N$icB(2) reaction pathway of cellulose may be incorrect. From the previously presented work here, there is a need to determine whether the $S_N$icB(2) mechanism, as implied by Lindberg,[4] occurs at 170°C and what is the significance of the levoglucosan yield.

THESIS OBJECTIVE

The objective of this thesis is to examine the high temperature alkaline degradation of phenyl β-D-glucopyranoside. This study will examine the inference that the mechanism at 170°C is similar to the $S_N$icB(2) pathway at 100°C. The question of whether levoglucosan formation is a quantitative indicator of the $S_N$icB(2) reaction mechanism at 170°C will also be addressed. From the knowledge of the phenyl β-D-glucopyranoside degradation mechanism and significance of levoglucosan yield, it may be possible to reexamine data generated from earlier cellulose models and to relate that data to propose a viable cellulosic random chain cleavage mechanism.

EXPERIMENTAL APPROACH

Examination of the alkaline degradation of phenyl β-D-glucopyranoside is divided into three phases. These include the change from the UV techniques[18,30] previously used to a gas chromatographic (GC) technique, an 100°C degradation in 1M NaOH, and the mechanistic study at 170°C.

In earlier phenyl β-D-glucopyranoside studies, researchers[18,30]followed model degradation by phenolate production with UV spectroscopy. A GC analysis was, however, chosen to monitor the degradation in this study. The GC technique allows for direct measurement of all neutral species and circumvents the possibility of interference of UV chromophores that could be formed from the degradation of possible glucose products.[31] After developing the GC techniques, it was found that Kiryushina *et al.*[32,33] had briefly examined the alkaline degradation of phenyl β-D-glucopyranoside at 170°C by UV and GC techniques. Their work indicated that the

UV technique grossly underestimated the amount of reaction that occurred.

The second phase was a degradation performed at 100°C in 1M NaOH. This experiment examined the change in analysis technique, determined a degradation rate constant for comparison with literature values, and provided a value for levoglucosan yield to compare with high temperature degradation values.

The high temperature degradation of phenyl β-D-glucopyranoside was examined by six different mechanistic tools. These tools were to determine which of five possible mechanisms, S_NicB(2), S_Ni1, S_Ni2, S_Ni2Ar, and S_NicB(2)-ro, occurred. The mechanistic tools used in this thesis include: determination of point of bond cleavage, addition of a strong nucleophile, blocking the S_Ni reactive site, determination of apparent thermodynamic functions of activation, effect of increasing the reaction medium's ionic strength at constant sodium hydroxide concentration, and effect of hydroxide concentration at constant ionic strength. Also, levoglucosan yield was monitored throughout the study. The expected mechanistic tool response for each mechanism is given in Table 2. Although some mechanisms give the same response to a certain mechanistic tool, there is an unique set of responses for each mechanism.

The point of bond cleavage experiment uses ^{18}O incorporation into the product phenol to determine the extent of oxygen-aglycon bond cleavage. Phenyl β-D-glucopyranoside is degraded in an alkaline solution of a known concentration of ^{18}O labeled water. It is assumed that the ^{18}O content of the hydroxide ions equilibrates to the same concentration as the ^{18}O labeled water. For oxygen-aglycon bond cleavage via the S_Ni2Ar reaction pathway (Figure 9), the phenol product would be proportionally enriched with the ^{18}O label equivalent to the ^{18}O water

Table 2. Summary of reaction mechanisms and responses to mechanistic tools.

Reaction Mechanism	Bond cleavage	Nucleophilic effect	C(2)-OH blocking	$\Delta S^{\ddagger a}$	salt effect	Levo yield
S_N1	G-O[b]	none	none	++	+	?
$S_N$icB(2)	G-O	none	decrease	-	-	high
$S_N$icB(2)-ro	C_1-O_5	none	decrease	-	-	none
S_N2	G-O	increase	none	--	-	none
S_N2Ar	O-A	increase	none	--	-	none

a. Entropy of activation as predicted by March.[33] The + symbolism denotes a positive value, the - denotes a negative value, and the double symbol denotes a more negative or more positive value.

b. G-O is the glucosyl-oxygen bond, C_1-O_5 is the anomeric-pyranose ring oxygen bond, O-A is the oxygen-aglycon bond.

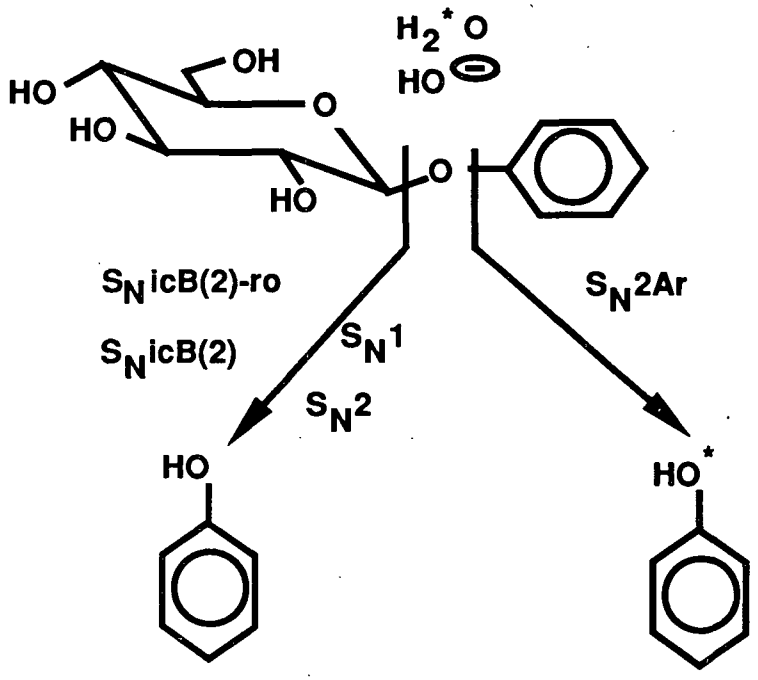

Figure 9. Distribution of enrichment (*) of ^{18}O in product phenol for the proposed mechanisms.

concentration in the reaction liquor. None of the other possible reaction mechanisms produce any ^{18}O enrichment of the phenol product. Therefore, the point of bond cleavage experiment indicates the extent of the S_N2Ar pathway.

The addition of a strong nucleophile to a reaction system provides a means to detect S_N2 mechanisms. March[33] stated that the addition of a strong nucleophile to an S_N2 mechanistic system caused an increase in the reaction rate constants, while for S_N1 pathways no change in rate constants would be seen. Sodium sulfide was chosen to provide the stronger nucleophile; under the conditions employed, sodium sulfide will effectively hydrolyze to sodium hydrosulfide and sodium hydroxide.[15] Blythe *et al.*[15] have shown for the S_N2 pathway in carbohydrate glucosyl-oxygen cleavage at 170°C that sodium hydrosulfide is a stronger nucleophile than sodium hydroxide. Maintenance of similar hydroxide ion concentrations and ionic strengths is important so that valid comparison of the nucleophilic effects can be made.

Formation of the C(2)-oxyanion is critical to the S_Ni type mechanisms (Figures 2 and 8). The addition of a non-ionizable alkyl blocking group on the C(2)-hydroxyl prevents the formation of the C(2)-oxyanion. This blockage stops any S_Ni type mechanism. Comparison of the reaction rate constants of blocked and unblocked C(2)-hydroxyl compounds is expected to show a large difference for S_Ni type pathways, while no difference in reaction rate constants should occur for S_N1 and S_N2 mechanisms. The extent of decrease in reaction rate constants associated with C(2) blocking for different $S_N$icB(2) reacting compounds has varied from 2400 times for p-nitrophenyl β-D-galactopyranoside[27] to 4 times for methyl β-D-glucopyranoside.[14] These differences in extent of the observed decrease can be associated with p-nitrophenyl β-D-galactopyranoside[27] degrading primarily by the

$S_N$icB(2) mechanism, while methyl β-D-glucopyranoside[16] exhibited several underlying reaction pathways. The C(2)-hydroxyl blocking study indicates both the presence of the S_Ni type mechanism and the extent of underlying reaction pathways.

The apparent thermodynamic functions of activation can be calculated for the phenyl β-D-glucopyranoside degradation from the reaction rate constants at various temperatures. The values obtained are enthalpy of transition ($\Delta H^{\ddagger}$) and entropy of transition ($\Delta S^{\ddagger}$). The $\Delta S^{\ddagger}$ value has generally been considered the most useful function for the comparison of mechanisms. The following generalization on the $\Delta S^{\ddagger}$ values were made from the discussion presented by March.[34] During the S_N1 transition state, two species are made from one molecule. The system entropy increases and a positive $\Delta S^{\ddagger}$ value results. For the S_N2 mechanism, two species come together in the transition state. This action decreases the degrees of freedom; therefore, the $\Delta S^{\ddagger}$ value will be negative. The degrees of freedom in S_Ni type mechanisms decrease due to the bridging of the C(2)-oxyanion to C(1). However, the $\Delta S^{\ddagger}$ value for the S_Ni mechanisms should be less negative than the S_N2 pathway's $\Delta S^{\ddagger}$ value, because less degrees of freedom are lost in the S_Ni transition state than in the S_N2 transition state. While earlier mechanistic tools indicate whether the S_Ni or S_N2 type mechanisms occur, the apparent thermodynamic functions of activation can reveal the presence of an S_N1 pathway.

An increase in the ionic strength in the reaction medium, while maintaining a constant hydroxide ion concentration, furnishes another technique to distinguish the reaction mechanisms. In the phenyl β-D-glucopyranoside S_N1 transition state, two charged species are produced from a neutral molecule. An increase in the medium's ionic strength for this type of S_N1 mechanism causes an increase in reaction rate constants.[33] The transition states of S_Ni and S_N2 type mechanisms

exhibit a dispersal of charge. For these reactions, an increase of the reaction medium's ionic strength should cause a small decrease in reaction rate constants.[34] The effect of increasing the ionic strength of the medium provides another method to indicate the presence of an S_N1 mechanism.

The final mechanistic tool used is the effect of hydroxide concentration at constant ionic strength. Lai and Ontto[18] suggested a modified version of this analysis procedure to distinguish between different mechanisms. In their work, the ionic strength was not maintained at a constant level. It was later proposed in the work of Brandon *et al.*[11] that the constraint of constant ionic strength was needed to provide a valid comparison of the experimental data. For the analysis, the reaction rate constants and hydroxide ion concentrations are plotted for derived linear relationships of observed reaction rate constants versus hydroxide ion concentrations for the various proposed mechanisms. Support for a particular mechanism is obtained when a linear plot results. However, with this analysis procedure many of the proposed mechanisms or combination of mechanisms can be made to give a linear relationship for the same functions of observed reaction rate constants versus hydroxide ion concentration.[12,14] Therefore, other mechanistic tools must be used to provide support for any conclusions made from this analysis procedure.

The levoglucosan yield provides another indication of the mechanisms present. It has been inferred that a near quantitative yield of levoglucosan should be obtained for an $S_N$icB(2) mechanism. Experimental evidence by Gilbert[12] has indicated that levoglucosan is not formed from the S_N2 pathway. In the S_N2Ar mechanism, levoglucosan should not be formed, because the glucosyl anion (Figure 7) should rapidly go to acidic products under the alkaline conditions. The S_N1

mechanism provides a pathway to produce levoglucosan. As seen in Figure 10, the S_N1 mechanism yields levoglucosan when the C(6) substituent attacks the C(1) cation as either hydroxyl or the oxyanion.

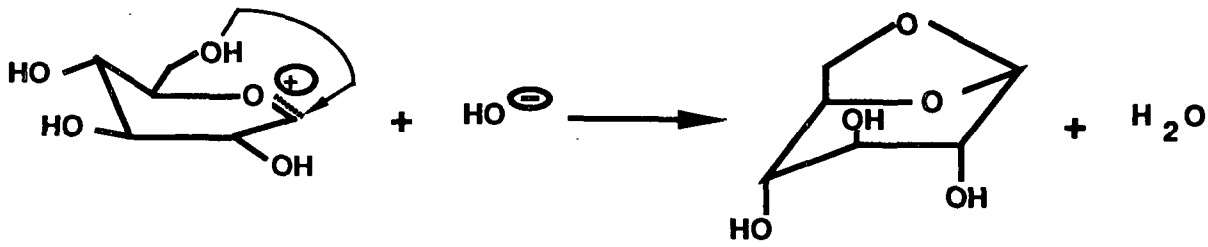

Figure 10. Possible formation route of levoglucosan during an S_N1 mechanism.

To date, the steps following ring opening in the $S_N$icB(2)-ro mechanism are unclear (Figure 8).[16] One can speculate (Figure 11) that for phenyl β-D-gluco-pyranoside, hydroxide ion attacks at C(1) to open the 1,2-epoxide and form a hemiacetal. The hydroxyl group of the hemiacetal would ionize to form an oxyanion; elimination would produce glucose. The glucose would rapidly form acidic products under the alkaline conditions. Therefore, levoglucosan formation should be absent in an $S_N$icB(2)-ro mechanism.

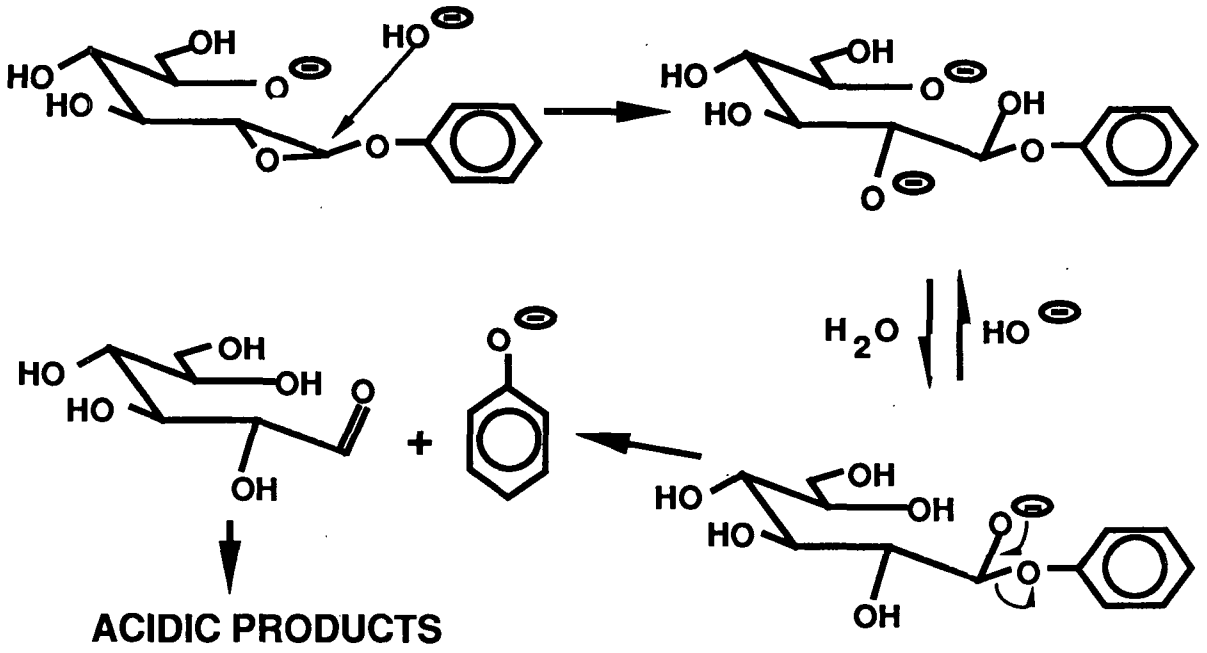

Figure 11. Possible degradation pathway after the presumed rate-determining step of $S_N$icB(2)-ro mechanism.[16]

RESULTS AND DISCUSSION

The results and discussion section is divided into three parts: kinetic studies, fast flow reactor, and alkaline degradation of phenyl β-D-glucopyranoside. The kinetic studies part illustrates the derivation of the kinetic equations used for analyzing the experimental data. The fast flow reactor portion presents the reactor choice and resulting problems encountered. The alkaline degradation part examines the 100°C degradation reaction and the mechanistic tools used in the high temperature degradation of phenyl β-D-glucopyranoside.

KINETIC STUDIES

Disappearance of Reactant

The fundamental rate expression at constant volume[35] for following the disappearance of reactant is:

$$\frac{dR}{dt} = -k R^{a} OH^{-b} \qquad (1)$$

where R = reactant concentration, mol L^{-1}

t = time, sec

k = specific rate constant, sec^{-1}

OH^- = hydroxide ion concentration, mol L^{-1}

a = constant

b = constant.

With a large ratio of hydroxide ion to reactant, the OH^- concentration is essentially constant and k becomes a pseudo-first-order rate constant. Dyferman and

Lindberg[25] determined that the exponent, a, was 1.0 for phenyl β-D-glucopyranoside degradations in an excess of hydroxide. These assumptions transform equation (1) to:

$$\frac{dR}{dt} = -k_r R \qquad (2)$$

where k_r = pseudo-first-order rate constant for the disappearance of reactant, sec^{-1}.

Integration yields:

$$R = R_o \exp(-k_r t) \qquad (3)$$

where R_o = initial reactant concentration, mol L^{-1}.

Rearrangement of equation (3) produces:

$$\ln R = \ln R_o - k_r t \qquad (4)$$

A least-squares regression analysis of ln R *vs.* t from equation (4) yields the pseudo-first-order rate constant for the disappearance of reactant. A representative plot of the experimental data from a phenyl β-D-glucopyranoside degradation at 171.6°C is given in Figure 12.

Formation of Stable Products

The oxygen-free alkaline degradation of phenyl β-D-glucopyranoside yields two neutral products, phenol and levoglucosan. In previous studies,[11,13-15] researchers have considered levoglucosan as an unstable product because it degraded faster than the reactant. The levoglucosan reaction rate constant data of

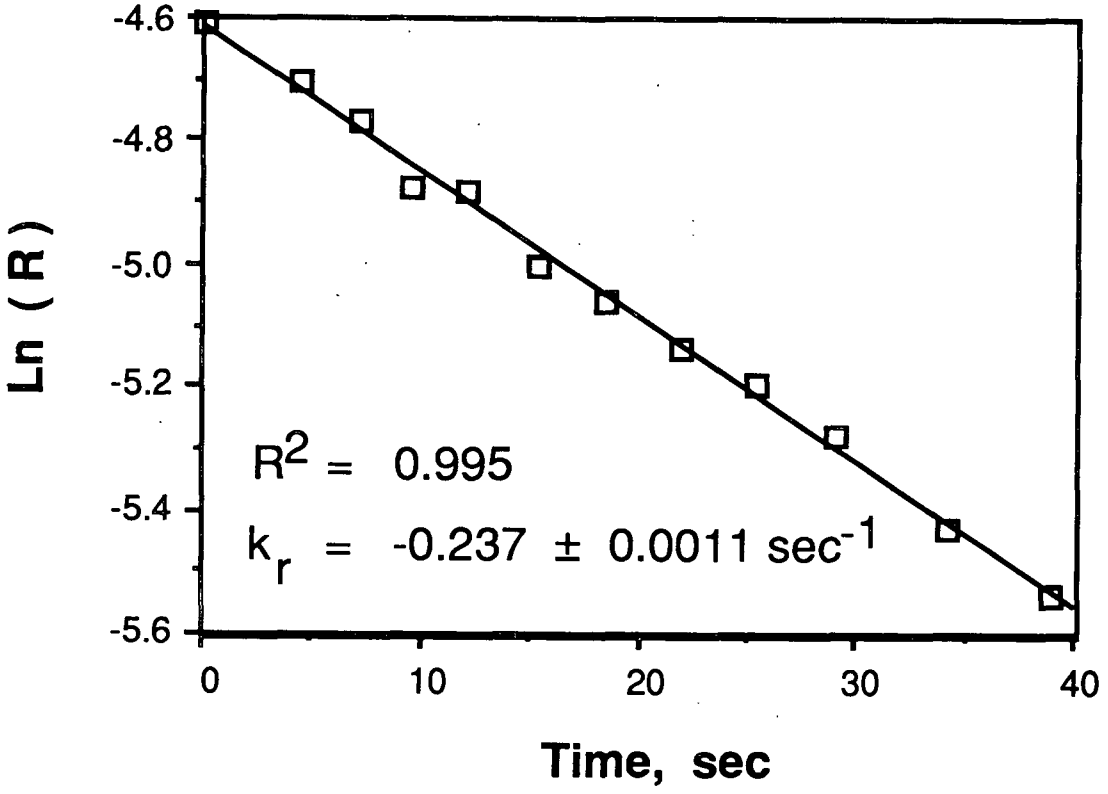

Figure 12. Disappearance of phenyl β-D-glucopyranoside in 1.0M NaOH and 1.5M NaCl at 171.6°C.

Gilbert[12] provided an indication that levoglucosan would degrade much slower than phenyl β-D-glucopyranoside. Therefore, levoglucosan was considered a stable product for the reaction times examined, and an analysis outlined in Appendix 1 confirmed this conclusion.

There were several possible reaction pathways that could independently occur during the degradation of phenyl β-D-glucopyranoside. Parallel reaction kinetics

were used to characterize this system. For the reaction,

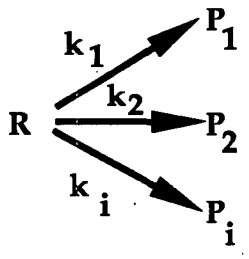

the general rate expression at constant volume[35] is:

$$\frac{dP_i}{dt} = k_i \, R^a \, OH^{-b} \qquad (5)$$

where P_i = concentration of product i, mol L^{-1}

k_i = specific reaction rate constant for i, sec^{-1}.

By use of pseudo-first-order assumptions in the kinetic description for the disappearance of reactant, equation (5) becomes:

$$\frac{dP_i}{dt} = k_i \, R \qquad (6)$$

where k_i = pseudo-first-order rate constant for appearance of product i, sec^{-1}.

Substitution of equation (3) into equation (6) yields:

$$\frac{dP_i}{dt} = k_i \, R_o \, \exp(-k_r \, t) \qquad (7)$$

Integration produces:

$$P_i = \left[\frac{-k_i R_o}{k_r}\right] \exp(-k_r t) + C \qquad (8)$$

where C = an integration constant.

At time $t = 0$, $P_i = P_{i,o}$, the integration constant becomes:

$$C = P_{i,o} + \left[\frac{k_i R_o}{k_r}\right] \qquad (9)$$

where $P_{i,o}$ = initial concentration of product i, mol L^{-1}.

Substitution of equation (9) into equation (8) and rearrangement produces:

$$(P_i - P_{i,o}) = k_i \left(\frac{R_o}{k_r}\right)\left[1 - \exp(-k_r t)\right] \qquad (10)$$

The pseudo-first-order rate constants for stable products were calculated from the linear regression analysis of $(P_i - P_{i,o})$ *vs.* $\{(R_o / k_r)[1 - \exp(-k_r t)]\}$ from equation (10). Figures 13 and 14, respectively, illustrate typical data plots of experimental data for phenol and levoglucosan formation from the alkaline degradation of phenyl β-D-glucopyranoside at 171.6°C.

Apparent Thermodynamic Functions of Activation

The apparent thermodynamic functions of activation for a chemical reaction can be calculated from temperature and reaction rate constant data. Since pseudo-first-order reaction kinetics are used, apparent thermodynamic functions of activation are obtained.

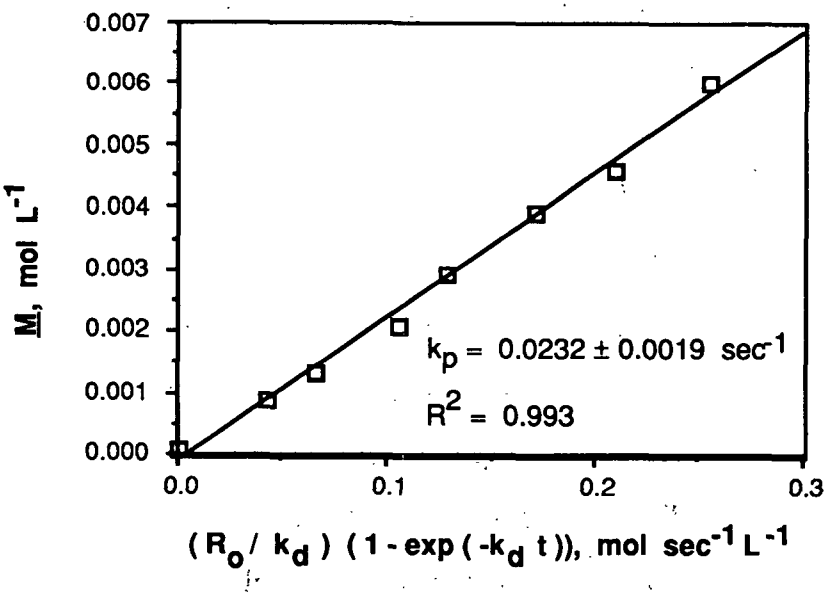

Figure 13. Appearance of phenol during the degradation of phenyl β-D-glucopyranoside in 1.0M NaOH and 1.5M NaCl at 171.6°C.

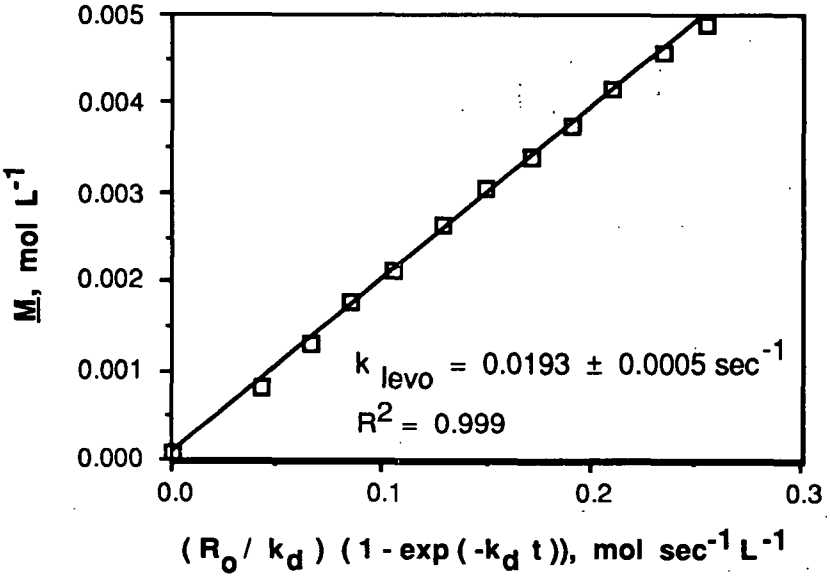

Figure 14. Appearance of levoglucosan during the degradation of phenyl β-D-glucopyranoside in 1.0M NaOH and 1.5M NaCl at 171.6°C.

The apparent rate constant for a constant volume system in transition state terms[34] is:

$$k_r = \left[\frac{k\ T}{h}\right] e^{\Delta S^{\ddagger}/R}\ e^{-\Delta H^{\ddagger}/RT} \qquad (11)$$

where k_r = apparent reaction rate constant, sec^{-1}

k = Boltzmann's constant, 1.38×10^{-6} erg $°K^{-1}$

T = absolute temperature, °K

h = Plank's constant, 6.625×10^{-27} erg sec

$\Delta S^{\ddagger}$ = entropy of activation, cal mol^{-1} $°K^{-1}$

$\Delta H^{\ddagger}$ = enthalpy of activation, cal mol^{-1}

R = the universal gas constant, 1.98 cal mol^{-1} $°K^{-1}$.

Rearrangement produces:

$$\ln\left(\frac{k_r}{T}\right) = \left[\ln\left(\frac{k}{h}\right) + \frac{\Delta S^{\ddagger}}{R}\right] - \frac{\Delta H^{\ddagger}}{RT} \qquad (12)$$

A least-squares regression analysis of equation (12) yields the apparent thermodynamic functions of activation ($\Delta H^{\ddagger}$ and $\Delta S^{\ddagger}$). Figure 15 presents the plot of $\ln(k_r/T)$ versus $1/RT$ from equation (12) obtained for the experimental data.

FAST FLOW REACTOR

Previous model compound studies have used Parr-like bomb reactors[11-16] or minibombs.[17-19] The projected reaction half life for phenyl β-D-glucopyranoside at 170°C under conditions considered for this study was calculated to be approximately 30 seconds. Bomb reactors would be unsuitable for such short reaction times,

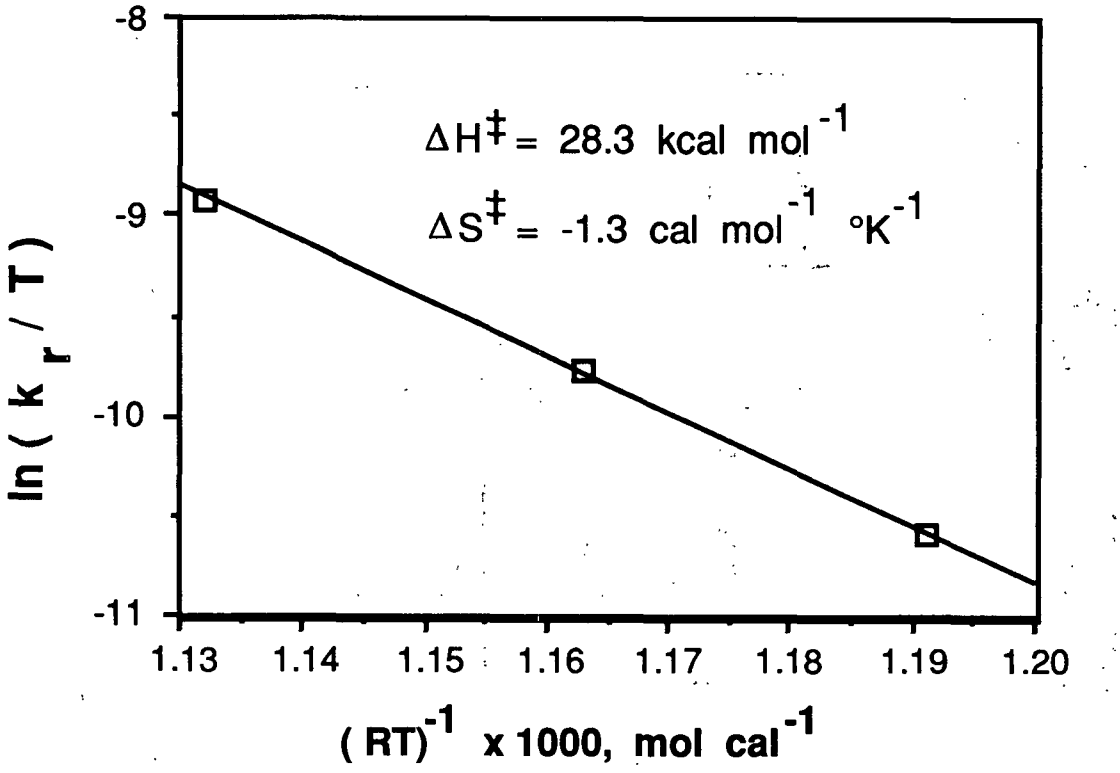

Figure 15. Temperature dependence of the reaction rate constants for phenyl β-D-glucopyranoside degradation in 2.5M NaOH

because warm-up and cool down times would be much greater than the projected reaction times. Therefore, the reactor chosen for this study was the fast flow reactor developed by Green *et al.*[36]

A brief description of the fast flow reactor (Figure 16) follows. Solutions were drawn into the syringes from their respective reservoirs by movement of the syringe pistons. Predetermined amounts of caustic and carbohydrate liquors were forced into their warm-up coils by movement of a piston and warmed to reaction

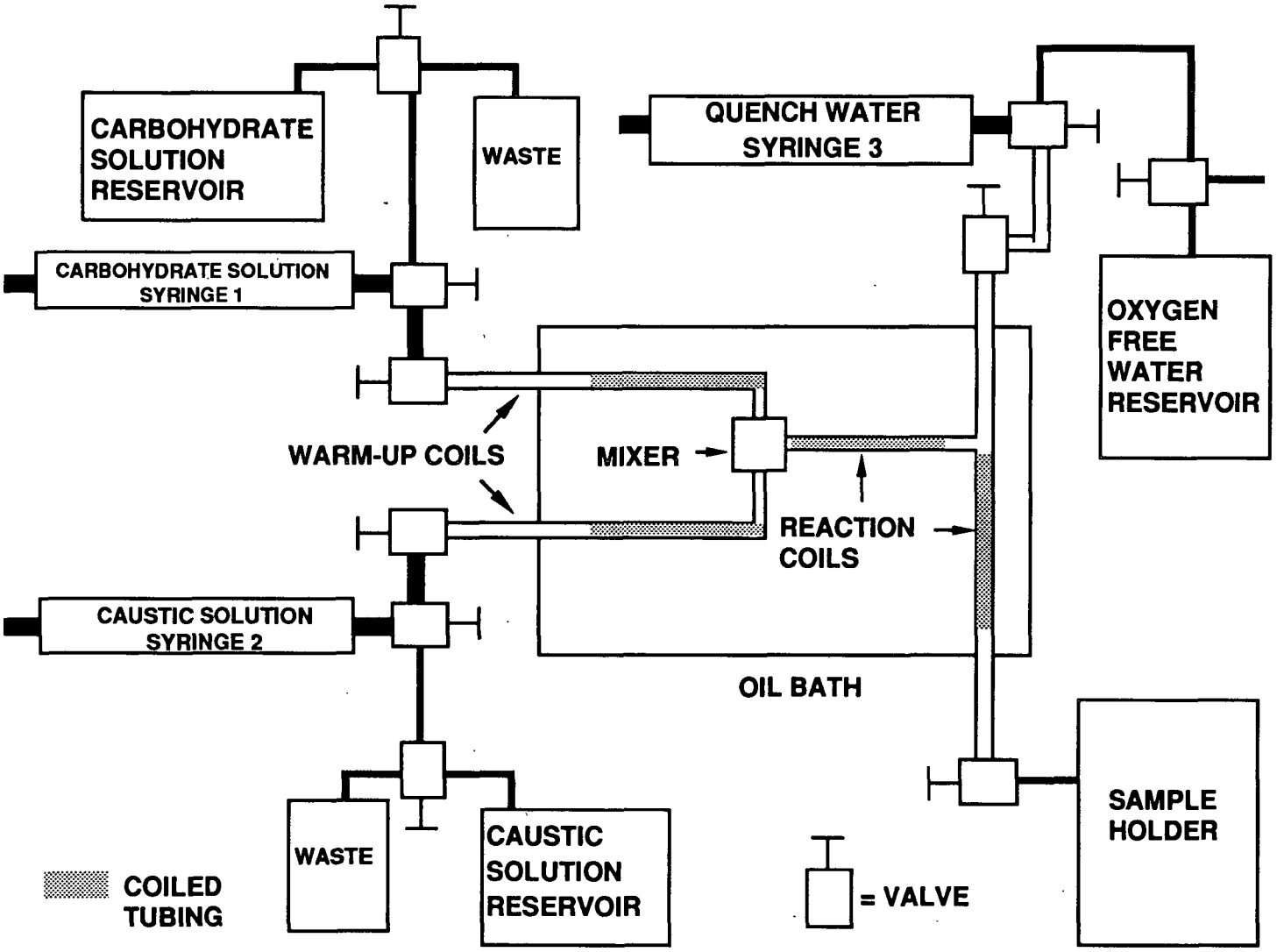

Figure 16. Fast flow reactor plumbing prior to degradation run.

temperature. In a preliminary experiment, phenyl β-D-glucopyranoside was shown to be stable in the aqueous medium at 170°C for periods longer than the typically employed warm-up period. These solutions were forced through the mixer by a second piston movement and reacted for a set time period. The reaction was stopped by forcing water, by the movement of the quench piston, to carry the reacted liquor into a sample holder where the all liquors were thermally quenched with iced water. Further discussion of the experimental procedure and apparatus are given, respectively, in the Experimental section and Appendix 2.

Prior to reactor use, a major overhaul of the reactor was performed. Hydraulic couplings were changed to safely use the hydraulic pump at rated pressures. Several hydraulic control valves were replaced, because they either leaked or were frozen in one position. The electronic system was rewired and simplified. An electronic stopwatch was used to time the reactions instead of the previously used recording oscilloscope.[36] Ram syringe bodies were rehoned to remove previous metal scoring. Several types of o-rings used between the syringe plunger and bodies were examined to determine what type would provide adequate sealing without metal scoring. The reaction mixer of Green *et al.*[36] was modified to prevent o-ring creep into the mixer holes. Further discussion of reactor redesign is given in Appendix 2.

ALKALINE DEGRADATION OF PHENYL β-D-GLUCOPYRANOSIDE

Low Temperature Degradation

Phenyl β-D-glucopyranoside was degraded in 1M sodium hydroxide at 100.6°C. The reaction rate constants were k_r (phenyl β-D-glucopyranoside pseudo-first-order degradation rate constant) of $5.02 \pm 0.04 \times 10^{-5}$ sec^{-1} and k_{levo} (levoglucosan pseudo-

first-order formation rate constant) of $4.43 \pm 0.03 \times 10^{-5}$ sec^{-1}. The phenyl β-D-glucopyranoside reaction rate constant was comparable to the degradation rate constant of 5.3×10^{-5} sec^{-1} which was calculated from the graphical data of Lai *et al.*[18] Conversion or yield from phenyl β-D-glucopyranoside to levoglucosan, as defined by the ratio of k_{levo} to k_r, was 0.88.

McCloskey and Coleman[22] reported a 88% gravimetric yield of levoglucosan from phenyl β-D-glucopyranoside for boiling 1.3N KOH. This data indicated that the calculated levoglucosan yield of 88% was consistent with the literature value. A comparison of kinetically derived levoglucosan yields can not be made, because Lai[18] and Moody and Richards[30] only examined phenyl β-D-glucopyranoside degradation by the production of phenolate and not by levoglucosan yields.

The 88% levoglucosan yield does not resolve the differences in the data interpretations of Lai[18] and Moody and Richards.[30] It can be speculated that the incomplete conversion of phenyl β-D-glucopyranoside to levoglucosan can come from one of three possibilities. Other mechanisms (i.e. S_N1, S_N2, etc.) could be present along with the $S_N$icB(2) pathway. Secondly, phenyl β-D-glucopyranoside reacts completely by the $S_N$icB(2) reaction mechanism, but the 1,2-anhydro-α-D-glucopyranose intermediate reacts with hydroxide ions to account for the remaining portion of the conversion. Or, a combination of these possibilities occur. Since the main thesis objective was to examine the high temperature alkaline degradation of phenyl β-D-glucopyranoside, no further work was performed at 100°C.

High Temperature Degradation

Point of Bond Cleavage

In the alkyl β-D-glucopyranoside,[12,14] p-nitrophenyl β-D-galactopyranoside,[27]

and cellodextrin[11,13,15,16] studies, researchers have shown that cleavage can occur at both the glucosyl-oxygen and the oxygen-aglycon bond. The amount of oxygen-aglycon cleavage ranged from 15% for p-nitrophenyl β-D-galactopyranoside[27] to 3-20% for 1,5-anhydro-2,3,6-tri-O-methyl-cellobiitol.[13]

Phenyl β-D-glucopyranoside was degraded at 171.6°C in 2.5M NaOH containing 8.6% ^{18}O labeled water. A modified data analysis program developed by Henderson[16] (Appendix 3) was used to calculate that 0.2% of the degradation reaction can be attributed to oxygen-aglycon cleavage. This value indicates that basically all cleavage occurs at the glucosyl-oxygen bond. The S_N2Ar mechanism, therefore, does not appear to be a viable degradation pathway for this model.

Effect of Addition of a Strong Nucleophile

The phenyl β-D-glucopyranoside reaction rate constants were 0.0345 sec^{-1} in caustic and 0.0349 sec^{-1} for the sodium sulfide addition (Table 3). A statistical test of these values indicated that they were significantly different. A 1.1% increase in the reaction rate constant was seen with sodium sulfide addition. This data was consistent with the increase seen by Blythe *et al.*[15] for the sodium sulfide addition to 1,5-anhydrocellobiitol. That model's degradation pathway was determined not to involve the S_N2 mechanism, so it appears that the S_N2 pathway is also unlikely to occur in the phenyl β-D-glucopyranoside degradation.

Effect of C(2)-OH Blocking With a Methyl Group

Blocking the C(2)-OH position provides a simple method to determine whether S_Ni type mechanisms occur and the relative importance of underlying pathways. Experimental data (Table 4) compares the blocked and unblocked analogs of phenyl β-D-glucopyranoside in 2.5M NaOH at 171.6°C. A reduction in reaction

Table 3. Effect of sodium sulfide on the degradation of phenyl β-D-glucopyranoside at 171.6°C.

M, NaOH	M, Na_2S	M, NaCl	k_r, x 10^2 sec^{-1}	k_{levo}, x 10^2 sec^{-1}	k_p[a], x 10^2 sec^{-1}
1.39	0.102	1.00	3.49 ± 0.18[b]	2.50 ± 0.12	3.24 ± 0.14
1.50	-	1.00	3.45 ± 0.19	2.92 ± 0.05	3.49 ± 0.11

a. k_p is the pseudo-first-order reaction rate constant for phenol formation.

b. All reaction rate constants will have the accompanying 95% confidence limits associated with the determination of the regression analysis.

Table 4. Degradation of phenyl β-D-glucopyranoside and phenyl 2-O-methyl-β-D-glucopyranoside in 2.5M NaOH at 171.6°C.

compound	k_r, x 10^2 sec^{-1}
phenyl β-D-glucopyranoside	5.99 ± 0.39
phenyl 2-O-methyl-β-D-glucopyranoside	0.00467 ± 0.00089

rate constants of 1300 times was evident. This reduction was consistent to the 2400 times reduction in reaction rate constants seen for p-nitrophenyl β-D-galacto-pyranoside.[27] It can be concluded that a S_Ni type mechanism is the dominant reaction pathway.

The large decrease in reaction rate constants with C(2) blocking also indicates the absence of an underlying S_N1 mechanism. A decrease in reaction rate constants

of 4 times, as seen for methyl β-D-glucopyranoside,[14] would have been expected when there are mixed $S_N$icB(2) and S_N1 mechanisms present. Therefore, the only remaining viable reaction mechanisms present for phenyl β-D-glucopyranoside alkaline degradation are the $S_N$icB(2) and $S_N$icB(2)-ro pathways.

Two neutral products were found in the phenyl 2-O-methyl-β-D-glucopyranoside (**8**) degradation (Figure 17). The Experimental section details isolation and identification of these compounds by nuclear magnetic resonance (NMR) and gas liquid chromatography/mass spectroscopy. One product, 1,6-anhydro-2-O-methyl-β-D-glucopyranose (**9**), was identified against an authentic standard.

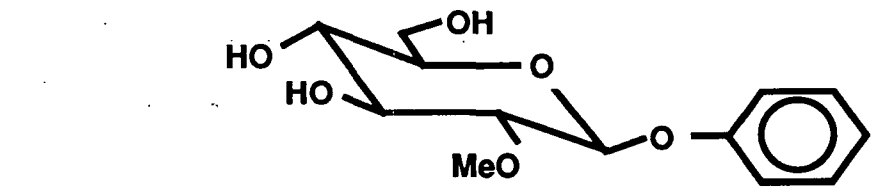

8

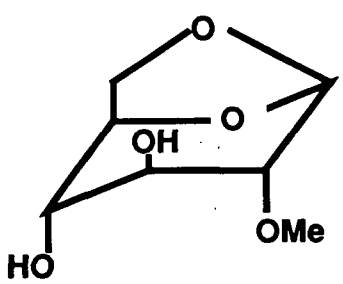

9

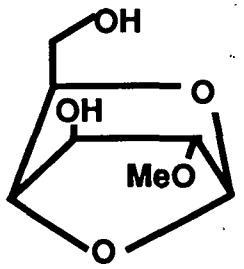

10

Figure 17. Compounds phenyl 2-O-methyl-β-D-glucopyranoside (**8**), 1,6-anhydro-2-O-methyl-β-D-glucopyranose (**9**), and 1,4-anhydro-2-O-methyl-α-D-glucopyranose (**10**).

The ^{1}H and ^{13}C NMR analyses of acetylated unknown product indicated: absence of the phenyl ring, the presence of one methoxyl and two acetate groups, and the presence of a low field ^{1}H signal (5.52 *ppm*). The two acetyl groups suggested the formation of an anhydro ring along with the pyranose ring. The low field signal suggested that the anhydro ring was at C(1);[37] the singlet suggested a rigid structure in which the C(1) and C(2) protons were 90° to each other.[38] A possible structure for this compound was 1,4-anhydro-2-O-methyl-α-D-glucopyranose (**10**) peracetate (**11**) (Figure 18). The C(1)-proton postulated for **11** and 1,4-anhydro-2,3-di-O-methyl-α-D-ribopyranose (**12**) are in very similar environments and would thus be expected to have similar ^{1}H NMR chemical shifts: C(1)-H in **11** is a singlet at 5.52 *ppm* and C(1)-H in **12** is a singlet at 5.52 *ppm*.[39] Also, **11** and 2,3,6-tri-O-acetyl-1,4-anhydro-α-D-glucopyranose[40] (**13**) have nearly identical C(5)-C(6) environments and show a great deal of similarities in the 3.9 to 4.8 *ppm* region of their ^{1}H NMR spectra. This NMR spectral data helps to confirm this compound assignment.

It is possible that 1,6-anhydro-2-O-methyl-β-D-glucopyranose may be a degradation product of 1,4-anhydro-2-O-methyl-α-D-glucopyranose; it has been postulated that 1,4-anhydro-α-D-mannopyranose degraded to 1,6-anhydro-β-D-mannopyranose by undetermined steps.[21]

Apparent Thermodynamic Functions of Activation

Previous analyses have indicated that S_N1, S_N2, and S_N2Ar mechanisms were unlikely to be degradative pathways. The apparent thermodynamic functions of activation should provide confirmation of these conclusions.

The apparent thermodynamic functions of activation were derived from phenyl β-D-glucopyranoside degradations at the temperatures of 149.6, 159.6, and

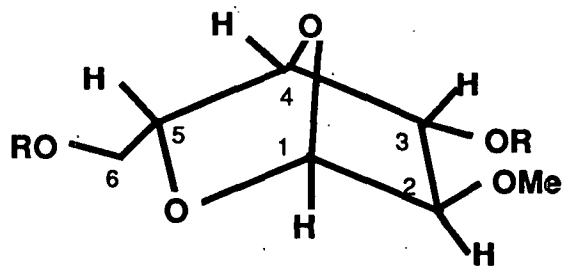

10 , R = H

11 , R = Ac

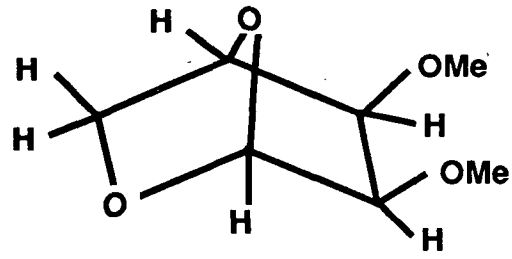

12

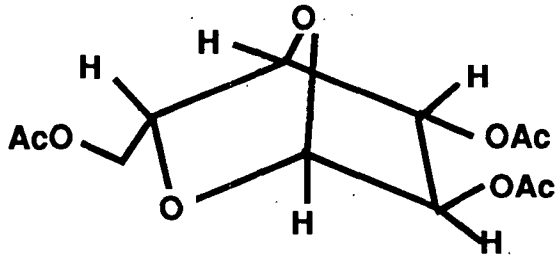

13

Figure 18. Compound analogs of 1,2-anhydro-α-D-glucopyranose (10).

171.6°C in 2.5M NaOH (Table 5). The apparent thermodynamic functions of activation as calculated from equation (12) were $\Delta H^{\ddagger}$ of 28.3 kcal mol^{-1} and $\Delta S^{\ddagger}$ of -1.3 cal mol^{-1} $°K^{-1}$.

Table 5. Effect of temperature on phenyl β-D-glucopyranoside degradation in 2.5M NaOH.

Temp., °C	k_r, x 10^2 sec^{-1}	k_{levo}, x 10^2 sec^{-1}	k_p, x 10^2 sec^{-1}
171.6	5.99 ± 0.39	4.71 ± 0.21	-
159.6	2.48 ± 0.01	2.02 ± 0.02	2.39 ± 0.06
149.6	1.07 ± 0.04	0.875 ± 0.020	1.07 ± 0.04

Values of $\Delta H^{\ddagger}$ and $\Delta S^{\ddagger}$ for selected model compounds degraded at 170°C in 2.5M NaOH are presented in Table 6. The $\Delta S^{\ddagger}$ value for phenyl β-D-glucopyranoside (-1.3 cal mol^{-1} $°K^{-1}$) is similar to those observed for presumed $S_N$icB(2) pathway models[12,13] and similar to the value for the $S_N$icB(2)-ro mechanism associated with cleavage of the C(1)-ring oxygen bond in 1,5-anhydromannobiitol.[18] The small difference between $\Delta S^{\ddagger}$ values of the S_Ni type pathways does not allow a distinction to be made as to which mechanism took place. However, it is apparent that an S_N1 mechanism, which has exhibited a large positive $\Delta S^{\ddagger}$ value, is unlikely to occur in the alkaline degradation of phenyl β-D-glucopyranoside.

Table 6. Thermodynamic data for phenyl β-D-glucopyranoside and selected model compounds.

model	proposed reaction mechanism	$\Delta H^{\ddagger}$, kcal mol^{-1}	$\Delta S^{\ddagger}$, cal mol^{-1} L^{-1}	ref
phenyl β-D-glucopyranoside	$S_N$icB(2)	28.3	-1.3	*
glucosyl-oxygen bond in 1,5-anhydromannobiitol	$S_N$icB(2)-ro	35.3	-4.3	16
1,6-anhydro-β-D-gluco-pyranose	$S_N$icB(2)	32.8	-3.8	12
glucosyl-oxygen bond in 1,5-anhydro-2,3,5-tri-O-methyl-cellobiitol	$S_N$icB(2)	35.5	-3.2	13
oxygen-aglycon in 1,5-anhydro-cellobiitol	S_N1	41.7	6.9	11
methyl α-D-glucopyranoside	S_N2	32.4	-13.6	12
glucosyl-oxygen bond in 1,5-anhydro-cellobiitol	mixed $S_N$icB(2) & S_N1	37.1	1.0	11

* Data generated in this thesis.

The 28.3 kcal mol^{-1} $\Delta H^{\ddagger}$ value for phenyl β-D-glucopyranoside was lower than the $\Delta H^{\ddagger}$ values for the other $S_N$icB(2) mechanistic models.[12,13] Differences in the $\Delta H^{\ddagger}$ value may be attributed to the fact that the phenoxy anion is a much better leaving group than those present in the other models. For the $S_N$icB(2)-ro mechanisms, the ring oxygen leaving groups of both 1,5-anhydromannobiitol and phenyl β-D-glucopyranoside contain similar substituents (*i.e.*, ring oxygen oxyanion and C(5) groups) and would be expected to exhibit similar $\Delta H^{\ddagger}$ values. The $\Delta H^{\ddagger}$ value for the $S_N$icB(2)-ro mechanism of phenyl β-D-glucopyranoside should be near the 35 kcal mol^{-1} associated with the $S_N$icB(2)-ro mechanism of 1,5-anhydro-mannobiitol.[16] The observed $\Delta H^{\ddagger}$ value of 28.3 ± 4.4 kcal mol^{-1} for phenyl β-D-glucopyranoside does not overlap the 90% confidence interval (the indicative ± error limits) of 35.3 ± 1.4 kcal mol^{-1} observed for the $S_N$icB(2)-ro mechanism, thus, indicating that the values are different and the $S_N$icB(2) pathway predominates. The width of the 90% confidence interval for the $\Delta H^{\ddagger}$ value of phenyl β-D-glucopyranoside is larger than that of 1,5-anhydromannobiitol, because the phenyl β-D-glucopyranoside value uses three data points while the other compound uses four data points. The lower $\Delta H^{\ddagger}$ value, as compared to the $\Delta H^{\ddagger}$ for the S_N1 mechanism, also indicates that the S_N1 mechanism is unlikely to have occurred.

Effect of Ionic Strength At Constant Hydroxide Concentration

A change in the ionic strength of the reaction medium by addition of a non-nucleophilic salt generally causes a predictable change in the reaction rate constants. Prior mechanistic tools have indicated that the predominant pathway for the alkaline degradation of phenyl β-D-glucopyranoside is the $S_N$icB(2) mechanism. Data obtained from this analysis should support this conclusion.

Before the salt effects were examined, a change in the salt used for altering the

ionic strength of the reaction medium was examined. This change was necessary, because the salt used in previous studies,[12-16] sodium tosylate, exhibits low solubility in alkali at room temperature and the insoluble salts could clog reactor parts. Sodium chloride was chosen as the replacement salt and was experimentally shown to be non-nucleophilic.

A fivefold change in ionic strength of the reaction medium with sodium chloride addition resulted in only a 2.5% decrease for the phenyl β-D-glucopyranoside reaction rate constant in 0.5M NaOH (Table 7). This decrease is much less than the 19% decrease (Table 8) seen for the presumed $S_N$icB(2) mechanistic model of levoglucosan.[14] This data was not unexpected, because the alkaline S_N2 degradation of methyl α-D-glucopyranoside at 170°C exhibited salt effects (Table 9) from -3.4% for NaCl to -25.2% for sodium tosylate.[12] Bunton and Robinson[41] have reported similar large differences in salt effects during the aqueous hydroxide S_N2 displacement of chloride in 2,4-dinitrochlorobenzene at 45°C. Sodium chloride decreased the reaction rate constants by 25%, sodium bromide by 35%, and sodium tosylate by 67%. From the trends seen, the salt effect from sodium chloride should be smaller than that derived from sodium tosylate. Therefore, the 2.5% decrease in reaction rate constants by the addition of NaCl would be consistent with an $S_N$icB(2) mechanism.

Table 7. Effect of NaCl addition on phenyl β-D-glucopyranoside degradation in 0.5M NaOH at 171.6°C.

M, NaOH	M, NaCl	k_r, x 10^2 sec^{-1}	k_{levo}, x 10^2 sec^{-1}
0.50	-	1.25 ± 0.06	1.05 ± 0.02
0.50	2.00	1.22 ± 0.04	1.03 ± 0.02

Table 8. Salt effect for phenyl β-D-glucopyranoside and selected model compounds at 170°C.

model	proposed reaction mechanism	salt effect, %	ref
phenyl β-D-glucopyranoside	$S_N$icB(2)	-2.5	*
1,6-anhydro-β-D-glucopyranose	$S_N$icB(2)	-19.0	12
oxygen-aglycon bond in 1,5-anhydro-cellobiitol	S_N1	64.0	11
methyl α-D-glucopyranoside	S_N2	-25.2	12
glucosyl-oxygen bond in 1,5-anhydro-mannobiitol	mixed S_N1 & $S_N$icB(2)-ro	11.0	16

* Data generated in this thesis.

Table 9. Effect of non-nucleophilic salt choice on salt effect for methyl α-D-glucopyranoside in 0.5M NaOH and 2.0M salt at 170°C.

salt	salt effect	ref
NaCl	-3.4	*
NaI	-14.8	12
NaOTs	-25.2	12

* Data generated in this thesis.

Effect of Varying the Hydroxide Concentration at Constant Ionic Strength

Since the $S_N$icB(2) reaction mechanism appears to be the only predominant degradation pathway still viable, the following data analysis can be used to provide further evidence for the presence of the $S_N$icB(2) mechanism.

For an $S_N$icB(2) pathway, the following equilibrium and reaction exist:

$$\underline{R} + OH^- \underset{}{\overset{K_e}{\rightleftharpoons}} \underline{R^-} + H_2O \qquad (13)$$

$$\underline{R^-} \xrightarrow{k} \underline{P} \qquad (14)$$

where $\underline{R}$ = glucoside

$\underline{R^-}$ = conjugate base of glucoside

$\underline{P}$ = product

K_e = equilibrium constant between the neutral glucoside and its conjugate base

k = reaction rate constant.

The rate expression at constant volume[35] for the product is:

$$\frac{dP}{dt} = k\,R^- \qquad (15)$$

where P = concentration of product, mol L^{-1}

t = time, sec

R^- = concentration of the glucoside conjugate base, mol L^{-1}.

K_e is derived by:

$$K_e = \frac{[R^-]}{[R]\ [OH^-]} \tag{16}$$

where R = concentration of glucoside, mol L^{-1}

OH^- = concentration of hydroxide ion, mol L^{-1}.

At anytime, R equals:

$$[R] = [R_o - R^- - P] \tag{17}$$

where R_o = initial glucoside concentration, mol L^{-1}.

Substitution of equation (17) into equation (16) yields:

$$K_e = \frac{[R^-]}{[R_o - R^- - P]\ [OH^-]} \tag{18}$$

Solving for R^- produces:

$$R^- = \frac{K_e\ [OH^-]}{1 + K_e\ [OH^-]}\ [R_o - P] \tag{19}$$

Substitution of equation (19) into equation (15) yields:

$$\frac{dP}{dt} = \frac{k\ K_e\ [OH^-]}{1 + K_e\ [OH^-]}\ [R_o - P] \tag{20}$$

The observed reaction rate constant (k_{obs}) is:

$$k_{obs} = \frac{k\ K_e\ [OH^-]}{1 + K_e\ [OH^-]} \tag{21}$$

Rearrangement yields:

$$\frac{1}{k_{obs}} = \frac{1}{K_e} + \frac{1}{k K_e [OH^-]} \qquad (22)$$

A plot obtained for the reciprocal of the observed reaction rate constant versus the reciprocal of hydroxide ion concentration should be linear for the presence of an $S_N$icB(2) pathway. The experimental data (Table 10) yielded a statistically linear plot (Figure 19). This provides further evidence for the presence of an $S_N$icB(2) mechanism. Similar parameters for observed reaction rate constants and hydroxide ion concentration can be made from other mechanisms; but since previous mechanistic tools suggest that only the $S_N$icB(2) pathway as a viable mechanism, these kinetic analyses were not examined.

Table 10. Effect of hydroxide ion concentration at constant ionic strength (2.5μ) for phenyl β-D-glucopyranoside degradations at 171.6°C.

M, NaOH	M, NaCl	k_r, x 10^2 sec^{-1}	k_{levo}, x 10^2 sec^{-1}	k_p, x 10^2 sec^{-1}
0.5	2.0	1.22 ± 0.04	1.03 ± 0.02	-
1.0	1.5	2.37 ± 0.11	1.93 ± 0.05	2.32 ± 0.19
1.5	1.0	3.45 ± 0.19	2.92 ± 0.05	3.49 ± 0.11
2.5	0.0	5.99 ± 0.39	4.71 ± 0.22	-

Formation of 1,6-Anhydro-β-D-glucopyranose and Phenol

Levoglucosan yield (Table 11) from the phenyl β-D-glucopyranoside degradations remained near the average value of 83% and, except for the sodium sulfide

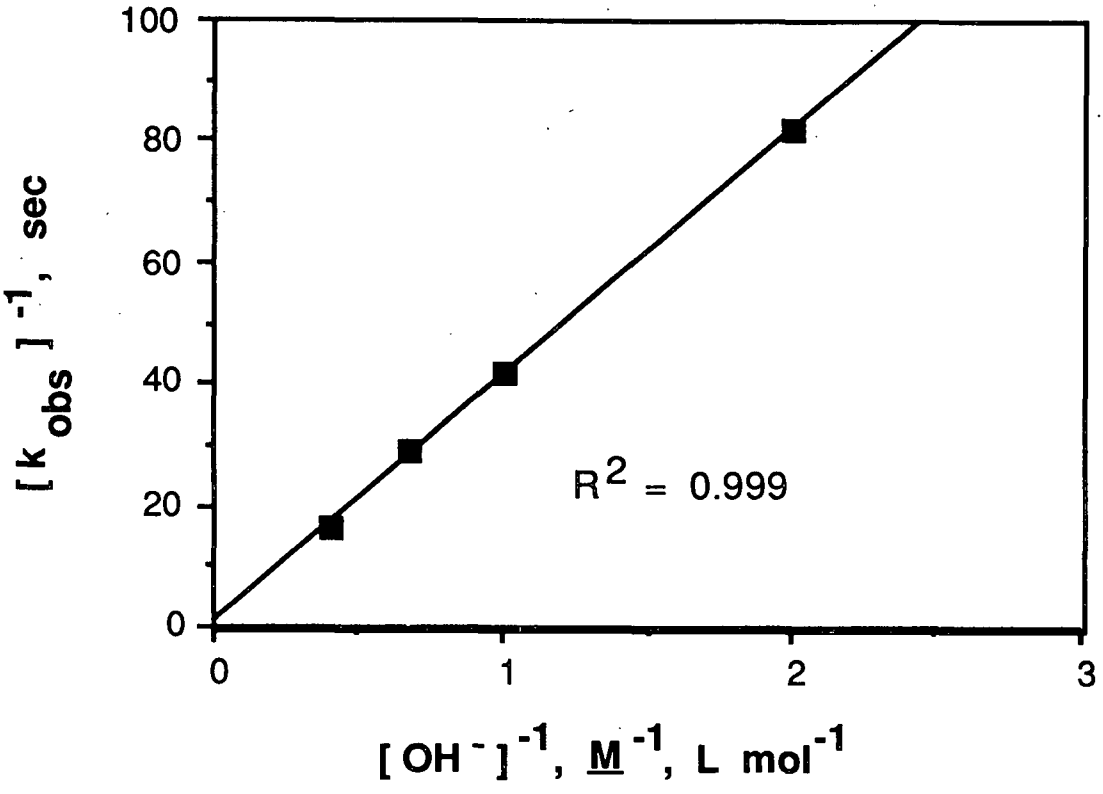

Figure 19. Relationship between the reciprocal hydroxide concentration and observed rate constants for phenyl β-D-glucopyranoside at constant ionic strength of 2.5μ and 171.6°C.

addition experiment, appeared independent of temperature, ionic strength, and hydroxide ion concentration at constant ionic strength. This behavior is different from what was seen by Wylie[13] where he noted that levoglucosan yield increased with decreasing temperature, increasing ionic strength, and decreasing hydroxide ion concentration. A probable cause for the difference in reaction behavior is that Wylie's model of 1,5-anhydro-2,3,6-tri-O-methyl-cellobiitol can undergo $S_N$icB(2)

Table 11. Levoglucosan (X_{levo})[a] and phenol (X_p)[b] conversions for phenyl β-D-glucopyranoside degradations.

Temp., °C	M, NaOH	M, NaCl	M, Na_2S	X_{levo}[c]	X_p
149.6	2.5	-	-	0.82	1.00
159.6	2.5	-	-	0.82	0.96
171.6	2.5	-	-	0.79	-
171.6	0.5	-	-	0.86	-
171.6	0.5	2.0	-	0.84	-
171.6	1.0	1.5	-	0.82	1.00
171.6	1.5	1.0	-	0.85	1.00
171.6	1.4	1.0	0.10	0.72	0.93

a. X_{levo} is the ratio of k_{levo} to k_r.

b. X_p is the ratio of k_p to k_r.

c. Each X_{levo} value has an accompanying 95% confidence interval of ±0.06, thus the X_{levo} confidence intervals overlap.

and S_N1 reactions along with oxygen-aglycon cleavage. Therefore, it would be difficult to determine how the different mechanistic tools would effect levoglucosan production from that model. In contrast, phenyl β-D-glucopyranoside appears to exhibit only the $S_N$icB(2) mechanism. Addition of hydrosulfide ion to the reaction system caused a 10% decrease in levoglucosan yield. From this data and the less than 100% yield of levoglucosan in the other degradations, C(1) of 1,2-anhydro-α-D-glucopyranose appears to be readily attacked by a variety of nucleophiles (Figure 20) that include OH^-, SH^-, and the C(6)-oxyanion.

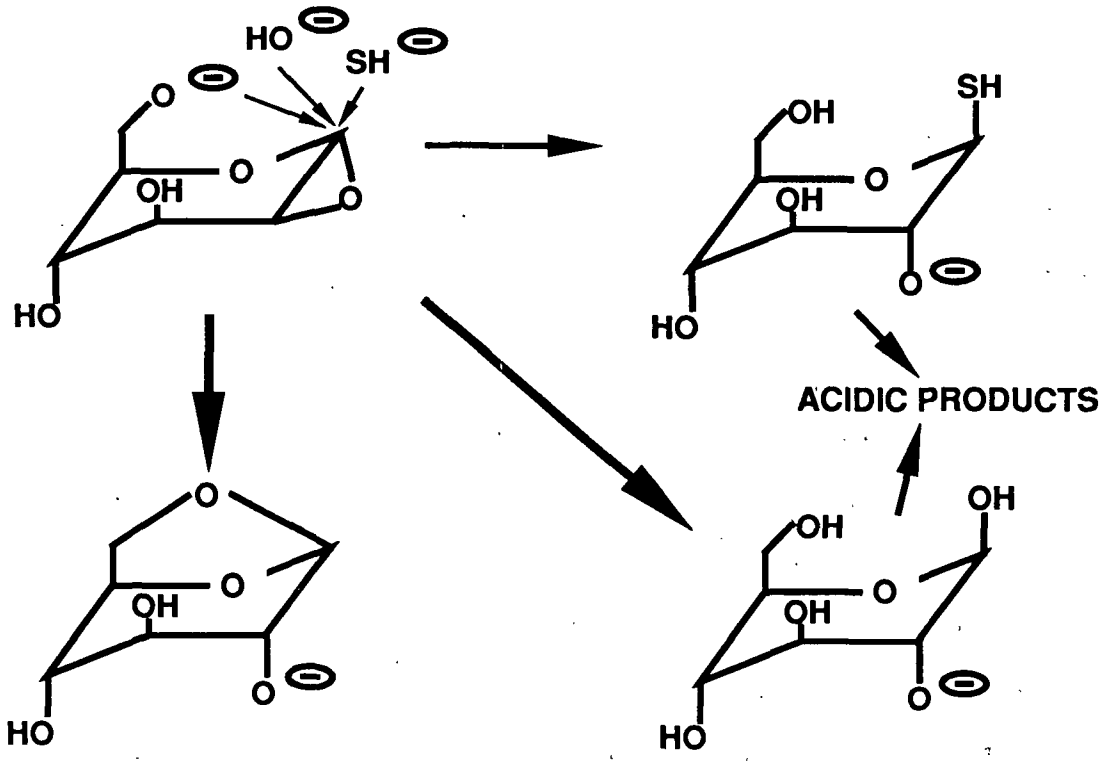

Figure 20. Nucleophilic attack at C(1) of 1,2-anhydro-α-D-glucopyranose.

The average levoglucosan yield of 83% at 170°C is only slightly lower than the 88% yield at 100°C. Thus, it may be concluded that the mechanisms are similar at the two different temperatures.

Levoglucosan data obtained in this thesis indicates that earlier model compounds studies, in which levoglucosan yield was used to indicate the extent of the $S_N$icB(2) mechanism, may have underestimated the amount of that pathway. As a first approximation of the amount of levoglucosan yield underestimated in previous caustic experiments, a 1.20 multiplying factor could be applied to original levoglucosan data. This multiplying factor represents the reciprocal of the 83%

levoglucosan yields found in this thesis. For example, Wylie[13] reported, for 1,5-anhydro-2,3,6-tri-O-methyl-cellobiitol (Table 1) in 0.5M NaOH, a 67% levoglucosan yield. The use of a multiplier factor changes that amount to 80%. Similarly, for the same model in 2.5M NaOH, the levoglucosan yield changes from 59 to 71%. The multiplying factor was not applied to sodium sulfide systems, because the reaction conditions used in this thesis did not match the conditions used by Blythe *et al.*[15]

Phenol formation was followed to provide another method to monitor phenyl β-D-glucopyranoside degradation. Phenol yield (Table 11), except for the sodium sulfide addition experiment, remained near 100%. The data presented in Table 11 includes only the experiments where 12 data points were used, because in earlier experiments where only six data points were used, the 95% confidence limits were greater than 10% or phenol formation exceeded 110%. This data illustrates that for every molecule of phenyl β-D-glucopyranoside degrading one molecule of phenol is produced. Therefore, the fraction of lost starting material not accounted for by levoglucosan formation should still represent a glucosyl-oxygen fragmentation process, such as those illustrated in Figure 20.

The cause of the 93% phenol yield in the sodium sulfide addition experiment was examined. It was found that no thiophenoxide product, which would indicate a possible S_N2Ar mechanism, was present and that phenol and it's internal standard were stable under the reaction conditions. Therefore, it is still undetermined why the phenol yield dropped with sodium sulfide addition.

IMPLICATIONS OF THIS STUDY ON PULPING SYSTEMS

Two implications arise from this study that may be applied to pulping systems. The first is that previous model compound data should be reexamined to

assess the amount of $S_N$icB(2) mechanism present. It may now be possible to determine the amounts of underlying pathways, and then apply that data to actual pulping systems. The second implication is that the use of salt effects as indicated from the model compound data may not directly correlate to pulping systems.

A problem encountered in earlier model compound systems was that cleavage on the glucosyl-oxygen bond could go by different pathways with only the $S_N$icB(2) mechanism giving a unique degradation product. From the data of this study, it may be possible to assign the portion of glucosyl-oxygen cleavage due to the $S_N$icB(2) mechanism in those models. With that pathway quantified, the remaining amounts of mechanisms may be determined. It would then be possible to apply the knowledge of the mechanisms present and their amounts from model systems to wood carbohydrates under pulping conditions. Therefore, mechanisms from model systems that would appear unlikely to occur in wood carbohydrates would not be applied to the real system, while viable mechanisms could be examined in further detail. For example, the model systems indicate that the $S_N$icB(2) pathway is a viable degradation route, but this mechanism would be unlikely to occur in cellulose random chain cleavage, because the necessary ring flip is not readily possible for cellulose. The model data does, however show that the S_N1 pathway may be an important mechanism for glucosyl-oxygen cleavage in wood carbohydrates.

The second implication comes from the salt effect data. In that data, it is evident that salt choice has a large impact on the salt effect. From earlier model work, the use of sodium tosylate exhibited a large effect on the reaction rate constants. If this data was applied to pulping systems, it would have been expected that, with the degradation mechanism known, changing the salts as indicated from

the salt effect data would have beneficial effects. However, as seen from this thesis, this may not be the case because salt effect is very much dependent on salt choice. Therefore, the earlier salt effect data can not be easily applied to pulping systems.

CONCLUSIONS

The 100°C alkaline degradation of phenyl β-D-glucopyranoside exhibited a reaction rate constant similar to that obtained by Lai, *et al.*[18] and a 88% levoglucosan yield consistent with the work of McCloskey and Coleman.[22] The high temperature (170°C) degradation of phenyl β-D-glucopyranoside was found to proceed by an $S_N$icB(2) pathway. This conclusion was made through the use of six mechanistic tools. No oxygen-aglycon cleavage was indicated by an ^{18}O labeled water study, thus the S_N2Ar mechanism appeared unlikely to occur. The lack of increase in reaction rate constants with addition of a strong nucleophile made the possible S_N2 pathway less plausible. The large difference (1300X) in reaction rate constants of C(2) blocked and unblocked anomers indicated an S_Ni type pathway. The $\Delta S^{\ddagger}$ value indicated an S_Ni type mechanism and not the possible S_N1 pathway. The $\Delta H^{\ddagger}$ value provided evidence that the $S_N$icB(2)-ro and S_N1 mechanisms were unlikely to have occurred. The salt effect and hydroxide ion concentration effect at constant ionic strength were found to be consistent with an $S_N$icB(2) mechanism. Finally, the levoglucosan yield of approximately 82% also indicated a large amount of $S_N$icB(2) pathway.

Sodium sulfide addition was not found to affect the phenyl β-D-glucopyranoside degradation rate constant, but did decrease the levoglucosan yield. The 72% levoglucosan yield in the Na_2S case and the 82% yields observed in the other runs indicates that the degradation of 1,2-anhydro-α-D-glucopyranose, a key intermediate in the $S_N$icB(2) reaction, was greatly influenced by the presence of nucleophiles (OH^- and SH^-) in the reaction system.

The experimental evidence supports the conclusion that phenyl β-D-glucopyranoside reacts similarly at 100°C and 170°C. From the observed levoglucosan

yields from the 170°C phenyl β-D-glucopyranoside degradation at 170°C and assuming the reaction is by a pure $S_N$icB(2) mechanism, it is now possible to recalculate the amount of the $S_N$icB(2) mechanism occurring in earlier carbohydrate model studies. For example, a multiplying factor of 1.20 (for caustic reactions) could be applied to those model systems to obtain the projected amount of the $S_N$icB(2) pathway. Knowledge of the percentage of the $S_N$icB(2) mechanism in those earlier studied systems would be useful in calculating the amount of other mechanisms present, because the earlier models exhibited multiple degradation pathways that produced non-unique degradation products. The calculation of the mechanisms present in the carbohydrate models could then be applied to pulping systems and predications of changes to lessen the impact of random chain cleavage in cellulose could then be made.

EXPERIMENTAL

GENERAL ANALYTICAL PROCEDURES

Melting points were determined on a Thomas Hoover capillary melting point apparatus calibrated against a standard thermometer and known compounds. Optical rotations were performed on a Perkin-Elmer 141 recording polarimeter at room temperature. Thin layer chromatography (TLC) was performed on microscope slides coated with silica gel (Merck Kielselgel D-5). Eluents are described in detail where TLC was used. Compounds were detected by spraying with concentrated sulfuric acid in methanol (1:4, v/v) followed by charring. Elemental analyses were performed by Midwest Microlab, LTD (Indianapolis, IN 46256).

Nuclear magnetic resonance (NMR) spectra were recorded on a Jeol FX-100 spectrometer. Samples were dissolved in deuterated dimethyl sulfoxide with tetramethylsilane as an internal standard. Microsample NMR was performed by Spectral Data Services (818 Pioneer, Champaign, IL 61820).

Sodium sulfide concentrations were measured by titration with 0.1M mercuric chloride by an Orion silver/silver sulfide specific ion electrode and an Orion 901 ionanalyzer.[42] Samples were titrated to an endpoint of -450 to -400 mV.[42] Liquor active alkali was determined by titration with 1.0M HCl in the presence of formaldehyde to a phenolphthalein endpoint. The sodium hydroxide concentration was calculated by subtraction of the sodium sulfide concentration from the active alkali.[43]

Gas liquid chromatography (GLC) was performed on a Hewlett-Packard 5890 instrument utilizing a flame ionization detector and interfaced to a Hewlett-Packard 3392A integrator. Helium was used as the carrier gas at a flow rate of 30 mL min^{-1}.

An OV-1 column on Supelcoport (100-120 mesh) in glass tubing (6 ft x 2 mm) rigged for on-column injection was used for GC analyses. The following conditions were used:

A Injector, 275°C; detector, 300°C; and column, 130°C, for 1 minute, and 7°C min^{-1} to 230°C.

B Injector, 275°C; detector, 300°C; and column, 60°C, for 1 minute, and 7°C min^{-1} to 110°C, and hold at 110°C for one minute.

For quantitative GLC analyses, various internal standards were used. Molar response factors were determined by subjecting authentic samples, in molar ratios expected to be encountered, to the appropriate analysis procedure. These factors (Table 12) were averaged from the values obtained from equation (23):

$$F_X = \frac{A_{IS} M_X w_X \rho_{IS}}{A_X M_{IS} w_{IS} \rho_X} \qquad (23)$$

where
- M = molarity of compound, mol L^{-1}
- A = peak area of compound
- w = weight of sample used, g
- ρ = density of sample used, g mL^{-1}
- X = compound X
- IS = internal standard.

Gas liquid chromatography/mass spectroscopy (GC/MS) was performed on a Hewlett-Packard 5895 system. The ^{18}O incorporated phenol was determined by electron impact (EI) mass spectroscopy on an OV-17 column. Operating conditions

Table 12. Gas chromatographic response factors.

Condition	Compound	Response Factor
A	levoglucosan	1.31[a]
A	phenyl β-D-glucopyranoside	0.67[a]
A	phenyl 2-O-methyl-β-D-glucopyranoside	0.70[a]
B	phenol	1.59[b]

a. As acetate derivative, calculated relative to the acetate derivative of methyl α-D-glucopyranoside (response factor = 1.00).

b. As methyl ether derivative, calculated relative to the methyl ether derivative of 4-isopropyl phenol (response factor = 1.00).

of the column were: start at 60°C and program at 7°C min^{-1} to 300°C. The ^{18}O enriched liquor was analyzed by EI on Porapak Q under the isothermal conditions of 100°C. All other samples were analyzed on an OV-1 column by EI with column conditions starting at 130°C and programming at 7°C min^{-1} to 300°C.

SOLUTIONS, REAGENTS, AND CATALYSTS

Anhydrous Methanol

Magnesium turnings (5 g) were covered with methanol (reagent grade, 1L) and iodine (0.1 g) was added.[44] After the reaction subsided, the mixture was refluxed for three hours and then fractionally distilled. The first 100 mL was discarded. The next 700 mL was collected and stored under nitrogen in tightly sealed bottles.

Acetic Anhydride

Acetic anhydride (reagent grade, 1.4 L) was fractionally distilled.[44] The first 150 mL was discarded, and the next 1 L was collected and stored under nitrogen in dark bottles.

Hydrogen Bromide in Glacial Acetic Acid

Hydrogen bromide in glacial acetic acid (32.9%, w/w) was obtained from Henderson.[16]

Methyl Iodide

Methyl iodide[45] (99%, 150 mL) was purified by short path distillation.[44] The first 40 mL was discarded. The next 70 mL was collected, stored over copper wire in a dark bottle, and refrigerated.

Oxygen-free Water

Distilled water (1.8 L) was boiled until the volume was reduced to 1.4 L. An 1 L bottle was rinsed with the heated water. The bottle was filled with the remaining water and purged with oxygen-free nitrogen while cooling in an ice bath. When the water was cool, the bottle was stoppered and sealed.

Piperidine

Piperidine[45] (98%, 580 mL) was fractionally distilled.[44] The first 100 mL was discarded, and the next 350 ml was collected and stored under nitrogen in a dark bottle.

Potassium Acid Phthalate

Potassium acid phthalate (reagent grade) was dried for four hours at 105°C and stored under vacuum prior to use.

Pyridine

Pyridine (reagent grade, 1.5 L) was refluxed over potassium hydroxide (300 g) for four hours and fractionally distilled.[44] The first 150 mL was discarded. The next 1 L was collected and stored under nitrogen in dark bottles.

Silver Oxide[46]

Silver nitrate (99.9%, 45 g) was dissolved in distilled water (450 mL) and heated to 70°C with constant stirring and exclusion of light. Sodium hydroxide (8.8 g) was dissolved in distilled water (235 mL) and heated to 70°C. The heated solutions were combined and allowed to cool to room temperature with constant stirring and exclusion of light. The resultant dirty brown precipitate was filtered and washed with warm distilled water (5 x 600 mL) and with acetone (4 x 150 mL). The solid was dried under vacuum at 50°C with exclusion of light. The sample (24.6 g, 96%) was stored in a foil lined bottle.

Sodium Chloride

Sodium chloride (reagent grade) was dried at 105°C for four hours and stored under vacuum prior to use.

Sodium Methoxide Solution

Sodium metal (1.15 g) was added to anhydrous methanol (100 mL). The 0.5M solution was stored under nitrogen in a tightly sealed bottle.

Stock Mercuric Chloride Solution

Mercuric chloride (reagent grade, 27.152 g) was dissolved in hot water (200 mL). The solution was diluted with water to 1 L to prepare a 0.1M stock solution.

Stock Sodium Hydroxide Solution

Sodium hydroxide (reagent grade, 500 g) was slowly added to distilled water (500 g) and stirred. Upon cooling, the solution was stored under nitrogen in a tightly sealed polyethylene bottle. Solution density was determined by filling tared 10 mL volumetric flasks. The solution concentration was determined by taking a known solution weight (~17.8 g), diluting to 100 mL, and titrating against potassium acid phthalate to a phenolphthalein endpoint.

Stock Sodium Sulfide Solution

Under nitrogen, sodium sulfide nonahydrate was washed with deoxygenated water in a buchner funnel until the crystals and filtrate were colorless. Crystals (100 g) were dissolved in oxygen-free water (400 mL). The solution was stored under nitrogen in a tightly sealed polyethylene bottle.

The stock sodium sulfide concentration was measured by titrating the solution (4 mL) with 0.1M mercuric chloride.[42] The density of the stock solution was determined by filling tared 10 mL volumetric flasks.

SYNTHESIS OF COMPOUNDS

1,6-Anhydro-β-D-glucopyranose

A sample of 1,6-anhydro-β-D-glucopyranose was supplied by L. R. Schroeder. The material was recrystallized from absolute ethanol: m.p. 179-180°C [Lit.[47]: 178-180°C].

Phenyl β-D-Glucopyranoside

Phenyl β-D-glucopyranoside[48] (10 g) was dissolved in 0.1M NaOH (100 mL) and heated at 45°C for two hours with constant stirring. The solution was diluted to

350 mL with distilled water and deionized with Amberlite MB-3 (H^+, OH^-) ion exchange resin (40 mL). The slurry was filtered through a coarse sintered glass filter funnel and the resin was washed with water (4 x 250 mL). The filtrates were concentrated *in vacuo* to a white crystalline solid. Recrystallization (2x) from water yielded white needles (5.1 g, 51%): m.p. 173.6-174.5°C, $[\alpha]_D$ -70.25 (c 1.519, water) [Lit.[49]: m.p. 174-175°C, $[\alpha]_D$ -71.0 (c 3.915, water)].

Methyl α-D-Glucopyranoside

Methyl α-D-glucopyranoside[50] (25 g) was dissolved in 1.25M NaOH (50 mL) and stirred at 80°C for four hours under nitrogen. The resultant yellow solution was diluted with 100 mL of distilled water and deionized with Amberlite MB-3 (H^+, OH^-) ion exchange resin (180 mL). The slurry was filtered through a coarse sintered glass filter funnel and the resin was washed with distilled water (4 x 200 mL). The colorless filtrates were combined and concentrated *in vacuo* to a white crystalline solid. Recrystallization (2x) from ethanol yielded white rod-life crystals (18.86 g, 75%): m.p. 166.5-167.5°C, $[\alpha]_D$ 160.1 (c 1.484, water) [Lit.[14]: m.p. 167-168°C, $[\alpha]_D$ 159.0 (c 2.0, water)].

N-(3,4,6-Tri-O-acetyl-D-glucosyl)-piperidine[51]

Piperidine (77 mL, 66.3 g) was placed in a 250 mL three necked, round bottom flask which was equipped with an overhead mechanical stirrer and a thermometer. β-D-glucose pentaacetate[45] (100 g) was added to the flask at the fastest possible rate that allowed for adequate mixing. The reaction temperature was maintained at 25 ± 5°C with an ice bath. Crystals formed within 15 minutes of the last addition of the sugar, and the slurry was stirred an additional 45 minutes. The resultant viscous cream colored slurry was cooled to 5°C. Cold ethyl ether (75 mL) was added to the slurry and thoroughly mixed in. The resultant precipitate was filtered off, washed

with cold ethyl ether (4 x 50 mL), and dried under vacuum. The dried crystal were slurried in absolute ethanol (100 mL). The solid was filtered off, washed with cold absolute ethanol (5 x 100 mL) and with cold ethyl ether (3 x 50 mL). The solid was dried under vacuum and ground to form white crystals (29.0 g, 27.3%): m.p. 123-124°C (decomp.) [Lit.[51]: m.p. 125°C (decomp.)].

N-(2-O-Methyl-3,4,6-tri-O-acetyl-D-glucosyl)-piperidine[51]

N-(3,4,6-tri-O-acetyl-D-glucosyl)-piperidine (34.3 g) was slurried in ethyl acetate (95 mL) and methyl iodide (45 mL, 109 g) for 20 minutes. Silver oxide (24 g) was added proportionwise to the slurry over a 30 minute period. Stirring was continued until the reaction was judged complete as indicated by TLC (benzene:methanol, 7:1, v/v). The slurry was filtered, and the filter cake was washed with ethyl acetate (3 x 50 mL). The filtrates were combined, decolorized with activated carbon (Darco), dried with Drierite, and reduced *in vacuo* to a sirup. The sirup was dissolved in isopropyl ether and placed in a freezer to yield a white solid. The solid was dried under vacuum and ground to white crystals (21.87 g, 62%): m.p. 111.8-113°C [Lit.[51]: m.p. 113°C].

2-O-Methyl-1,3,4,6-tetra-O-acetyl-D-glucopyranose[14]

N-(2-O-methyl-3,4,6-tri-O-acetyl-D-glucosyl)-piperidine (10 g) was added to 0.5M HCl (50 mL) and shaken. The pH of the solution was maintained under pH 5 by addition of 1M HCl. Completion of the reaction was determined by TLC (isopropyl ether:pyridine, 10:1, v/v). The solution was deionized by passing through an Amberlite MB-3 (H^+, OH^-) ion exchange resin (150 mL) column eluted with water (550 mL). The solution was reduced *in vacuo*. The resultant sirup was acetylated in pyridine (40 mL) and acetic anhydride (50 mL) overnight with gentle shaking. The solution was poured into vigorously stirring ice water (280 mL) and

stirred for 20 minutes. Chloroform (120 mL) was added and stirred for five minutes. The chloroform layer was removed, and the aqueous layer was back-extracted with chloroform (2 x 200 mL). The chloroform layers were combined and washed with 1M HCl (2 x 200 mL) and water (3 x 200 mL). The chloroform layer was dried with sodium sulfate and reduced *in vacuo* to a sirup. The sirup was dissolved in absolute ethanol and yielded upon vacuum drying white crystals (5.5 g, 56%): m.p. 88-105°C (as α and β anomers) [Authentic sample[14]: m.p. 88-103°C].

Phenyl 2-O-Methyl-β-D-glucopyranoside

2-O-methyl-1,3,4,6-tetra-O-acetyl-D-glucopyranose (9.0 g) was dissolved in 1,2-dichloroethane (30 mL). A solution of HBr in glacial acetic acid (32.9%, w/w, 100 mL) was added to the 1,2-dichloroethane solution.[14] The resulting yellow solution was occasionally shaken over a two hour period. The solution was diluted with chloroform (270 mL). The chloroform layer was washed with iced water (3 x 200 mL), saturated sodium bicarbonate solution (2 x 100 mL), and water (3 x 150 mL). The chloroform layer was dried over anhydrous sodium sulfate and reduced *in vacuo* to a light sirup.

The sirup was dissolved in acetone (45 mL). A solution of phenol (reagent grade, 2.34 g), 2M KOH (12.4 mL), and acetone (31.5 mL) was added to the dissolved sirup, and the resulting solution was stirred overnight.[52] The solution was diluted with chloroform (100 mL), and the chloroform layer was washed with 0.5M NaOH (2 x 75 mL) and distilled water (3 x 150 mL). The chloroform layer was dried over anhydrous sodium sulfate and reduced *in vacuo* to a white solid.

A 0.5M sodium methoxide solution (2 mL) in methanol (58 mL) was added to the white solid and stirred for several hours. The reaction was judged complete by

TLC (9:1, chloroform:ethyl acetate, v/v). The solution was neutralized with glacial acetic acid and reduced *in vacuo* to a solid. Crystallization from water yielded white rod-like crystals (2.39 g, 35.6%): m.p. 165-166°C, $[\alpha]_D$ -62.3 (c 0.836, EtOH) [Lit.[23]: m.p. 167-168°C, $[\alpha]_D$ -63 (c 1, EtOH)].

^{13}C NMR data (d-DMSO): *ppm* 59.9, 60.7, 70.0, 75.8, 76.8, 83.2, 100.2, 116.0, 121.8, 129.3, and 156.9.

PROCEDURES FOR KINETIC ANALYSIS

The following discussion details procedures used for the fast flow reactor. A description and discussion of the reactor are given in Appendix 2. Procedures and equipment used for the low temperature degradation were outlined by previous researchers.[11-16]

Solution Preparation

All reaction solutions for the fast flow reactor were made under oxygen-free nitrogen conditions in a glove bag that had been through four deflation-inflation cycles. Solutions were made the day prior to the degradation and sealed under nitrogen in bottles.

Standard sodium hydroxide solutions were made from stock solution to a concentration four times the reaction concentration. The amount of stock solution needed was determined from the equation (24):

$$X = \frac{4\, M_R\, V_S\, \rho}{M} \qquad (24)$$

where X = grams of stock solution required, g

M_R = target molarity of reaction solution after mixer, mol L^{-1}

V_S = desired volume of standard solution, mL

ρ = density of stock solution, g mL^{-1}

M = molarity of stock solution, mol L^{-1}.

In a tared volumetric flask, the calculated amount of stock solution was weighed and diluted with oxygen-free water. The density was determined from the final weight of the contents or through tared 10 mL volumetric flasks. The molarity of the standard solution was measured by titration against potassium acid phthalate to a phenolphthalein endpoint.

For the fast flow reactor degradations, two room temperature reaction liquors were made, one for the caustic syringe and the one for the carbohydrate syringe. The molarities of these solutions were targeted at twice the molarity of the reacting liquor to account for the mixing of equal volumes of the carbohydrate and caustic solutions and a value which accounted for volume expansivity of the room temperature liquor at reaction temperature. Volume expansivity (F_V) is defined by equation (25):

$$F_V = \frac{V_T}{V_{RT}} \qquad (25)$$

where V_T = standard water volume at reaction temperature, L

V_{RT} = standard water volume at room temperature, L.

The amount of standard solution necessary for the room temperature caustic

reaction liquor was calculated using equation (26):

$$X_S = \frac{2\, M_R\, V_{RT}\, \rho_S\, F_V}{M_S} \qquad (26)$$

where X_S = weight of standard solution required, g

V_{RT} = volume of reaction solution at room temperature, mL

ρ_S = density of standard solution, g mol^{-1}

M_S = molarity of standard solution, mol L^{-1}.

After addition of the standard solution, the phenol internal standard, 4-isopropylphenol[44] (98%, 0.05M at reaction conditions after mixer), was added to the room temperature reaction liquor volumetric flask prior to dilution. The amount of solid additive was determined by equation (27):

$$Y = 2\, M_R\, V_{RT}\, W_M\, F_V \qquad (27)$$

where Y = weight of compound required, g

W_M = molecular weight of compound.

For caustic experiments the stock solution was then diluted.

In the salt addition experiments, sodium chloride was added in the amount calculated from equation (27) to the volumetric flask of the room temperature caustic reaction liquor after addition of internal standard and standard NaOH. The amount of sodium sulfide stock solution, in the nucleophilic effect experiment, used was calculated from equation (26). The stock solution was weighed into the volumetric flask of the room temperature reaction liquor after the standard sodium hydroxide liquor and internal standard were added. The molarity of the sodium

sulfide was calculated by the method previously outlined in the General Analytical Procedures section.

For the room temperature carbohydrate reaction liquor, carbohydrate (0.01M at reaction conditions after the mixer) and internal standard (0.005M at reaction conditions after the mixer), methyl α-D-glucopyranoside, were weighed into a volumetric flask in amounts indicated by equation (27) and diluted with deoxygenated water.

Initial Loading of Syringes

Prior to reaction, the caustic, carbohydrate, and oxygen-free water reservoirs were attached to their inlets to the reaction system (Figure 16). Pistons were retracted to fill each syringe with fluid via suction. Then the piston was advanced so that the liquor goes to waste. This process was repeated until all air bubbles were removed from the syringes and tubing.

Reaction Run

With the caustic and carbohydrate syringes full, the reactor system was depressurized. Initially the system was pressurized to maintain oxygen-free conditions in the coils. Their warm-up coils were partially filled with solution (10.2 mL); and the reaction coils repressurized to 150 psi gage. The coils were lowered into the oil bath and allowed to warm-up for 10 minutes. A rapid pulse of the remaining solution forced the warm solutions through the mixer and into the reaction coils. The electronic stopwatch was started, the reaction was run the desired time, the quench ram was activated, and the stopwatch was stopped. The quench water pushed the reacted liquor into a polypropylene bottle (250 mL) that contained iced water (100 mL). The iced water thermally quenched the reaction. The system

was depressurized, the headspace of the bottle was flushed with nitrogen, and the bottle was tightly sealed. The sample bottle was placed in ice water for further cooling and then refrigerated until samples were taken for analysis.

Reactor Cleaning

After the degradation was completed, the coils, mixer, quench line, and lines to the sample holder were flushed with water and acetone. The line to the quench syringe was disconnected. Vacuum was applied through a three-way valve connection to the warm-up ram. Water, then acetone, were suctioned through both the quench line and the line to the sample holder. After the acetone rinse, the tubing was dried by connection to a vacuum line for 15 minutes. The syringes were then refilled and a new sample bottle was placed in the sample holder. The system was pressurized. Nitrogen was blown through the tubing and the quench line was connected. During pressurization, leaks were checked for. The reactor system was ready for the start of the next degradation.

Reaction Liquor Analysis

The carbohydrate reaction liquor sample (16 mL) which contained internal standard was neutralized to pH 7 with acetic acid (1M). The solution was reduced *in vacuo* to a sirup. Isopropyl alcohol (reagent grade, 12 mL) was added to the sirup and the resultant slurry was reduced *in vacuo* to dryness. The white salt containing residue was acetylated overnight with pyridine/acetic anhydride (2:1, v/v, 2 mL) with gentle shaking. The acetylation reaction was quenched with cold water (10 mL), shaken for two minutes, and extracted with chloroform (2 x 5 mL). The chloroform layers were combined and washed with 1M hydrochloric acid (2 x 75 mL) and water (3 x 10 mL). The chloroform layer was reduced *in vacuo* to dryness; the residue was transferred to a 4 mL vial with chloroform (2 mL). The sample was

reduced *in vacuo* to dryness and taken up in ethyl acetate for GLC analysis.

The sample (16 mL) for phenol analysis which already contained internal standard was placed in a 50 mL erlenmeyer flask and the solution NaOH molarity was adjusted to 0.5M by addition of 5M NaOH. Dimethyl sulfate (98%, 2 mL) was added and the flask was stoppered. The two phase solution was vigorously stirred for 15 minutes. Concentrated ammonium hydroxide (9 mL) was added to quench the excess dimethyl sulfate and the solution was stirred for another 15 minutes. The solution was extracted with chloroform (2 mL) by stirring for two minutes. The chloroform layer was drawn off and placed in a 4 mL vial. A sample was injected on the GLC for analysis.

Concentration of the analyzed compounds were calculated from equation (28):

$$M_X = \frac{A_X}{A_{IS}} M_{IS} \qquad (28)$$

where M = molarity of compound, mol L^{-1}

A = peak area of compound

X = compound X

IS = internal standard.

Linear regressions and confidence limits on the experimental data were performed on LOTUS-123 (LOTUS Software) to give pseudo-first-order reaction rate constants.

^{18}O Incorporation Experiment

The experimental procedure for this analysis utilized previously described

fast flow reactor methods. A 25 mL carbohydrate liquor size was used. The model compound was diluted with 2 g of 90.7% ^{18}O water[53] and 10 g of 25% ^{18}O water.[16] This produced an 8.6% ^{18}O water level in the reaction liquor after mixing. When filling the carbohydrate syringe, bubbles were removed as described previously except the solution was recycled back for reactor use. The sample was reacted in 2.5M NaOH at 171.6°C for 20.62 seconds.

The phenol product with incorporated ^{18}O was derivatized as indicated above. Analysis by GC/MS was used to measure the isotopic levels of ^{18}O in the product, the reaction liquor, and the water. The amount of oxygen-aglycon cleavage was calculated by a modified program developed by Henderson.[16]

Isolation of Unknowns from Phenyl 2-O-Methyl-β-D-glucopyranoside Degradation

Phenyl 2-O-methyl-β-D-glucopyranoside (0.01M) was reacted in 2.5M NaOH for 24 hours in the reactor described by Brandon.[11] The solution was deionized with Amberlite MB-3 (H^+, OH^-) ion exchange resin (500 mL), and the resin was washed with 1L water. The water fractions were combined and reduced *in vacuo* to a solid. The solid was acetylated with a mixture of acetic anhydride and pyridine (5 mL, 1:2, v/v) for two days with gentle agitation. The acetylation reaction was quenched with iced water (100 mL) and stirred for 20 minutes. The solution was extracted with chloroform (2 x 50 mL). The chloroform layers were combined and washed with 1M HCl (3 x 25 mL) and water (4 x 25 mL). The chloroform layer was reduced *in vauco* to a sirup.

The sirup was placed on a silica gel column (Merck Kieselgel 60, 35 cm x 1.2 cm) and eluted with a mixture of ethyl acetate and chloroform (1:5, v/v). Fractions of 5 mL were collected. Fractions 21 and 22 yielded the unknown tentatively

identified as 1,4-anhydro-2-O-methyl-α-D-glucopyranose. Fractions 28-30 yielded a product identified as 1,6-anhydro-2-O-methyl-β-D-glucopyranose. Portions of the samples was sent for GC/MS analysis, while the remainder of the samples were reduced *in vacuo* to a residue and sent for microsample NMR.

An authentic sample of 1,6-anhydro-2-O-methyl-β-D-glucopyranose[12] (2 mg) was acetylated by the procedure outlined for the reaction samples.

1,6-anhydro-2-O-methyl-β-D-glucopyranose as acetate derivative: ^{13}C NMR data ($CDCl_3$) *ppm* 170.2, 169.3 (-C(=O)CH_3); 100.2 (C-1), 76.9, 73.5, 70.6, 68.9, 65.2 (C-2, C-3, C-4, C-5, C-6), 58.3 (-OCH_3), 21.1 (-C(=O)CH_3) (Appendix 4, Figures 24 and 25); ^1H NMR data ($CDCl_3$) *ppm* 5.50 (1H, s, -C(1)H-), 4.88 (1H, t, J = 1.4 Hz), 4.67 (1H, s), 4.60 (1H, d, J = 5.2 Hz), 4.09 (1H, d, J = 7.6 Hz), 3.79 (1H, d of d, J = 7.6 Hz and 5.8 Hz), 3.52 (3H, s, -OCH_3), 3.07 (1H, s), 2.17 (3H, s), 2.12 (3H, s) (-C(=O)CH_3) (Appendix 4, Figures 27 and 28); EI mass spectrum in *m/z* (relative intensity) 158 (32), 129 (56), 126 (12), 116 (17), 113 (78), 112 (46), 97 (12), 87 (64), 85 (13), 81 (41), 74 (100), 71 (11), 70 (9), 43 (51).

Fraction 28-30: ^{13}C NMR data ($CDCl_3$) *ppm* 100.1 (C-1), 73.5, 70.6, 68.8, 65.2, 58.4 (-OCH_3), 21.1 (-C(=O)CH_3); ^1H NMR data ($CDCl_3$) *ppm* 5.50 (1H, s, -C(1)H-), 4.88 (1H, t, J = 2.5 Hz), 4.67 (1H,s), 4.60 (1H, d, J = 5.3 Hz), 4.09 (1H, d, J = 7.6 Hz), 3.79 (1H, d of d, J = 7.5 Hz and 6.4 Hz), 3.52 (3H, s, -OCH_3), 3.07 (1H, s), 2.18 (3H, s), 2.12 (3H, s) (-C(=O)CH_3); EI mass spectrum in *m/z* (relative intensity) 158 (12), 129 (22), 126 (5), 116 (8), 113 (28), 112 (18), 97 (5), 87 (37), 85 (7), 81 (20), 74 (64), 71 (6), 70 (6), 43 (100). The NMR spectra of this product is virtually identical to that of 1,6-anhydro-2-O-methyl-β-D-glucopyranose. However due to small sample size not all ^{13}C-NMR signals were visible above the noise level. The EI mass spectrum provided a close match to the known: the signals were similar but not identical.

Fractions 21 and 22: ^{13}C NMR data ($CDCl_3$) *ppm* 102.7 (C-1), 97.0, 85.9, 79.1, 75.9, 63.0, 57.2, 55.4, 20.7 (-C(=O)$\underline{C}H_3$) (The ^{13}C NMR data appears incomplete, because the small sample size caused signals that were expect to occur, such as the carboxyl carbons, to be hidden in the background noise.) (Appendix 4, Figure 26); ^1H NMR data ($CDCl_3$) *ppm* 5.52 (1H, s, -C(1)$\underline{H}$-), 4.90 (2H, t of d, J = 3.0 Hz and 7.6 Hz, -C(6)$\underline{H}_2$-), 4.42 (1H, d of d, J = 8.6 Hz and 11.7 Hz), 4.27 (1H, d of d, J = 11.7 Hz and 4.5 Hz), 4.12 (1H, t of d, J = 3.0 Hz and 8.3 Hz), 3.63 (1H, d, J = 1.4 Hz), 3.41 (1H, d, J = 3.6 Hz), 3.39 (3H, s, -OC$\underline{H}_3$), 2.12 (3H, s, -C(=O)C$\underline{H}_3$), 2.08 (3H, s, -C(=O)C$\underline{H}_3$), (signals at 2.02, 2.10, 2.17, and 3.41 *ppm* appear to be related to a possible contaminant) (Appendix 4, Figures 29-31); EI mass spectrum in *m/z* (relative intensity) 177 (7), 141 (4), 140 (4), 129 (26), 115 (13), 113 (32), 112 (21), 87 (71), 85 (11), 81 (13), 74 (20), 71 (11), 69 (15), 43 (100).

ACKNOWLEDGEMENTS

The author would like to acknowledge the encouragement and guidance provided by his thesis advisory committee: Dr. L. E. Schroeder, Dr. D. R. Dimmel, Dr. E. W. Malcolm, and Dr. N. S. Thompson.

Thanks are also extended to The Institute of Paper Chemistry and its member companies for the opportunity that made this work possible, and to my fellow students for making the time so enjoyable.

I also wish to express my appreciation for the encouragement and love of my family, and especially of my wife, Susan, throughout the course of this thesis.

LITERATURE CITED

1. American Paper Institute. 1986 Statistics of Paper, Paperboard, and Wood Pulp: Data Through 1985. New York, American Paper Institute, 1986. 76 p.

2. Smook, M.A. Handbook for Pulp and Paper Technologists, Joint Committee of Vocational Educational Committees of the Pulp and Paper Industry, Montreal, 1984:66-75.

3. Samuelson, O.; Grangard, G; Jonsson, K. and Schram, K; Svensk Papperstidn. 56:779-84(1953).

4. Rydholm, S. A. Pulping Processes, John Wiley and Sons, Inc., New York, 1965:576-649.

5. Matthews, C., Svensk Papperstidn. 77:629-35(1974).

6. Gentile, V. Effects of Physical Structure of the Alkaline Degradation of Hydrocellulose, Doctoral Dissertation, The Institute of Paper Chemistry, Appleton, WI, 1986. 110 p.

   Gentile, V.; Schroeder, L.; and Atalla, R.; ACS Symp. Ser. 340:272-9(1987).

7. Corbett, W. and Richards, G., Svensk Papperstidn. 60:791-4(1957)

8. Lindberg, B., Svensk Papperstidn. 59:531-4(1956).

9. Robins, J. and Green, J., Tappi 52(7):1346-51(1969).

10. Best, E. and Green, J., Tappi 52(7):1321-5(1969).

11. Brandon, R. Alkaline Degradation of 1,5-anhydrocellobiitol, Doctoral Dissertation, The Institute of Paper Chemistry, Appleton, WI, 1973. 164 p.

    Brandon, R.; Schroeder, L.; and Johnson, D.; ACS Symp. Ser. 10:125-46(1975).

12. Gilbert, F. Mechanisms of High Temperature Alkaline Degradation of Methyl α-D-glucopyranoside and 1,6-anhydro-β-D-glucopyranose, Doctoral Dissertation, The Institute of Paper Chemistry, Appleton, WI, 1975. 97 p.

13. Wylie, T. The Alkaline Degradation of 1,5-anhydro-2,3,6-tri-O-methyl-cellobiitol, Doctoral Dissertation, The Institute of Paper Chemistry, Appleton, WI, 1979. 87 p.

14. Nault, J. Alkaline Degradation of Methyl β-D-glucopyranoside and Methyl 2-O-methyl-β-D-glucopyranoside, Doctoral Dissertation, The Institute of Paper Chemistry, Appleton, WI, 1979. 112 p.

15. Blythe, D. An Investigation of the Role of Sodium Sulfide in Cellulosic Chain Cleavage During Kraft Pulping, Doctoral Dissertation, The Institute of Paper

Chemistry, Appleton, WI, 1984. 151 p.

Blythe, D., and Schroeder, L., J. Wood Chem. Technol. 5(3):313-34(1985).

16. Henderson, M., Mechanisms of Alkaline Glycosidic Bond Cleavage in 1,5-anhydro-4-O-β-mannopyranosyl-D-mannitol, Doctoral Dissertation, The Institute of Paper Chemistry, Appleton, WI, 1986. 142 p.

17. Lai, Y.-Z., Carbohydr. Res. 24:57-65(1972).

18. Lai, Y.-Z. and Ontto, D., Carbohydr. Res. 75:51-9(1979).

19. Lai, Y.-Z., SPCI Int. Symp. Wood and Pulping Chem., Vol 2, 26-32, (June 9-12, 1983).

20. Ballou, C., Adv. Carbohydr. Chem. Biochem. 9:59-95(1954).

21. Capon, B., Chemical Reviews 69(4):407-98(1969).

22. McCloskey, C. and Coleman, G., J. Org. Chem. 10:184-93(1945).

23. Bardolph, M. and Coleman, G., J. Org. Chem. 15:169-73(1950).

24. Montgomery, E.; Richtmeyer, N.; and Hudson, C.; JACS 65:3-7(1943).

25. Dyferman, A. and Lindberg, B., Acta Chem. Scand. 4:878-84(1950).

26. Hickinbottom, W., JCS 1928:3140-7.

27. Gasman, R. and Jonhson, D., J. Org. Chem. 31:1830-8(1966).

28. Tsai, G. and Reyes-Zamora, C., J. Org. Chem. 37(17):2725-9(1972).

29. DeBruyne, C; Van Wijnendaele, R.; and Carchon, H.; Carbohydr. Res. 33:75-87(1974).

30. Moody, W. and Richards, G., Carbohydr. Res. 93:83-90(1981).

31. Forskahl, I.; Popoff, T.; and Theander, O.; Carbohydr. Res. 48:13-21(1976).

32. Kiryushina, M.; Repilo, E.; and Chirkin, G.; Khim. Drev. (5);46-52(1977).

33. Bennaser, E.; Kiryushina, M.; and Zarabin, M.; Khim. Drev. (2):59-70(1987).

34. March, J. Advanced Organic Chemistry: Reactions, Mechanisms, and Structure. 2nd ed. McGraw-Hill, Inc., New York, 1977.

35. Hill, C., Jr. An Introduction to Chemical Engineering Kinetics and Reactor Design. John Wiley and Sons, Inc., New York, 1977.

36. Green, J.; Pearl, I.; Hardacker, K.; Andrews, B.; and Haigh, F.; Tappi 60(10):120-

5(1977).

37. Hall, L., Adv. Carbohydr. Chem. Biochem. 19:51-91(1964).

38. Anet, F., Can. J. Chem. 39:789-94(1961).

39. Uryu, T.; Yamanouchi, J.; Kato, T.; Higuchi, S.; and Matsuzaki, K.; JACS 105(23):6865-71(1983).

40. Bochkov, A. F. and Vaznyi, Ya. V., Zh. Org. Khim. 13(4):750-5(1977).

41. Bunton, C. and Robinson, L., JACS 90(22);5965-71(1968).

42. TAPPI Standard Method T694 pm-82.

43. TAPPI Standard Method T625 cm-85.

44. Perrin, D.; Armarego, W.; and Perrin, D. Purification of Laboratory Chemicals, Pergamon Press, New York, 1966.

45. Aldrich Chemical Company, Inc., Milwaukee, WI 53233.

46. Millard, E. The Degradation of Selected 1,5-anhydroalditols by Molecular Oxygen in Alkaline Media, Doctoral Dissertation, The Institute of Paper Chemistry, Appleton, WI, 1976. p.159

47. Cerny, M. and Stanek, J., Adv. Carbohydr. Chem. Biochem. 34:164-(1977).

48. Sigma Chemical Company, St. Louis, MO 63178.

49. Fischer, E. and Armstrong, E., Chem. Ber. 34:2885-2900(1901).

50. Pfanstiehl Laboratories, Inc., Waukegan, IL 60085.

51. Hodge, J. and Rist, C., JACS 74:1498-1500(1952).

52. Jermyn, M., Australian J. Chem. 10:448-54(1957).

53. Alfa Products, Danvers, MA 01923.

APPENDIX 1

ANALYSIS OF LEVOGLUCOSAN AS AN UNSTABLE PRODUCT

Earlier researchers have considered levoglucosan an unstable product, because it degraded faster than the reactant. In those cases, the levoglucosan formation rate had to account for the simultaneous degradation of levoglucosan. Consecutive first-order reaction kinetics were used to determine the levoglucosan reaction rate constants.

For the product levoglucosan, the rate equation at constant volume[35] is:

$$\frac{dP}{dt} = k_{levo} R - k_d P \qquad (29)$$

where R = reactant concentration, mol L^{-1}

P = levoglucosan concentration, mol L^{-1}

k_{levo} = pseudo-first-order rate constant for formation of levoglucosan, sec^{-1}

k_d = pseudo-first-order rate constant for degradation of levoglucosan, sec^{-1}.

Substitution of equation (3) into equation (29) produces:

$$\frac{dP}{dt} = k_{levo} [R_o \exp(-k_r t)] - k_d P \qquad (30)$$

where R_o = initial reactant concentration, mol L^{-1}

k_r = pseudo-first-order constant for the degradation of reactant, mol L^{-1}.

Equation (30) rearranges to:

$$k_d P\,dt - k_{levo} R_o \exp(-k_r t)\,dt + dP = 0 \qquad (31)$$

The solution of the linear first order differential equation is:

$$P \exp(k_d t) - \left[\frac{k_{levo} R_o}{k_d - k_r}\right] \exp[(k_d - k_r)t] = C \qquad (32)$$

where C = the integration constant.

At $t_o = 0$ and $P = P_o$, the integration constant C becomes:

$$C = P_o - \frac{k_{levo} R_o}{(k_d - k_r)} \qquad (33)$$

Substitution of equation (33) into equation (32) and rearrangement yields:

$$P - P_o \exp(-k_d t) = k_{levo}\left[\frac{R_o}{k_d - k_r}\right][\exp(-k_r t) - \exp(-k_d t)] \qquad (34)$$

For this analysis, values of k_r and k_d are needed to calculate k_{levo} in equation (34). The k_r value was experimentally determined, while the value of k_d was obtained from the data of Gilbert.[12]

One problem arising from using the literature derived k_d value is that the number may be incorrect. An analysis was run to determine the effect on levoglucosan formation rate constants when different values of k_d, which were multiples of Gilbert's levoglucosan degradation rate constant, were used in equation (34). Table 13 shows this effect on the levoglucosan formation rate constants in 0.5M NaOH at 170°C with various k_d values.

When the analysis for stable products was run, k_{levo} was determined to be 1.05×10^{-2} sec^{-1}, k_{levo} from the unstable analysis with Gilbert's value[14] becomes 1.06×10^{-2} sec^{-1}. The differences in the reaction rate constants are small enough that the unstable product analysis appears to be unnecessary. When the k_d value goes from 6.8 x 10-5 sec^{-1} to 1.7×10^{-5} sec^{-1}, the levoglucosan reaction rate constant goes from 1.07×10^{-2} sec^{-1} to 1.10×10^{-2} sec^{-1}, respectively. From data obtained from Gilbert[12] and Blythe *et al.*[15], there appeared to be only a 5% difference in the reaction rate constants when the same model was degraded under similar conditions by the different researchers. Thus, the best estimate for k_d was 3.4×10^{-5} sec^{-1}, and levoglucosan can be considered a stable product

Table 13. Levoglucosan formation rate constants and its dependence upon k_d values used in equation (34).

k_d value used, $\times 10^5$ sec-1	levoglucosan formation rate constants, $\times 10^2$ sec^{-1}
3.4	1.06
6.8	1.07
17.0	1.10

APPENDIX 2

REACTOR SYSTEM

The flow reactor contained four interrelated systems: hydraulics and controls, syringe assembly, gas and liquid delivery, and the oil bath.

The hydraulic system was divided into the electronic controls and the hydraulic hardware (Figure 21). The hydraulic hardware consisted of a pump (Fluid Controls Inc., Power-One, 100- psi max., 346 cu in. min^{-1}), flow control valves (Racine, 2-MEPW-50H-1231), directional control valves (Racine, FD4-DSNS-701-QD), pressure gages (Ashcroft, 0-100- psig), the caustic and carbohydrate hydraulic ram (Tomkins Johnson Co., LSM1,1 in. diam.), and the quench hydraulic ram (Tomkins Johnson Co., LSM1, 1.5 in. diam.). The electronic controls for each ram allowed for retraction (fill syringe), stoppage of movement, and advance (empty syringe). The carbohydrate and caustic hydraulic ram also had an advance to set point switch that advanced piston movement to a preset position determined by the closing of a microswitch (Micro Switch, BZE6-2RQ2).

The syringe assembly consisted of three syringes mounted on an iron rail. The syringes were stainless steel tubes and pistons sealed with BUNA rubber o-rings. Caustic and carbohydrate syringe tubes (0.459 in. ID) had a stroke volume of 21.0 mL. Their pistons were attached to a bar whose movement was controlled by the caustic and carbohydrate hydraulic ram piston rod. The quench syringe tube (1.01 in. ID) had a 100.0 mL stroke volume and its piston was attached to the quench hydraulic ram rod.

The gas and liquor delivery system (Figures 16 and 22) included liquor storage

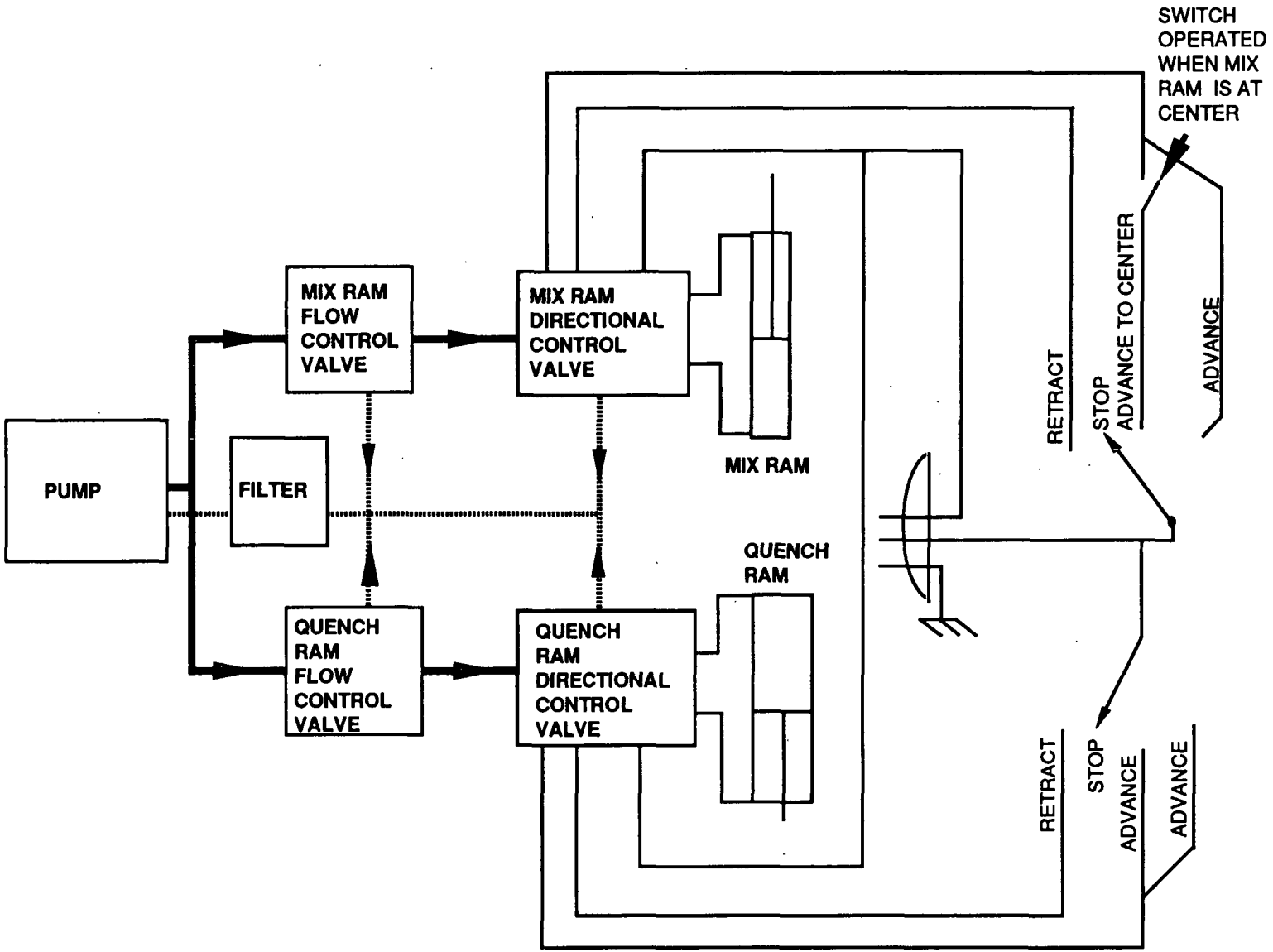

Figure 21. Electronic and hydraulic schematic of the fast flow reactor.

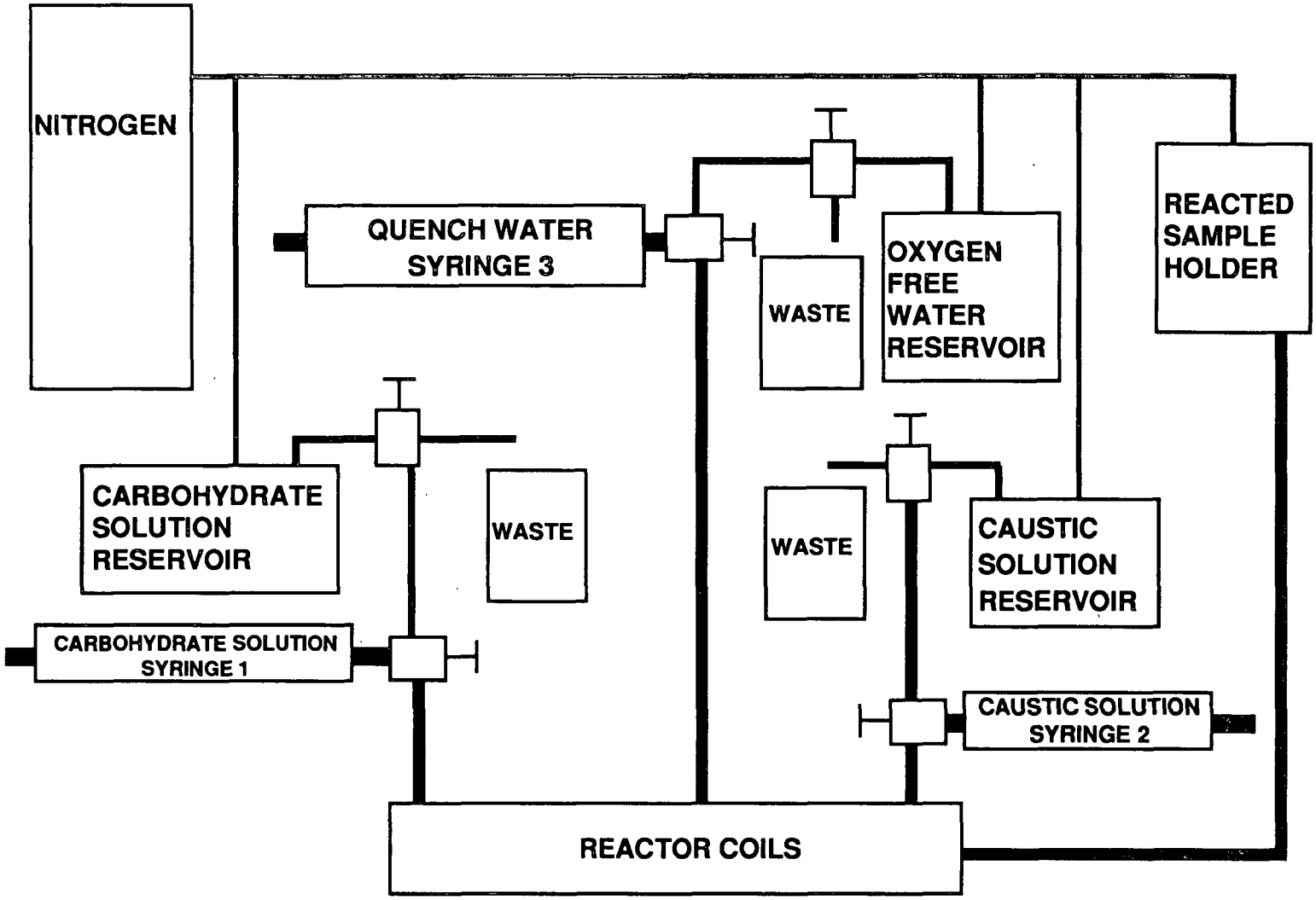

Figure 22. Liquor and gas handling schematic for the fast flow reactor.

and the reactor parts. The reservoirs for quench water, carbohydrate liquor and caustic liquor were maintained with oxygen-free headspaces by blowing nitrogen from tubes connected to a nitrogen gas cylinder. The reservoirs were attached to the appropriate syringes through tubing that had two three-way valve connections. One valve was for the removal of air bubbles that occur when the syringes are initially filled. The second valve allowed for connection to the reactor coils. From the caustic and carbohydrate syringes, tubing lead to their respective warm-up coils (13.9 mL). The warm-up coils were connected to the mixer inlet. The mixer (Figure 23) was divided into the inlet body, the stainless steel Gibson Eight-Jet Mixer (Durrum Co.) and housing, and the the mixer outlet body. The mixer was sealed with Viton o-rings. From the mixer outlet body, a reaction coil (5.1 mL) was attached. At the other end of the reaction coil, a tee connection was connected to a second reaction coil (15.3 mL) and tubing to the quench syringe. The two coil arrangement was used so that the first coil would retain any liquor that may have gone through the mixer due to thermal expansion, while the second coil would contain liquor of a known reaction history. Between the tee and the quench syringe, a valve was located near the oil bath. This valve prevented movement of the reaction liquor into unheated tubing. Tubing from the second reaction coil led to the reacted liquor sample holder. The sample holder was connected to a nitrogen gas cylinder that provided 150 psi gage pressure. This pressure prevented the reactions liquors from boiling in the reaction tubing and maintained oxygen-free conditions in the reaction tubing. The liquor handling tubing was 1/8 in. stainless steel tube (Kilsby-Roberts, 304 or 314), the connections were 1/8 in. stainless steel Swagelock, and the valves were 1/8 in. stainless steel Whitey.

For a degradation, the reaction coils were placed in an oil bath containing

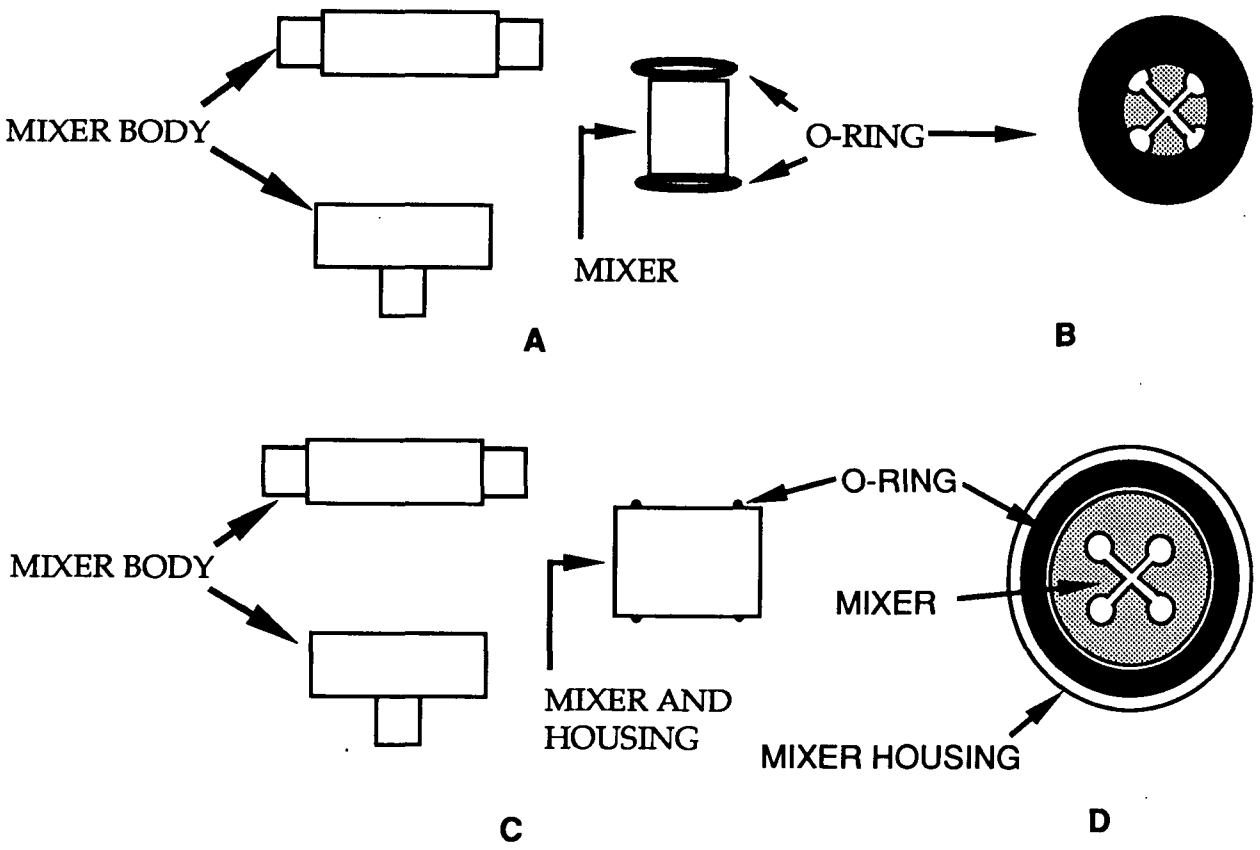

Figure 23. Side (A) and top inlet mixer (B) view of Green's mixer[36] and side (C) and top inlet mixer (D) views of modified mixer.

UCON Heat Transfer Fluid 500 (Union Carbide, 8 gal). The bath was heated continuously with two 500 Watt glass knife heaters. Temperature control was through intermittently heating one 250 and one 500 Watt glass knife heaters controlled by a RTD digital controller with probe (Omega Engineering, 4201-PF2 and PR-11-2-100-1/4-12 1/2-E). Temperature readings were measured from the controller

and by a standardized thermometer.

For this thesis, the mixer used by Green *et al.*[36] was modified. This modification was necessary, because the reactor was cleaned while the coils were attached to the reactor, in contrast to Green *et al.*[36] who took the reactor apart after each data point. The cleaning process helped to cause the o-rings to disintegrate and plug the mixer holes. Plugging prevented mixing and subsequent control of the reaction time. Mixer changes (Figure 23) prevented the o-rings from contacting the mixer holes while providing a seal between mixer parts.

APPENDIX 3

OXYGEN-AGLYCON CLEAVAGE PROGRAM AND RAW DATA

COMPUTER PROGRAM FOR ^{18}O DETERMINATION

```
10    REM  This a modified program of M. E. Henderson
20    REM  This program calculates the fraction of phenol that forms from
30    REM  oxygen-aglycon cleavage of phenyl β-D-glucopyranoside
35    DIM  A(25), T(25), U(25),V(25)
40    INPUT  "Label for degradation run ", LABEL$
50    'PRINT  LABEL'
60    LPRINT  "This degradation is  "; LABEL$
70    REM  This section calculates the fractions of the various isotopes
80    REM  present for natural methylated phenol
90    'PRINT  PROMPT'
100   PRINT  "Enter MS counts for natural phenol"
110   INPUT  "No. counts at M=108 "; M108
120   INPUT  "No. counts at M=109 "; M109
130   INPUT  "No. counts at M=110 "; M110
140   INPUT  "No. counts at M=111 "; M111
150   'PRINT HEADER AND LABEL'
160   LPRINT  "This is the natural phenol for degradation  "; LABEL$
170   LPRINT "Pass      Alpha          M      MO17 MO18 DIFA  ANEW       "
175   A=0.725
180   I=0
190   I=I+1
200   'Calculate MO17 and MO18'
205   M=M108
210   MO17=M109-(A*M)
220   MO18=M110-(A*MO17)
230   'Write values from this pass'
240   LPRINT USING  "##          " I;
250   LPRINT USING  "#.####  "; A;
260   LPRINT USING  "######.#### "; M;MO17;MO18;DIFA;ANEW
```

```
270   'Calculate new A'
280   ANEW=M111/MO18
290   'Compare Last Two A values'
300   IF I < 25, GOTO 330
310   PRINT  "25 passes, no convergence"
320   GOTO 1400
330   DIFA=ABS(A-ANEW)
335   A=A+0.0001
340   IF DIFA > 0.0001, GOTO 190
345   ALPHA=A
350   'Calculate Isotope Fractions'
360   MC13=ALPHA*M
370   MC13O17=ALPHA*MO17
380   MC13O18=ALPHA*MO18
390   MTOT=M+MO17+MO18+MC13+MC13O17+MC13O18
400   BETA=MO17/MTOT
410   GAMMA=MO18/MTOT
420   DELTA=M/MTOT
430   REM  End of this section
440   REM  Calculation of the number of various phenol species
450   RTOT=100
460   RO17=BETA*RTOT
470   RO18=GAMMA*RTOT
480   R=DELTA*RTOT
490   RC13=ALPHA*R
500   RC13O17=ALPHA*RO17
510   RC13O18=ALPHA*RO18
520   REM  End of this section
530   REM  This section inputs the counts observed for the
540   REM  experimentally observed mixture of natural and
550   REM  enriched phenol and normalizes them.
580   PRINT  "Enter MS counts for product phenol "
590   INPUT  "No. counts at M=108"; M108P
600   INPUT  "No. counts at M=109"; M109P
```

```
610   INPUT  "No. counts at M=110"; M110P
620   INPUT  "No. counts at M=111"; M111P
630   ETOT=RTOT
640   ETOTP=M108P+M109P+M110P+M111P
650   NORMF=ETOTP/ETOT
660   E108=M108P/NORMF
670   E109=M109P/NORMF
680   E110=M110P/NORMF
690   E111=M111P/NORMF
700   REM   End of this section
710   REM   This section calculates the fractions of the various
720   REM   isotopic species present in the liquor.
730   'Print  Prompt'
740   PRINT  "Enter MS counts for liquor"
750   INPUT  "No. counts at M=16 "; M16
760   INPUT  "No. counts at M=17 "; M17
770   INPUT  "No. counts at M=18 "; M18
780   INPUT  "No. counts at M=19 "; M19
790   INPUT  "No. counts at M=20 "; M20
800   HTOT=M16+M17+M18+M19+M20
820   'Enter initial values for T, U, and V'
830   T(1)=0.75
840   U(1)=0.2
850   V(1)=0.05
860   'Print header and label'
865   PRINT
870   LPRINT "THIS IS THE LIQUOR FOR DEGRADATION "; LABEL$
880   LPRINT "Pass      T      U      V      O16    O17    O18"
890   I=0
900   I=I+1
910   'Calculate O16, O17, and O18'
920   O18=M20/T(I)
930   O17=(M19-(U(I)*O18))/T(I)
940   O16=(M18-(U(I)*O17)-(V(I)*O18))/T(I)
```

```
950  'Write values form this pass'
960  LPRINT USING  "##      "; I;
970  LPRINT USING  "#.##### "; T(I); U(I); V(I);
980  LPRINT USING  "######.# ; O16; O17; O18
990  'Calculate new T, U, and V'
1000 V(I+1)=M16/O16
1010 U(I+1)=(M17-(V(I+1)*O17))/O16
1020 T(I+1)=1-U(I+1)-V(I+1)
1030 'Compare last two T, U, and V values'
1040 IF I < 25, GOTO 1400
1050 PRINT  "25 passes, no convergence"
1060 GOTO 1400
1070 DIFT=ABS(T(I)-T(I+1))
1080 IF DIFT > 0.0002, GOTO 900
1090 DIFU=ABS(U(I)-U(I+1))
1100 IF DIFU > 0.0002, GOTO 900
1110 DIFV=ABS(V(I)-V(I+1))
1120 IF DIFV > 0.0002, GOTO 900
1130 'Now calculate fractions of various species'
1140 C=O16/HTOT
1150 D=O17/HTOT
1160 E=O18/HTOT
1170 REM  End of liquor calculation section
1180 REM  This section calculates the fraction of cleavage
1190 REM  at the oxygen-aglycon bond
1195 LPRINT
1200 PRINT  "Theses are the O-A fraction for degradation "; LABEL$
1210 'Calculate OA from M108 measurement'
1220 OA108=(E108-R)/(R*C-R)
1230 LPRINT  " From M108, OA=  ";
1240 LPRINT USING "##.####; OA108
1250 'Calculate OA from M109 measurement'
1250 OA109=(E109-(RC13+RO17))/(RC13*C-RC13+R*D+RO17*C-RO17)
1270 LPRINT  "From M109, OA=  ";
```

```
1280  LPRINT USING "##.#####  ; OA109
1300  'Calculate OA from M110 measurement'
1310  NUM=E110-RO18-RC13O17
1320  DEN=R*E+RO18*C+RC13*D+RC13O17*C+RO17*D-RO18-RC13O17
1330  OA110=NUM/DEN
1340  LPRINT  "From M110, OA=  ";
1350  LPRINT USING  "##.#####    "; OA110
1400  END
```

RAW DATA FOR OXYGEN-AGLYCON DETERMINATION

Table 14. Mass chromatogram for water used in ^{18}O experiment.

m / z	Multiplier counts
16.0	3265
17.0	51191
18.0	217798
19.0	321
20.0	499

Table 15. Mass chromatogram for natural phenol as methyl ether derivative.

m / z	Multiplier counts
108.0	98596
109.0	6800
110.0	400
111.0	31

Table 16. Mass chromatogram for the ^{18}O incorporated phenol as methyl ether derivative.

m / z	Multiplier counts
108.0	124767
109.0	8490
110.0	529
111.0	33

APPENDIX 4

NMR SPECTRA OF PHENYL 2-O-METHYL-β-D-GLUCOPYRANOSIDE DEGRADATION PRODUCTS

Authentic Sample, *ppm*	Fractions 28-30, *ppm*	Assignment
170.2		-C(=O)CH_3
169.3		-C(=O)CH_3
100.2	100.1	C(1)
76.9		
73.5	73.5	
70.6	70.6	
68.9	68.8	
65.2	65.2	
58.3	58.4	-OCH_3
21.1	21.1	-C(=O)CH_3

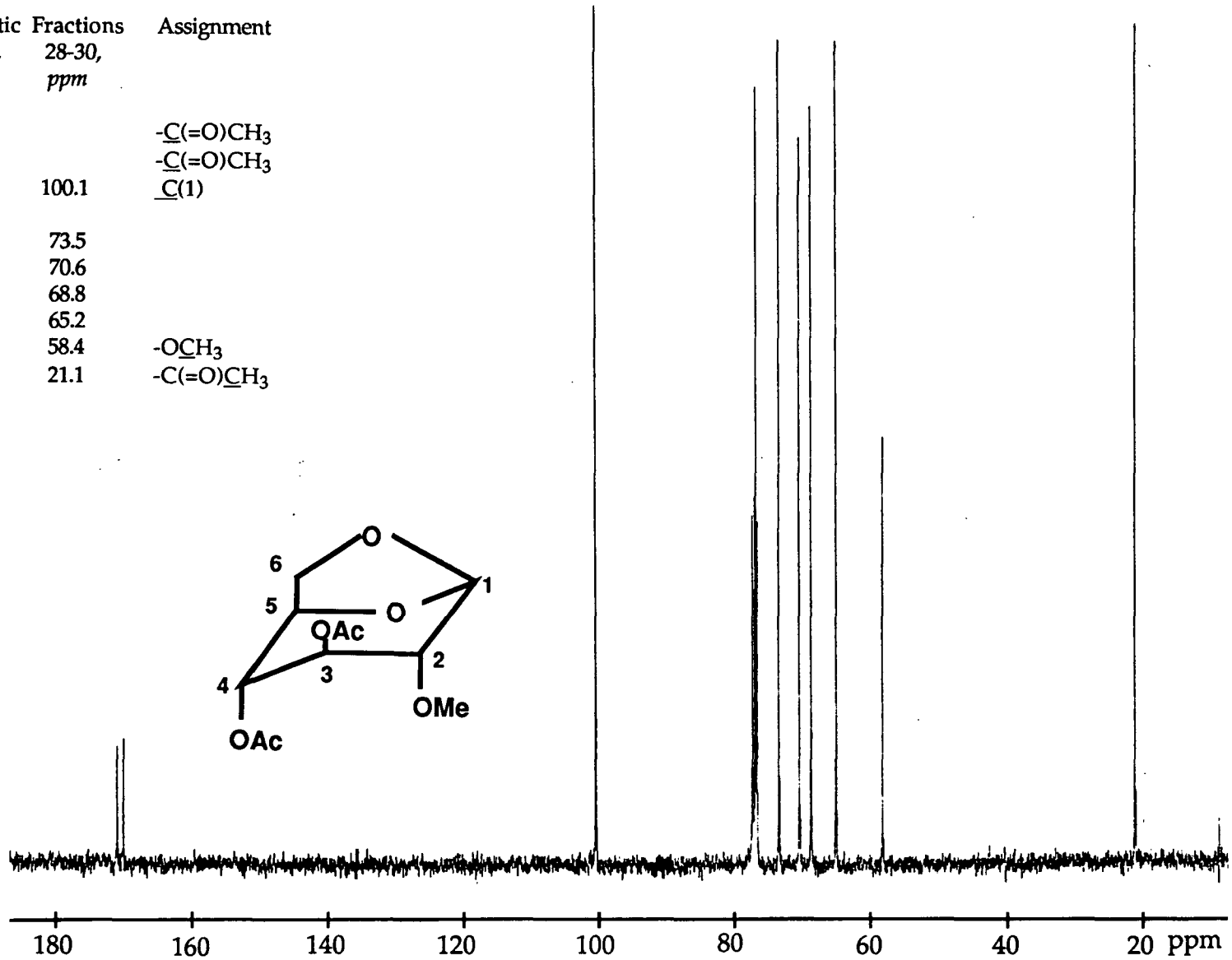

Figure 24. The ^{13}C NMR (91 MHz) spectrum of an authentic 1,6-anhydro-3,4-di-O-acetyl-2-O-methyl-β-D-glucopyranose sample with the NMR listing of Fractions 28-30 which were identified as 1,6-anhydro-3,4-di-O-acetyl-2-O-methyl-β-D-glucopyranose.

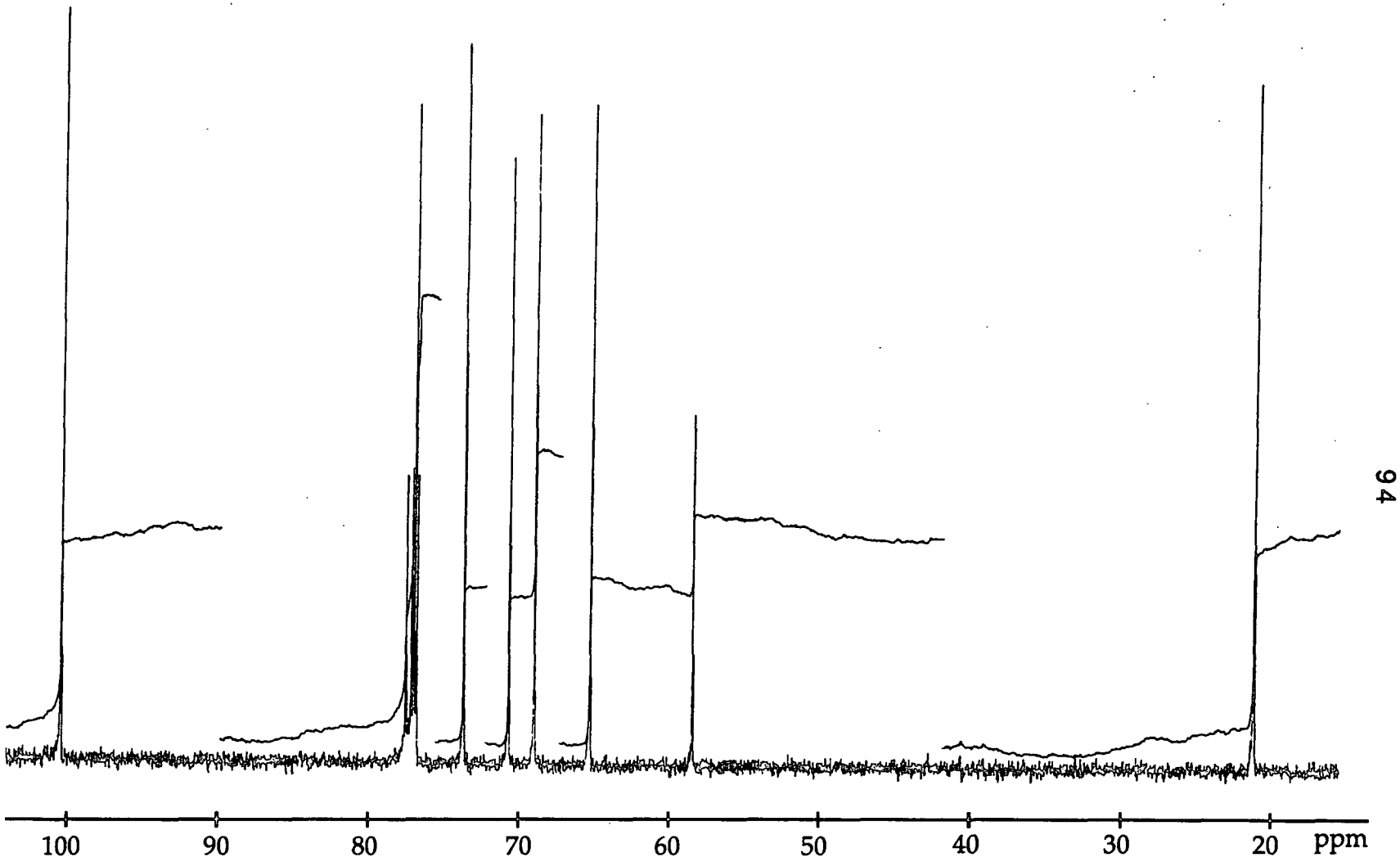

Figure 25. The expanded view of 20-100 *ppm* region of Figure 24.

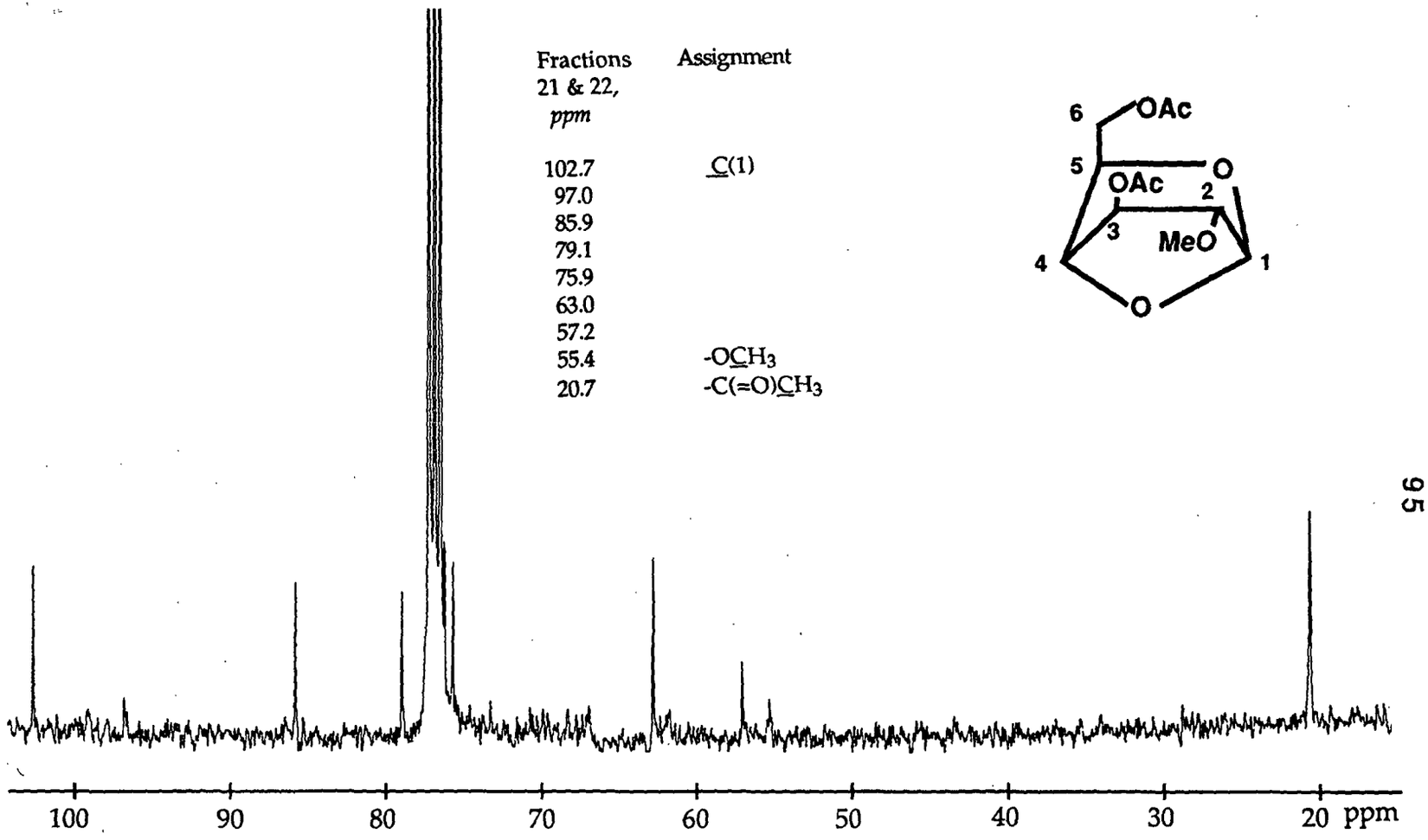

Figure 26. The ^{13}C NMR (91 MHz) spectrum of Fractions 21 and 22 which were tentatively identified as 1,4-anhydro-3,6-di-O-acetyl-2-O-methyl-α-D-glucopyranose; the signals normally associated with the carbonyl groups of the acetates (~170 *ppm*) were too weak to be distinguished from the noise with this very dilute sample.

Authentic Sample, *ppm*	Fractions 28-30, *ppm*	Splitting	Assignment
5.50	5.50	s	C(1)H
4.88	4.88	t	
4.67	4.67	s	
4.60	4.60	d	
4.09	4.09	d	
3.79	3.79	d of d	
3.52	3.52	s	
3.07	3.07	s	-OCH$_3$
2.17	2.18	s	-C(=O)CH$_3$
2.12	2.12	s	-C(=O)CH$_3$

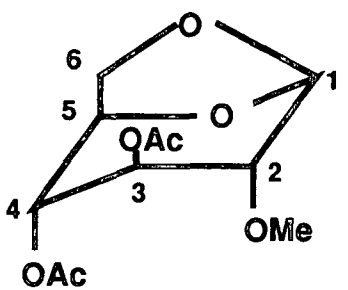

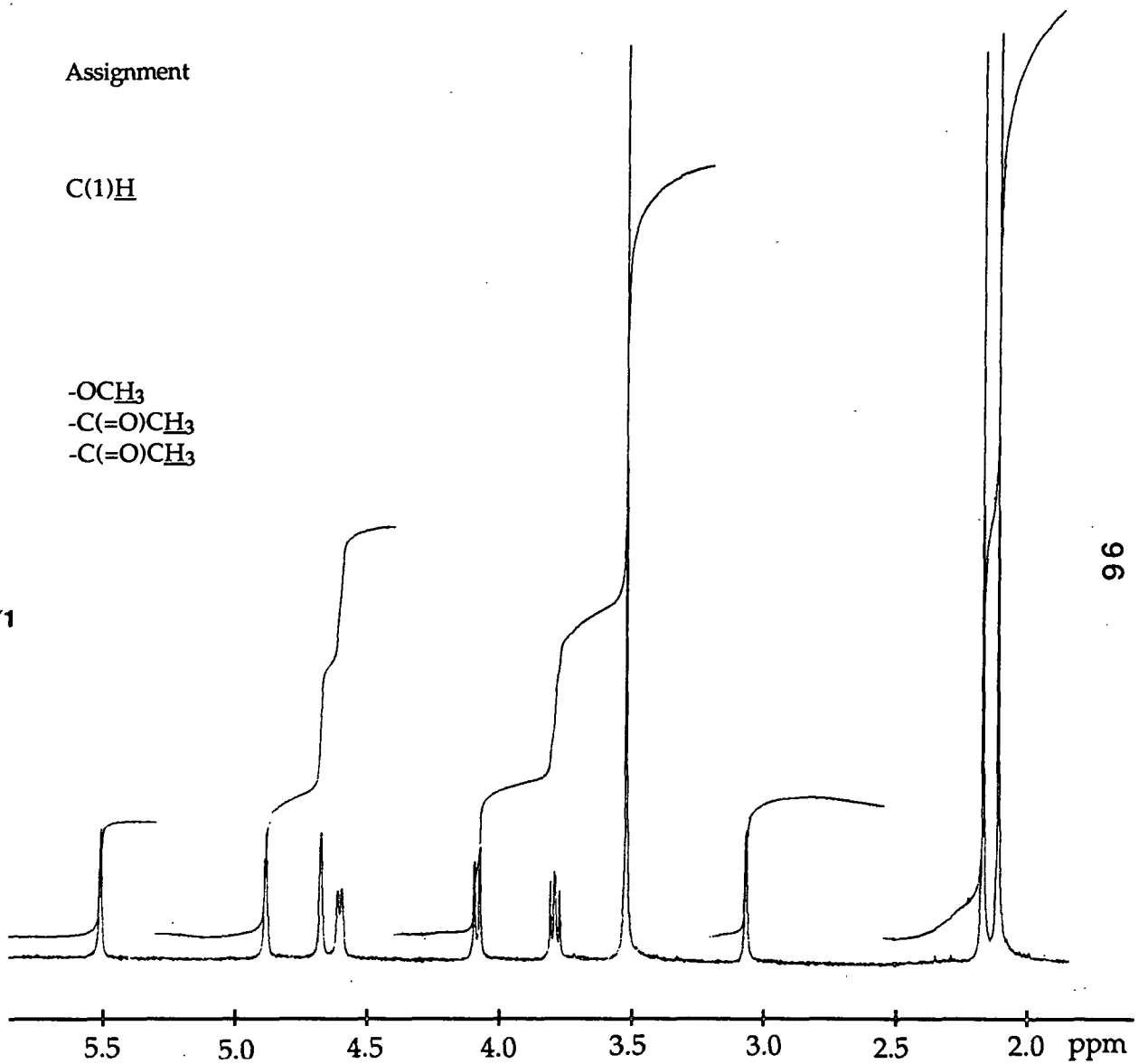

Figure 27. The ^{1}H NMR (363 MHz) spectrum of an authentic 1,6-anhydro-3,4-di-O-acetyl-2-O-methyl-β-D-glucopyranose sample with the NMR listing of Fractions 28-30 which were identified as 1,6-anhydro-3,4-di-O-acetyl-2-O-methyl-β-D-glucopyranose.

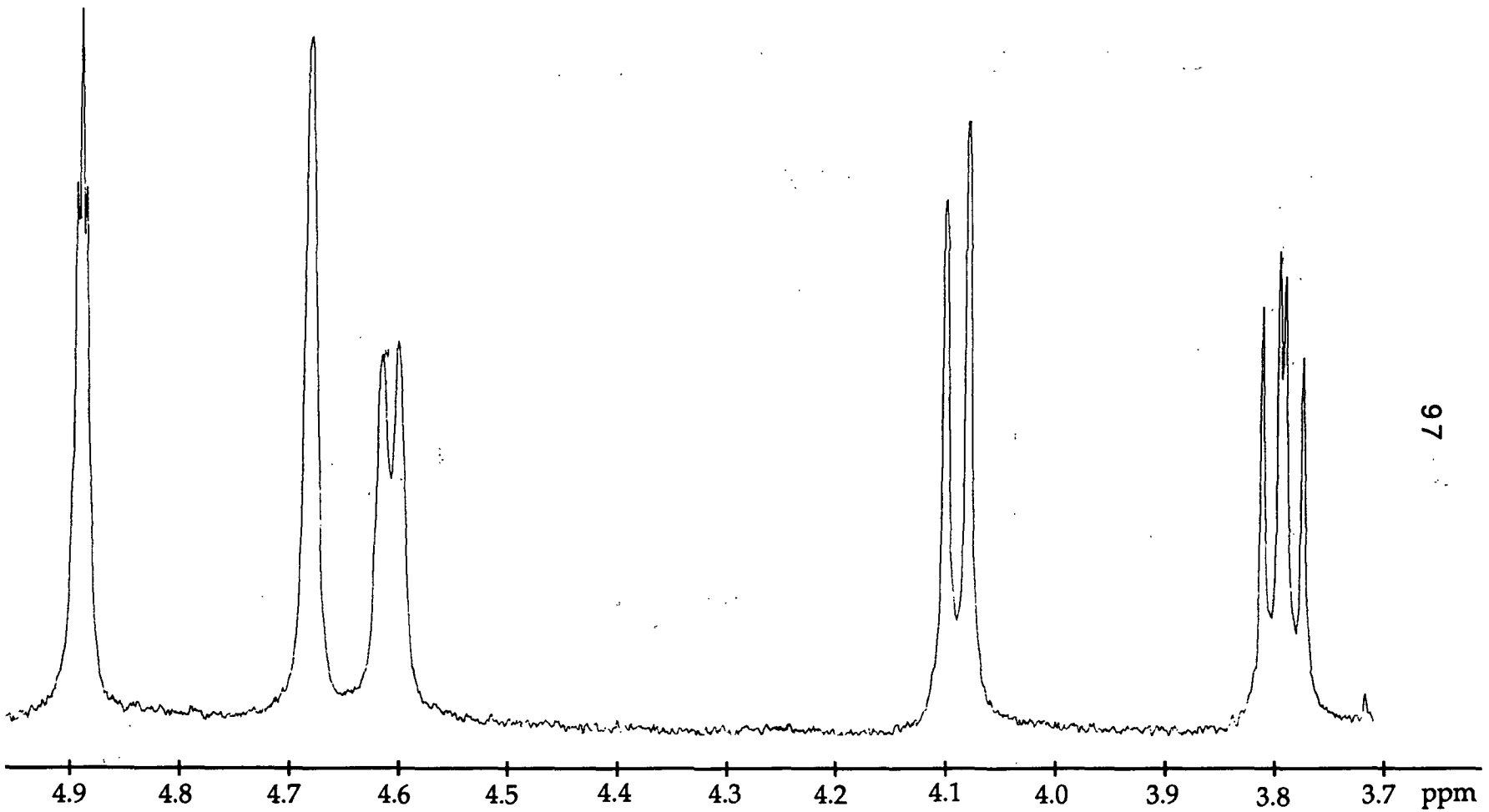

Figure 28. The expanded view of 3.7-4.9 *ppm* region of Figure 27.

Fractions 21 & 22, *ppm*	Splitting	Assignment
5.52	s	C(1)H
4.90	t of d	C(6)H_2
4.42	d of d	
4.27	d of d	
4.12	t of d	
3.63	d	
3.39	s	-OCH_3
2.12	s	-C(=O)CH_3
2.08	s	-C(=O)CH_3

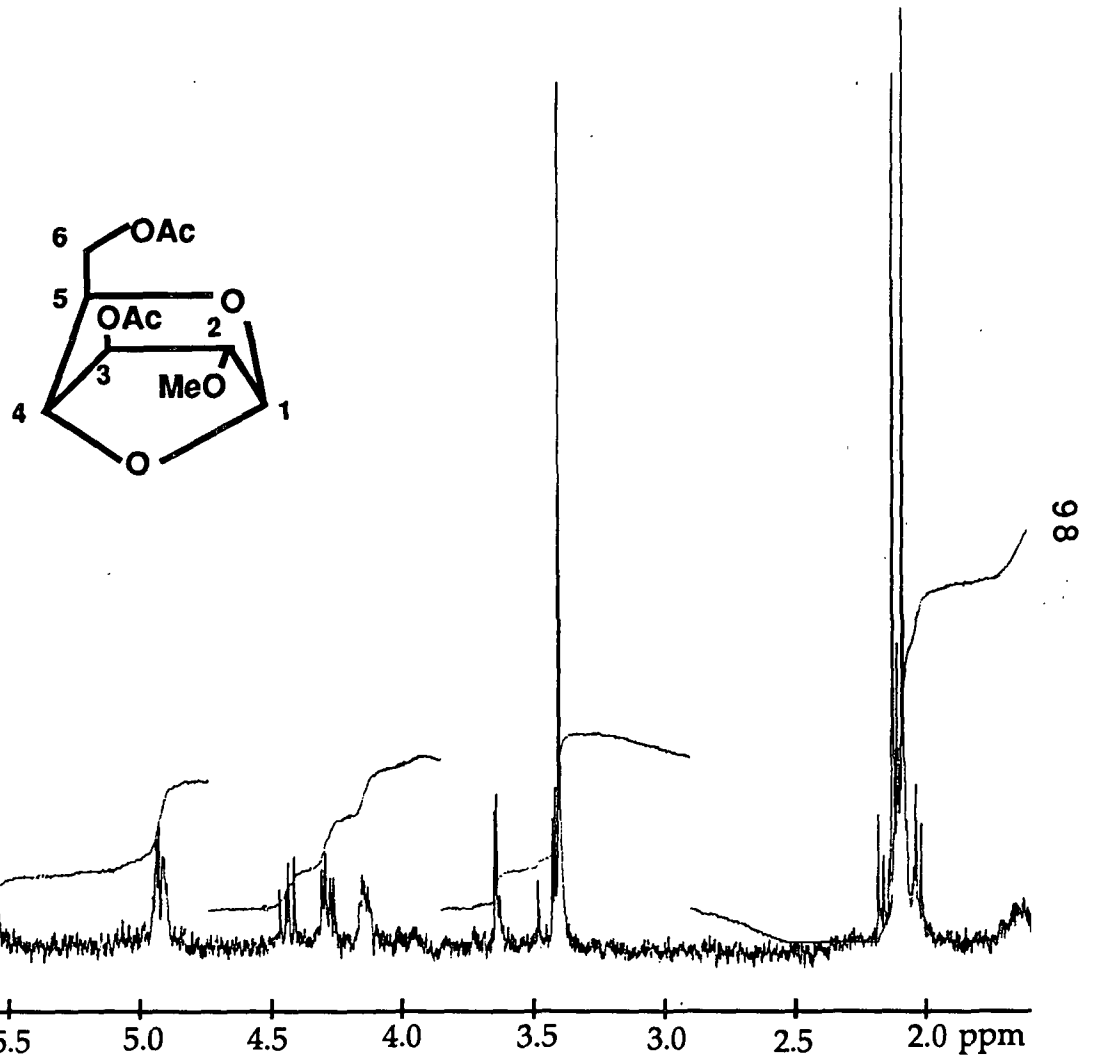

Figure 29. The ^{1}H NMR (363 MHz) spectrum of Fractions 21 and 22; the sample was tentatively identified as 1,4-anhydro-3,6-di-O-acetyl-2-O-methyl-α-D-glucopyranose.

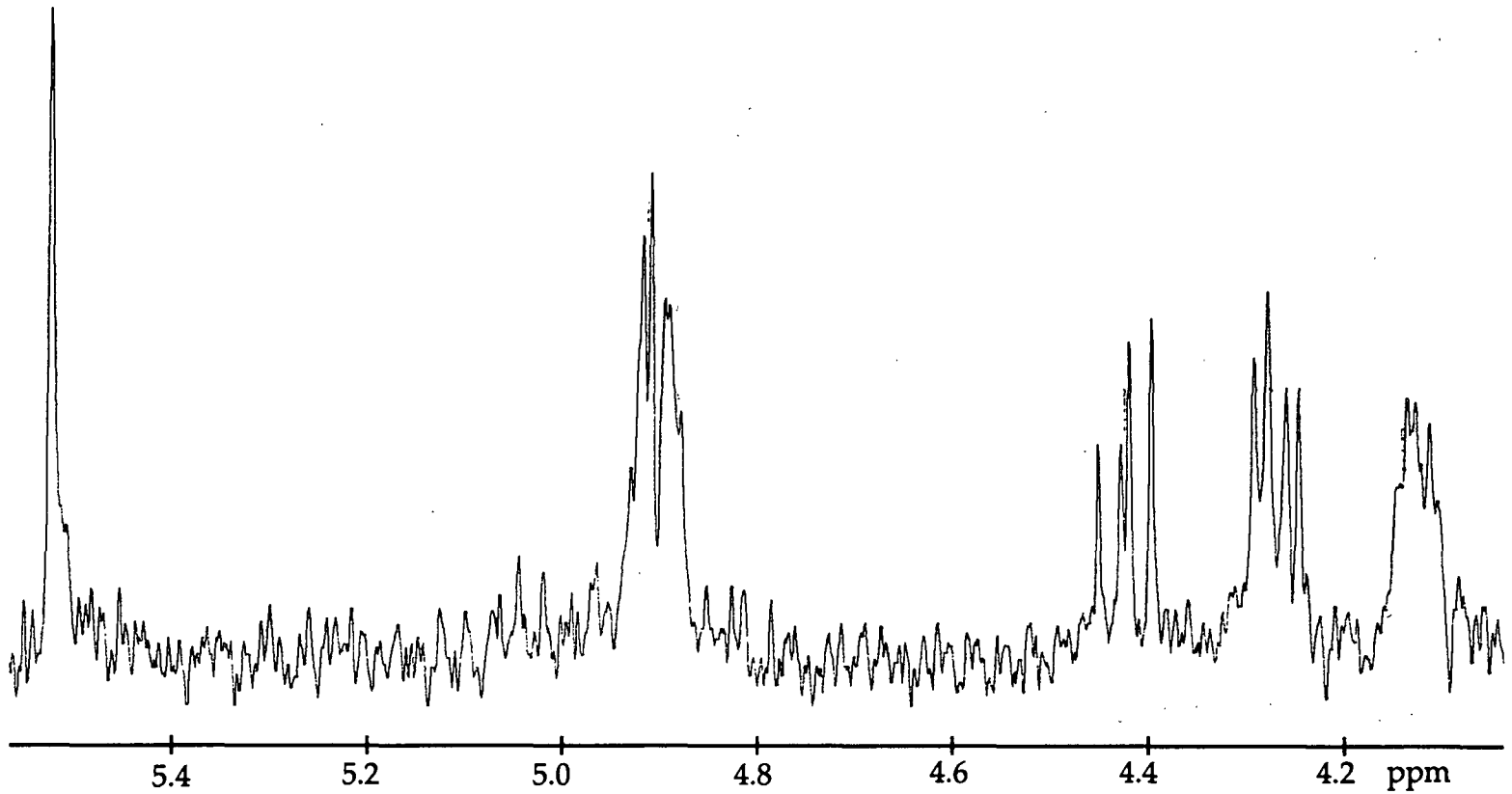

Figure 30. The expanded view of 4.2-5.4 *ppm* region of Figure 29.

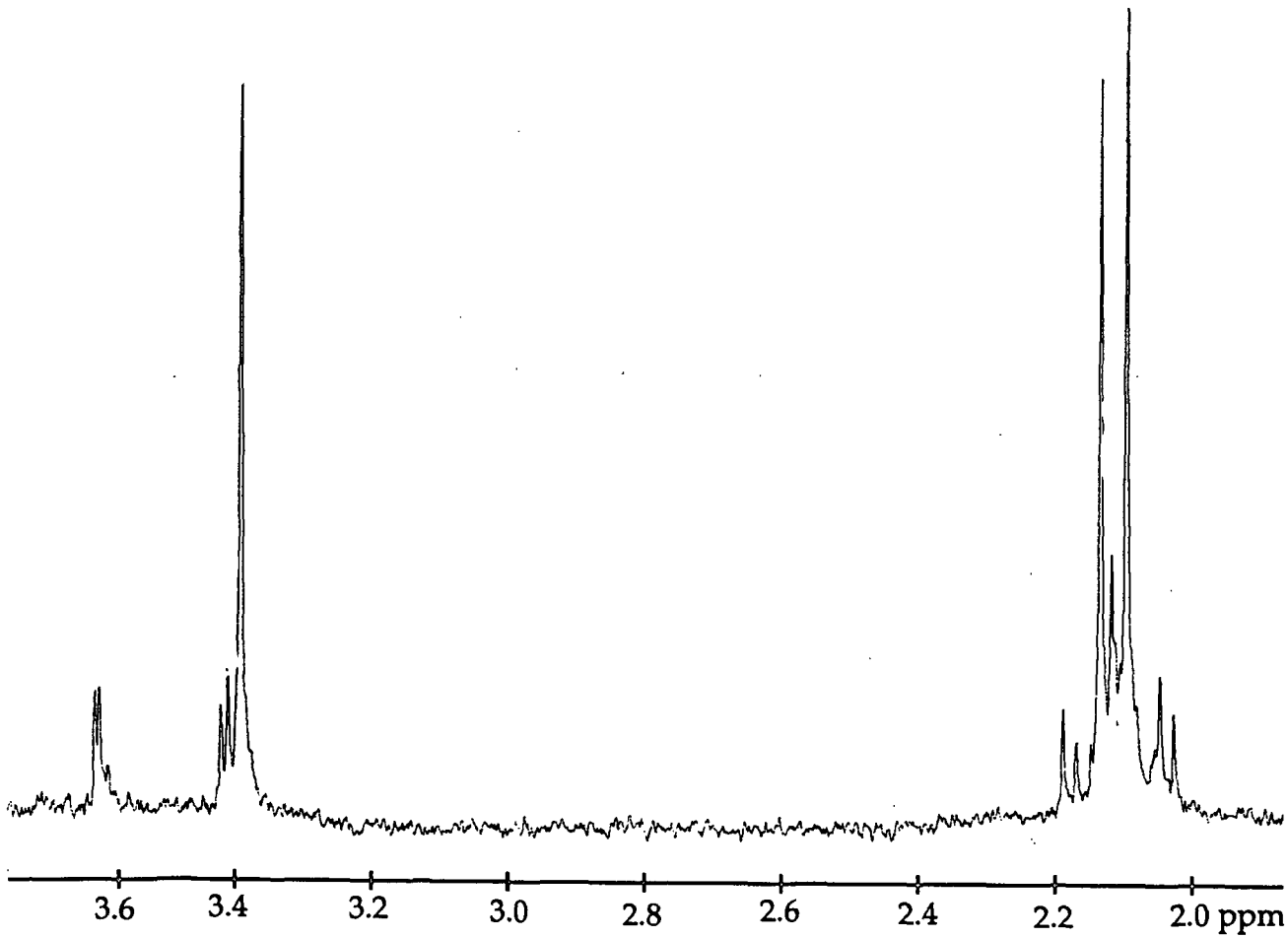

Figure 31. The expanded view of 2.0-3.6 *ppm* region of Figure 29.

APPENDIX 5

EXPERIMENTAL RAW DATA

The following tables include the raw data obtained for the experiments discussed in the Results and Discussion section. Also included in this section are two experiments not included in the Results and Discussion section. These degradations were run in 0.25M NaOH to demonstrate reproducibility between experiments. From this finding, no further duplication of experiments was performed.

Concentrations listed in the tables are at reaction temperature with thermal expansivity of reaction liquors accounted. At the bottom of the raw data columns is the degradation and formation rate constants (k). The subscripts used were r for phenyl β-D-glucopyranoside, levo for 1,6-anhydro-β-D-glucopyranose, p for phenol, r-2 for phenyl 2-O-methyl-β-D-glucopyranoside, and m for methyl α-D-glucopyranoside.

Table 17. Degradation of phenyl β-D-glucopyranoside (0.01M) in 1.000M sodium hydroxide at 100.6°C.

time, seconds	phenyl β-D-glucopyranoside, M ($\times 10^3$)	1,6-anhydro-β-D glucopyranose, M ($\times 10^3$)
0	9.198	0.000
900	8.670	0.342
3912	7.546	1.410
5700	6.907	1.985
7500	6.275	2.493
9600	5.677	3.064
12000	5.039	3.655
14700	4.370	4.240
21900	3.063	5.395
26100	2.461	5.912

$k_r = 5.02 \pm 0.04 \times 10^{-5}$ sec-1

$k_{levo} = 4.43 \pm 0.03 \times 10^{-5}$ sec-1

Table 18. Degradation of phenyl β-D-glucopyranoside (0.01M) in 0.5000M sodium hydroxide at 171.6°C.

time, seconds	phenyl β-D-glucopyranoside, M (x 10^3)	phenol, M (x 10^3)	1,6-anhydro-β-D glucopyranose, M (x 10^3)
5.34	8.723		0.515
19.97	7.899	2.417	1.896
40.51	5.930		3.463
61.11	4.473	5.496	4.611
80.46	3.435	6.327	5.526
100.70	2.712	7.532	6.091
135.52	1.655		7.099
161.26	1.179	8.444	7.463
190.17	0.954		7.635
220.37	0.532		7.939
252.00	0.397	9.400	8.163
281.64	0.332		8.131

$k_r = 1.25 \pm 0.06 \times 10^{-2}$ sec-1

$k_p = 1.18 \pm 0.11 \times 10^{-2}$ sec-1

$k_{levo} = 1.08 \pm 0.03 \times 10^{-2}$ sec-1

Table 19. Degradation of phenyl β-D-glucopyranoside (0.01M) in 0.5000M sodium hydroxide and 2.002M sodium chloride at 171.6°C.

time, seconds	phenyl β-D-glucopyranoside, M (x 10^3)	phenol, M (x 10^3)	1,6-anhydro-β-D glucopyranose, M (x 10^3)
0.00	10.21		0.000
5.55	9.388	0.593	0.570
9.93	8.918	0.903	1.035
15.93	8.162	1.625	1.523
22.29	7.753	2.714	2.015
29.86	6.920	2.298	2.619
35.45	6.462	2.908	3.009
41.93	5.972		3.492
50.32	5.379		3.920
58.37	4.949		4.325
67.73	4.296		4.833
78.86	3.963		5.139

$k_r = 1.22 \pm 0.04 \times 10^{-2}$ sec-1

$k_p = 0.945 \pm 0.213 \times 10^{-2}$ sec-1

$k_{levo} = 1.03 \pm 0.02 \times 10^{-2}$ sec-1

Table 20. Degradation of phenyl β-D-glucopyranoside (0.01M) in 2.496M sodium hydroxide at 171.6°C.

time, seconds	phenyl β-D-glucopyranoside, M (x 10^3)	phenol, M (x 10^3)	1,6-anhydro-β-D glucopyranose, M (x 10^3)
0.00	9.755		0.000
3.60	8.588	1.474	1.277
6.46	7.277	3.348	2.242
9.58	5.893	4.597	3.350
13.00	5.921	5.983	3.403
15.94	4.347	6.308	4.548
18.25	3.866	7.095	4.859
23.95	3.970		4.889
26.46	2.275		6.126
30.27	1.705		6.539
34.57	2.413		5.962
37.62	1.032		6.952

$k_r = 5.99 \pm 0.39 \times 10^{-2}$ sec-1

$k_p = 6.94 \pm 0.22 \times 10^{-2}$ sec-1

$k_{levo} = 4.71 \pm 0.22 \times 10^{-2}$ sec-1

Table 21. Degradation of phenyl 2-O-methyl-β-D-glucopyranoside (0.01M) in 2.503M sodium hydroxide at 171.6°C.

time, seconds	phenyl 2-O-methyl-β-D-glucopyranoside, M (x 10^3)	phenol, M (x 10^3)
0.00	10.26	0.0000
240.06	10.01	0.1641
480.00	9.753	0.2690
720.73	9.948	0.4143
1023.32	9.399	0.518
1260.49	9.503	0.618
1560.71	9.183	0.756
1920.51	9.070	0.897
2280.67	9.040	1.063
2640.59	8.985	1.217
3060.87	8.694	1.400
3540.50	8.679	1.604

$$k_{r\text{-}2} = 4.67 \pm 0.89 \times 10^{-5} \text{ sec-1}$$

$$k_p = 4.77 \pm 0.13 \times 10^{-5} \text{ sec-1}$$

Table 22. Degradation of phenyl β-D-glucopyranoside (0.01M) in 2.509M sodium hydroxide at 159.6°C.

time, seconds	phenyl β-D-glucopyranoside, M (x 10^3)	phenol, M (x 10^3)	1,6-anhydro-β-D glucopyranose, M (x 10^3)
0.00	10.57	0.058	0.000
3.59	10.70	0.764	0.639
6.52	8.759	1.346	1.191
9.38	7.927	2.008	1.677
12.12	7.699	2.486	2.124
15.66	6.857	3.034	2.591
20.29	6.259	3.811	3.207
24.01	5.628	4.384	3.207
29.96	5.287	5.080	4.234
35.00	4.369	5.389	4.635
39.99	3.909	5.086	5.001
46.45	3.198	6.476	5.522

$k_r = 2.48 \pm 0.10 \times 10^{-2}$ sec-1

$k_p = 2.39 \pm 0.06 \times 10^{-2}$ sec-1

$k_{levo} = 2.02 \pm 0.02 \times 10^{-2}$ sec-1

Table 23. Degradation of phenyl β-D-glucopyranoside (0.01M) in 2.489M sodium hydroxide at 149.6°C.

time, seconds	phenyl β-D-glucopyranoside, M (x 10^3)	phenol, M (x 10^3)	1,6-anhydro-β-D glucopyranose, M (x 10^3)
0.00	9.921	0.000	0.029
5.48	9.541	0.552	0.457
9.39	9.116	1.090	0.784
13.14	8.878	1.326	1.083
17.90	8.242	1.810	1.433
24.48	7.830	2.436	1.878
29.40	7.240	2.528	2.266
35.78	6.558	2.696	2.686
44.25	6.347	3.847	3.081
49.34	5.937	4.068	3.258
56.41	5.183	4.610	3.771
65.26	4.948	4.421	4.111

$k_r = 1.07 \pm 0.04 \times 10^{-2}$ sec-1

$k_p = 1.07 \pm 0.03 \times 10^{-2}$ sec-1

$k_{levo} = 0.875 \pm 0.020 \times 10^{-2}$ sec-1

Table 24. Degradation of phenyl β-D-glucopyranoside (0.01M) in 0.9982M sodium hydroxide and 1.501M sodium chloride at 171.6°C.

time, seconds	phenyl β-D-glucopyranoside, M (x 10^3)	phenol, M (x 10^3)	1,6-anhydro-β-D glucopyranose, M (x 10^3)
0.00	10.02	0.096	0.082
4.45	9.077	0.889	0.813
7.21	8.505	1.356	1.318
9.45	7.653	1.186	1.793
12.13	7.588	2.095	2.118
15.36	6.711	2.946	2.635
18.41	6.360	1.559	3.061
21.84	5.901	3.923	3.395
25.35	5.546	3.389	3.752
29.04	5.124	4.582	4.161
34.11	4.394	4.829	4.598
38.88	3.949	6.007	4.907

$k_r = 2.37 \pm 0.11 \times 10^{-2}$ sec-1

$k_p = 2.32 \pm 0.19 \times 10^{-2}$ sec-1

$k_{levo} = 1.93 \pm 0.05 \times 10^{-2}$ sec-1

Table 25. Degradation of phenyl β-D-glucopyranoside (0.01M) in 1.500M sodium hydroxide and 1.000M at 171.6°C.

time, seconds	phenyl β-D-glucopyranoside, M (x 10^3)	phenol, M (x 10^3)	1,6-anhydro-β-D glucopyranose, M (x 10^3)
0.00	9.726	0.153	0.000
4.08	8.956		1.091
5.14	8.665	1.614	1.343
6.76	8.142	2.097	1.795
8.15	7.765	2.514	2.058
10.21	7.201	3.005	2.516
11.99	6.493	3.448	2.890
13.96	6.264	3.824	3.295
15.76	5.738	4.381	3.554
19.11	5.194	4.983	4.100
22.73	4.590	5.637	4.646
26.15	4.161	6.000	4.947

$k_r = 3.45 \pm 0.19 \times 10^{-2}$ sec-1

$k_p = 3.49 \pm 0.11 \times 10^{-2}$ sec-1

$k_{levo} = 2.92 \pm 0.05 \times 10^{-2}$ sec-1

Table 26. Degradation of phenyl β-D-glucopyranoside (0.01M) in 1.39M sodium hydroxide, 0.102M sodium sulfide, and 1.00M sodium chloride at 171.6°C.

time, seconds	phenyl β-D-glucopyranoside, M (x 10^3)	phenol, M (x 10^3)	1,6-anhydro-β-D glucopyranose, M (x 10^3)
0.00	10.05	0.239	0.225
3.86	8.848	1.110	0.886
5.44	8.402	1.665	1.265
6.19	8.388	1.799	1.357
8.15	7.764	2.436	1.863
10.04	7.126	2.899	2.141
12.54	6.639	3.330	2.562
14.64	6.243	3.986	2.907
16.10	5.910	4.075	3.183
19.15	5.130	4.743	3.411
22.98	4.369	5.250	4.046
27.38	4.017	5.677	4.585

$k_r = 3.49 \pm 0.18 \times 10^{-2}$ sec-1

$k_p = 3.24 \pm 0.11 \times 10^{-2}$ sec-1

$k_{levo} = 2.50 \pm 0.12 \times 10^{-2}$ sec-1

Table 27. Degradation of methyl α-D-glucopyranoside (0.01M) in 0.497M NaOH and 2.00M NaCl at 182.7°C.

time, seconds	methyl α-D-glucopyranoside, M ($\times 10^3$)
0	9.29
75290	8.80
173500	8.23
258200	7.90
334600	7.52
421800	7.07
505400	6.75
595100	6.45
681000	5.97
782400	5.68
862900	5.28
940000	5.09

$$k_m = 6.01 \pm 0.68 \times 10^{-1}\ sec^{-1}$$

Table 28. Degradation of phenyl β-D-glucopyranoside (0.01M) in 0.2498M NaOH and at 171.6°C.

time, seconds	phenyl β-D-glucopyranoside, M ($\times 10^{-3}$)	1,6-anhydro-β-D glucopyranose, M ($\times 10^{-3}$)
7.20	9.468	0.293
20.66	8.436	1.068
40.23	7.305	2.958
58.56	6.277	2.942
90.57	5.090	3.896
121.01	4.129	4.863
150.40	3.383	5.441
180.56	2.687	6.093
210.97	2.155	6.488
250.50	1.656	7.008
300.86	1.124	7.391
345.98	0.921	7.635

$k_r = 6.99 \pm 0.18 \times 10^{-3}$ sec-1

$k_{levo} = 5.94 \pm 0.11 \times 10^{-3}$ sec-1

Table 29. Degradation of phenyl β-D-glucopyranoside (0.01M) in 0.2496M NaOH at 171.6°C.

time, seconds	phenyl β-D-glucopyranoside, M (x 10^3)	1,6-anhydro-β-D glucopyranose, M (x 10^3)
6.92	9.787	0.229
20.44	8.860	0.955
40.16	7.784	1.975
60.94	6.709	2.679
90.84	5.354	4.025
120.66	4.648	4.572
150.37	3.656	5.405
180.80	3.446	5.636
209.95	2.462	6.412
250.20	2.119	6.704
294.07	1.436	7.206

$k_r = 6.44 \pm 0.29 \times 10\text{-}^3$ sec-1

$k_{levo} = 5.52 \pm 0.23 \times 10^{-3}$ sec-1